Volume 7, No. 1
December, 1960

THE SOVIET JOURNAL OF

ATOMIC ENERGY

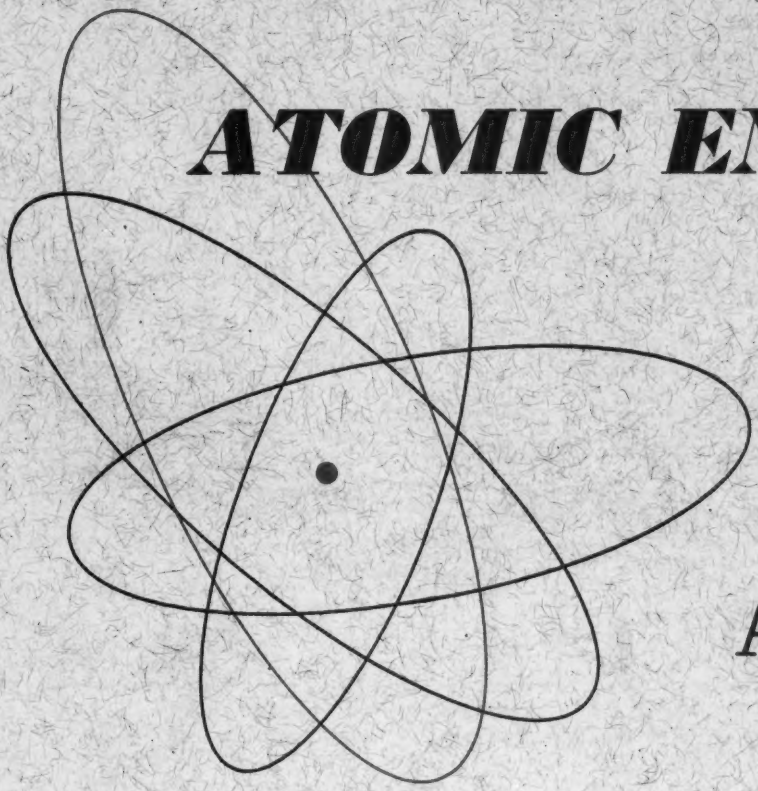

Атомная
энергия

TRANSLATED FROM RUSSIAN

CONSULTANTS BUREAU

THE SOVIET JOURNAL OF

ATOMIC ENERGY

A translation of ATOMNAYA ÉNERGIYA,
a publication of the Academy of Sciences of the USSR

(Russian original dated July, 1959)

Vol. 7, No. 1 December, 1960

CONTENTS

Annual subscription $75.00
Single issue 20.00
Single article 12.50

CONTENTS (continued)

NOTE

The Table of Contents lists all material that appears in Atomnaya Énergiya. Those items that originated in the English language are not included in the translation and are shown enclosed in brackets. Whenever possible, the English-language source containing the omitted reports will be given.

Consultants Bureau Enterprises, Inc.

FIVE YEARS OF NUCLEAR POWER

N. A. Dollezhal' and A. K. Krasin

Original article submitted April 27, 1959

A tremendous event in science and engineering transpired on June 27, 1954: the world's first atomic electric-power generating station, built near Moscow (in the town of Obninsk), delivered current into the electric power grid. Although the power produced by the station's only turbine was not large (5000 kw), the First Atomic-Power Station exhibited all of the features of the full-scale large electric-power station. This made it possible to acquire operating experience with relatively moderate expenditures on capital outlays and, in the case of successful performance, to extend the example to more powerful scaled-up power stations of a similar type.

Nuclear power engineering, the basis of which was laid by the starting-up of the First Atomic-Power Station in the USSR, is characterized by a very swift growth in atomic power levels (see Fig. 1). This intense rate of growth will continue, since quite a few large-scale atomic power generating stations are nearing completion. The successes achieved in nuclear power engineering are obvious and imposing.

However, at the time the First Atomic-Power Station was commissioned, and even more so while it was still in the beginning of the design stage, there was not only no definite opinion on the technical pathways for developing nuclear power, but even skeptical views as to the feasibility of developing nuclear power as a branch of the economy were occasionally voiced.

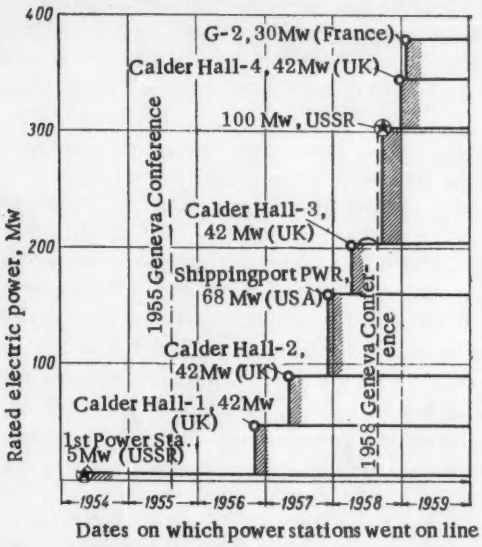

Fig. 1. The increase in power ratings of the large-scale atomic-power generating stations during the past five years.

The start-up and the five-year history of performance of the atomic power station have radically altered those views. In the first instance, the start-up of the power station was fraught with great social significance (a fact acknowledged by all) in that it became clear that atomic energy might serve the aims of progress, rather than military objectives. And in the second instance, the five-year operation of the station is of great engineering significance in that, as a result of that history, one of the variants of power-reactor design has been confirmed with respect to its viability, a point which met with doubt even after the station was first put on the line.

In the past five years, a great variants of power reactors, differing in design and materials, have been proposed and partially tried out. This has,to an appreciable degree,made it possible to feel out the areas of scientific and engineering research which will be decisive in the further development of nuclear power.

The operation of the station not only has enabled us to evaluate the station as one of the variants to be considered in resolving the problem of utilization of atomic energy for power generation, but also has enabled us to derive reliable conclusions bases on the operating experience.

Several papers devoted to a description of the design and performance of the atomic electric-power station [1–6] have been published, and show that the tasks posed when the station was being built have been fulfilled, and that the accumulated experience is proving highly valuable in the resolution of problems associated with the design of scaled-up atomic electric-power stations employing reactors of similar design.

Let us now consider some of the more important conclusions which may be arrived at on the basis of the experience accumulated over the five-year period of operation of the reactor.

In atomic electric-power stations, as in conventional heat-power stations, raising the plant efficiency is a prime concern. The effort exerted to raise the steam parameters in graphite-moderated reactors inevitably leads to high graphite temperatures. The experience gained in the protracted reliable operation of the reactor at graphite temperatures of 700-750°C attests to the possibility of attaining high coolant temperatures in graphite-moderated reactors. This has found its expression in the subsequent design project of the reactor for the Ural atomic-power station [4], and in recent plans for graphite-moderated re-

actors, e.g., the British "ZENITH" [7] and AGR [8] reactors, and the American GCR-2 reactor [9].

The continuous rise in coolant temperature at exit from the reactor is a distinctive trend noted in modern reactor design. The increased plant efficiency, due to efforts aimed at raising the steam temperature and pressure to values used in modern steam turbines leads to a reduction in rated power costs, i.e. to improvement in the economic performance of the stations. The reliable performance of graphite under the temperature conditions indicated in the First Atomic-Power Station has opened the way for planning the production of steam suitable to drive modern turbines in the Ural power-station reactor design. The use of nuclear superheating of steam in the Ural station reactor is a distinguishing feature of this reactor: its efficiency is much higher than in other known reactor types.

The possibility of boiling water and superheating steam in a reactor has been confirmed by special experiments carried out on the reactor of the First Atomic-Power Station [4]. Important experiments relating to the study and control of transients in the Ural atomic station now being built were also carried out. The production of superheated steam in the reactor is bound up with the need to alter the cooling of the channels (designed for superheating of the steam), i.e. to switch from water-heat transfer to steam-heat transfer, in starting-up the reactor from cold. A similar problem is encountered in shutting down the reactor, when heat transfer by steam is replaced by water cooling. The experiments have demonstrated that the transients are fully realizable in practice, and do not impose any difficulties on the operating performance of such systems. This yields the possibility of using several different design approaches to atomic electric-power stations incorporating steam superheat in the reactor.

This leads to the following conclusion based on the results of operating of the First Power Station: the reactor design proved to be technically extremely flexible; it permitted large-scale experiments on introducing the reactor to a progressive operating regime of boiling and superheating of the coolant in the core, without necessitating any far-reaching redesigning work.

The technical flexibility of the reactor is contained in the very concept underlying its design: in the use of channels with individual coolant leads. The absence of a pressurized containment vessel made it possible to use the reactor for a broad range of experiments, which would be difficult, if not simply impossible, to carry out in a reactor enclosed in a pressure vessel. The testing of samples of different structural materials, the design of test loops for fuel elements and operating conditions research, is accomplished with relative ease in a reactor of this type. The choice of reactor type for the First Atomic-Power Station proved to be a fortunate one in this respect as well.

It is still difficult to determine at this stage in what area the optimized economical performance of the station, dependent on steam pressure and temperature, is to be found, but the perspectives for direct enhancement of station performance by means of the heat of the fission reaction are highly promising.

The use of nuclear superheating of steam in nuclear power stations not only makes it possible to lower the cost per 1 kwh of the electric power generated, but also (no less important) to reduce rated power costs.

Another important factor determining the economics of nuclear power is the use of both charged and regenerated fuel, as well as the use of neutrons.

The percent burnup of the nuclear fuel, i.e., the ratio of the amount of U^{235} consumed during a reactor period to the original amount present, has a significant effect on the cost of generated electric power. The percent fuel burnup (especially in reactors working on enriched uranium) is characterized to a certain extent by the amount of heat which may be successfully extracted from a unit weight of loaded uranium fuel. The greater the burnup, the less frequently fuel elements have to be replaced in the reactor and the lower fraction of unit cost of electric power generated attributable to expenditures in the perparation of operating channels (with fuel elements), chemical reprocessing of spent fuel discharged from the reactor, etc.

High burnup may be attained by using fuel elements stable to corrosion attack, radiation effects, temperature, stress, and other factors. The reactor of the First Atomic-Power Station contains channels which have been operating without letup since the first charging of fuel, i.e., for five years. The original design of the reactor was carried out in order to obtain a fuel burnup corresponding to a fuel heat rating of ~10,000 Mwd/ton. However, operating experience has shown that the fuel elements retained their operating efficiency even at much higher heat ratings; e.g., in some fuel elements subjected to special tests, a specific energy yield reaching 30,000 Mwd/ton was reported, which gave promise of achieving very efficient use of the fuel in reactors of their design. The operating experience of the station thus allows one further conclusion to be drawn, namely that the elaboration of projects involving full-scale nuclear power stations incorporating similar reactors may proceed with assurance of achieving high economic performance, on account of the excellent reliability of the fuel elements used.

Burnup is dependent largely on when and how recharging of the operating channels takes place. It is common knowledge that fuel burnup does not proceed at a uniform pace at all points in the pile. By dividing the core of the reactor in the First Atomic-Power Station arbitrarily into 7 annular regions [3] shown in Fig. 2, for example, we see that, following the first run, fuel burnup proceeds in the different annuli according to the curve in Fig. 3. Inspection of the curve shows that U^{235} burnup is much less in the peripheral channels, which are the majority, than in the centrally placed channels, i.e., the uranium is not completely burned, and the channels fail to produce the rated amount of heat. In order to achieve uniform and increased fuel burnup at the First Atomic-Power Station, recourse was had with success to a method of partial recharging of the

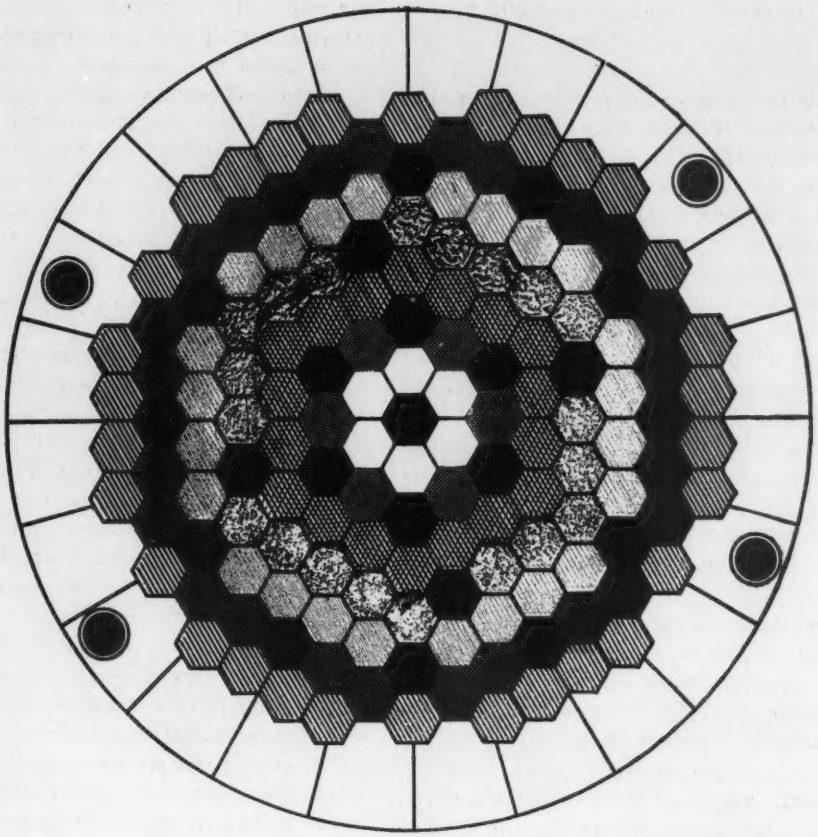

Fig. 2. Annular regions for partial (staggered) recharging of reactor fuel channels.

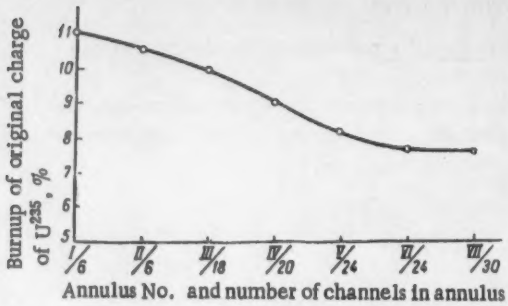

Fig. 3. Amount of spent U^{235} along radius of reactor (in percentage of original fuel charged) after the first run.

channels [6] involving the shifting of peripheral channels to the center of the core and the loading of fresh channels into the peripheral region. This approach made is possible to achieve high fuel burnup and to increase the economic efficiency of the power station at the same time. This manner of utilizing the fuel has already been considered in several nuclear electric-power stations being planned abroad [13], and will undoubtedly meet with great favor in the future.

High burnup of U^{235} by means of the partial recharging method, in order to be economically feasible, requires a reactor design allowing convenient recharging of fuel without lengthy downtime. This is facilitated in the reactor of the First Atomic-Power Station by designing each operating channel to allow easy extraction and replacement of the channels independently of each other. In principle, the operation may be carried out even while the reactor is in operation.

This prominent positive feature of the reactor, with its individual channels, confers a high plant duty factor on the operating economics of the station, which in turn has a favorable effect on the cost of electric power generated. The principle of individual coolant ducting serving the fuel channels has been adopted outside the USSR, e.g., in the Swiss heavy-water organic-coolant reactor [14], in the sophisticated USA sodium-cooled reactor [15], and in the Canadian heavy-water reactor [16]. A variant of the design of heterogeneous reactors with individual distribution of coolant flow to the channels, together with a variant of the reactor enclosed in a pressure vessel, has thus won its right to existence.

It is common knowledge that the economic performance of a nuclear electric-power generating station is significantly affected by the unit power rating of the generating unit: the higher the thermal power of the reactor, the cheaper electric power will be, other conditions being equal. The observed tendency of the unit thermal power of reactors now being built to increase is evident and easily understood. The increase in the thermal power of the reactors is due not only to more intense heat removal, but fundamentally to increased core dimensions. The possibilities of expanding the dimensions of the core, and consequently of increasing the thermal power of the reactors by individual handling of the channels, are virtually unlimited, whereas these possibilities are restricted in reactors enclosed in pressure vessels by virtue of the highly complicated engineering problems involved in the construction of the enclosure.

In spite of the use of stainless steel in fuel assemblies, a rather favorable neutron balance is successfully achieved. The breeding ratio of the fuel is from 0.50-0.65 in such reactors, i.e., it is not inferior to the value found in water-moderated, water-cooled reactors.

Whatever the parameters of a nuclear power installation may be, the prime requirements are reliability in operation and safety factors for the operating personnel and the population of the surrounding area.

Safety and health standards require that special measures be taken to ensure safe operation of the facility, when designing and building a reactor installation. It is also essential that the costs of safety provisions not entail an exorbitant increase in the electric power costs.

In particular, a substantial fraction of the capital outlay goes into the protective shielding of the nuclear power station, if such shielding is planned as part of the installation. No protective shielding is used in the First Atomic-Power Station or in the Ural power-station project. This is not accidental, for the principle of individual coolant flow along the reactor fuel channels provides for an explosion-proof reactor. While the potential energy in reactors of the pressure-vessel type is concentrated within the large unit volume of the pressure enclosure and may be suddenly liberated in large quantity in the event of an accident, this type of accident is excluded in reactors with discrete channels. The five-year experience in reliable operation of the First Atomic-Power Station brings a powerful argument to support the concept of the safety inherent in that type of reactor, and attests to the infeasibility of using protective shields. The experience acquired in experimental research wherein meltdown or breakup of fuel assemblies took place demonstrated that no danger of radioactive contamination of the station grounds and facilities or of the surrounding locality resulted.

On the whole, operation of the First Atomic-Power Station has shown that favorable radiation-biological circumstances both for the servicing personnel and the population of the surrounding area in reactors of that type do not involve expenditures or unusual engineering difficulties.

Operation of the First Atomic-Power Station has provided opportunity for the training of cadres of reactor operating personnel. The successful performance of the power station was contributed to in large degree by the guidance and supervision of A. N. Grigor'yants, G. N. Ushakov, L. A. Kochekov, V. T. Lytkin, and others.

In taking note of the Fifth Anniversary of the start-up of the world's First Atomic-Power Station, one cannot help but acknowledge that it has played an important social and technical role in the development of nuclear power, and has become the prototype of a broad class of reactors.

COMMENTS ON THE FIRST ATOMIC POWER STATION

Recorded in the Visitors' Book:

The late G. M. Krzhizhanovskii, Academician of the Academy of Sciences of the USSR (1956):

"The practical use of each new energy form signifies grandiose stages on the road of mankind's forward motion. The ability to harness the colossal energy contained in the atomic energy is an outstanding even in science and technology. In our country, setting the example for all nations in the harnessing of atomic energy, the world's first atomic electric power generating station, producing 5000 kw, has been built. The day is not far off when atomic electric power generating stations delivering fifty and even a hundred thousand kilowatts will be going into operation . . .".

Prime Minister Jawaharlal Nehru of India (1955):

"I am glad that I visited this power station, and am thrilled by it. This has made it possible to glimpse into the future, opening up before my eyes. . .".

President Sukarno of the Republic of Indonesia (1956):

"There is no limit to the human intellect. Evolution is still going on. The visit to this power station reinforces our faith that mankind must develop his knowledge, in order to reach a higher living standard. . . ".

Ambassadors of the USA, Britain, Sweden (1955):

"The scientists and engineers of the USSR, in being the first in the world to harness atomic energy for peaceful purposes, have earned themselves unforgettable honors before all of humanity. This atomic electric-power station is a tremendous achievement of Soviet science and a symbol of the profoundly human character of Soviet society. We wish the Soviet scientists new successful firsts on the road to the practical utilization of atomic energy. . . ".

Professor Chou Pei-Wang, Hu Chung-Ming, Tsiang Nan-Hsiang, People's Republic of China (1955):

"We are very happy that we have had the opportunity to visit the atomic electric-power station. The building of the first atomic electric-power station in the world is a victory for Soviet science and victory for the Socialist system.

"This combination of science and engineering put to the service of Socialist construction is a shining example for the Chinese people. We hope that with the noble international aid rendered by great Soviet people, we shall, relying on our own labor, be able to contribute our share to the cause of the peaceful utilization of atomic energy for Socialist construction in the interest of peace."

Former member of the British atomic energy planning commission, S. G. Reason (1955):

"I am very grateful at having had the opportunity to witness the great progress made by Soviet scientists in the peaceful utilization of atomic energy. As a former member of the British atomic-energy planning commission, I am aware of the broad scope of the problems to be solved in order to harness this new source of energy, and the manner in which these problems have been resolved in the USSR has made a great impression on me . . . ".

Professor Gustav Hertz of Leipzig University, German Democratic Republic (1956):

"I have already heard much and read much about atomic electric-power stations, but what I saw here surpassed all of my expectations . . . ".

Dean Hewlett Johnson of Cantebury Cathedral (1956):

"More than 40 years have passed since I first became interested in science and technology. I have dreamed of the creation of such a power station as this one. I was convinced that a Socialist country would be the first in the world to harness atomic energy, and I knew that this power would be used for peaceful purposes. I am happy that I have lived to see the day when I could view this station with my own eyes, and greet all of those who made it possible, and all of those who worked on it . . . " .

LITERATURE CITED

1. D. I. Blokhintsev and N. A. Nikolaev, "Reactor design and theory," Geneva, 1955, p. 615.
2. D. I. Blokhintsev, N. A. Dollezhal', and A. K. Krasin, Atomnaya Énergiya No. 1, 10 (1956).*
3. N. A. Dollezhal', A. K. Krasin, N. A. Nikolaev, A. N. Grigor'yants, and G. N. Ushakov, Geneva, 1958, p. 2183; Russian edition: Nuclear Reactors and Nuclear Energy. 2 (Atomizdat, 1959) p. 15.
4. N. A. Dollezhal' et al., Geneva, 1958 p. 2183; Russian edition: Nuclear Reactors and Nuclear Energy. 2 (Atomizdat, 1959) p. 36.
5. N. A. Dollezhal', Atomnaya Énergiya 3, 391(1957).*
6. A. N. Grigor'yants, Atomnaya Énergiya 2, 109 (1957).*
7. K. Mitchell and R. Geary, "The high-temperature energy reactor 'Zenith'," Geneva 1958, p. 1463.
8. R. Moore, H. Kronberger, and L. Grainger, "Advance in the design of gas-cooled graphite-moderated power reactors," Geneva, 1958, p. 312.
9. R. Charpie, M. Bender et al., "Design study for a graphite-moderated gas-cooled reactor using partially enriched uranium," Geneva, 1958, p. 950.
10. Atomnaya tekhnika za rubezhom No. 3, 85 (1959).
11. Nuclear Reactor Plant Data. ASME, 1958.
12. Nucleonics 17, 63 (1959).
13. W. Zinn, J. West, and G. Tavernier, "A 125 Mw indirect-cycle boiling-water reactor," Geneva, 1958, p. 1801.
14. W. Hälg and T. Schaub, "Diphenyl cooled, heavy-water moderated, natural uranium reactor prototype," Geneva, 1959, p. 259.
15. S. Levy, B. Voorhees, P. Aline, and K. Cohen, "Advance design of a thermal sodium-cooled reactor for power production," Geneva, 1958, p. 604.
16. H. Smith, W. Walker, N. Williams, and E. Critoph, "A study of a full-scale uranium and heavy-water nuclear power plant," Geneva, 1958, p. 208.

* Original Russian pagination. See C.B. translation.

THE DESIGN AND OPERATION OF SOME PUMPS FOR SODIUM AND SODIUM-POTASSIUM ALLOYS

P. L. Kirillov, V. A. Kuznetsov, N. M. Turchin, and Yu. M. Fedoseev

Original article submitted February 10, 1959

This article gives a description of some designs, testing results, and operational experience of centrifugal and electromagnetic pumps for sodium and sodium-potassium alloys. During the past two years these pumps have been used in experimental and semiindustrial plant.

In developing reactors cooled with liquid metals (sodium or sodium-potassium alloys), the problem of pumping liquid metals arose. Pumps designed for water, petroleum products, etc. could not be employed for this purpose because they failed to provide a complete seal and reliable operation at metal temperatures of 300-500 °C.

In centrifugal pumps the seal can be obtained by the following four methods: 1) by means of sealing rings pressed against the shaft; 2) by sealing all rotating parts (shaft, rotor, etc.); 3) by placing the entire machine under a casing; and 4) by sealing the shaft by means of a ring of frozen sodium.

The first problem is complicated and no reliable solution exists for it as yet. The second problem is, in essence, reduced to the development of a special machine. We have therefore selected the two last-mentioned methods, which are easy to achieve in laboratory conditions.

No difficulties are encountered at present in the operation of centrifugal pumps at temperatures below 400°C [1-4]. Pumps have also been designed which are capable of operating at a temperature of 550-600 °C.

The high electrical conductance of liquid metals made possible the development of new types of pumps in which the hydrodynamic head is produced by electromagnetic forces. The use of electromagnetic pumps makes the problem of sealing the circuit easier. The main shortcoming of these pumps is their low efficiency, which is only about half that of centrifugal pumps designed for the same operating conditions. However, for the experimental plants this fact is of little importance. Therefore, electromagnetic pumps are being increasingly used in laboratory practice, their main advantages being that they have no moving parts and are simpler to make and operate than the centrifugal pumps.

The problem of selection of a suitable type of pump (centrifugal or magnetic) for full-scale plants is as yet not solved. Only the experience obtained in the operation of a large number of pumps of various types can lead to correct conclusions on the advantages of one design or the other.

CENTRIFUGAL PUMPS

The schematic diagram of a centrifugal pump is shown in Fig. 1. At 990 rpm this pump produces a head of 23 m of the liquid being handled, and at 1450 rpm a head of 55m. The delivery of the pump at 990 rpm is more than 10 m^3/hr. The built-in asynchronous motor 2 has a power of 10 kw. The 415 mm diameter impeller 1 has 14 blades. In order to reduce the axial force, the working-wheel disk has 7 holes of 8 mm diameter. The electric motor and the impeller are mounted on the same shaft. The shaft has three supports, the upper support consisting of two thrust journal-ball bearings 3, the central support consisting of one journal-ball bearing 4, and the lower support which is the sliding bearing 5. In order to prevent the lubricant from escaping into the liquid metal, the shaft was made with a stepped contour and provided with the protective collar 7 below the central bearing. The sleeve of this bearing is made of RF-1 high-speed steel and the bush 6 from Br. B2 beryllium bronze, which contains 2% beryllium. The sealing rings 8 are made of the same bronze. When the bearing is cold the clearance between the sleeve and the bush is 0.2-0.25 mm. All other parts of the pump are make of 1Kh18N9T steel.

The metal leaking through the upper sealing ring rises along the shaft and is led through the special hole 9 into the tank of the pump. Above and outside this hole are mounted removable cooling chambers 10. The electric motor is cooled by an inert gas contained inside it. The coil 11 through which water can be circulated is also mounted inside the motor. It was found that when the pump was in operation there was no need to use this coil for cooling since water circulating in the outer jacket proved adequate. The pump is connected into the circuit by means of removable "ball-cone"-type connecting fittings. A nickel packing is used for sealing the motor housing.

The pump was first tested, and its characteristics determined, on water. At 990 rpm and a volume flow of liquid of 6.5 m^3/hr, the efficiency of the machine was 40%. After this test the machine worked for 2000 hr on a sodium-potassium alloy at temperatures ranging from 200 to 400 °C. After 1500 hr the bush of the lower bearing had to be replaced because its wear reached 2 mm on one side.

The greatest shortcomings of these pumps' design are their complicated dismantling (replacement of bearings, removal of the housing, etc.) and heavy weight. Figure 2 shows another centrifugal pump which is more compact

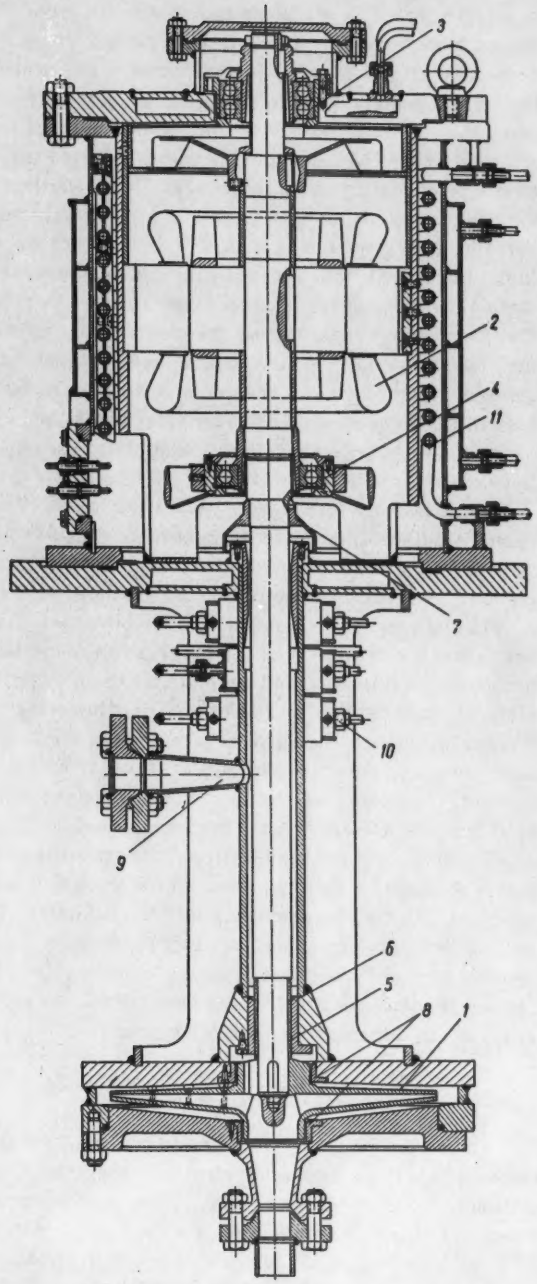

Fig. 1. Centrifugal pump with bearing of beryllium bronze and a built-in electric motor: 1) impeller; 2) asynchronous motor; 3) journal-thrust ball bearing; 6) bush; 7) protective collar; 8) sealing rings; 9) hole for the removal of leakage; 10) cooling chambers; 11) coil.

and simpler in design. In order to make the machine more compact while retaining its characteristics, motor 2 with 2900 rpm was chosen. The electric motor was sealed by covering it with a water-cooled casing 3. An inert gas was circulated in the casing by means of the fan of the electric motor. The bed plate was cooled with water. The impeller 1 with a diameter of 164 mm is fixed on the shaft which is supported at two points—at the top (4) and at the bottom (5). Metal which flows in an axial direction lubricates the lower bearing and then flows into the tank of the pump. According to the resistance of the main circuit, the amount of metal which flows along the shaft can vary from 50 to 200 liter/hr.

The pump was tested at temperatures reaching 450°C. It was found that the service life of bearings was reduced to less than hundreds of hours by a sudden drop in the strength of the beryllium bronze at such temperatures. Attempts to use other pairs of metals for this bearing, which is immersed into sodium (RF-1 steel-cast iron, RF-1 steel—EI-220 steel) produced no satisfactory results. The best results were obtained with a bearing having the sleeve made of RF-1 steel and a bush of Br.B2 bronze. The clearance between the sleeve and bush of the bearing, which was determined by experiment, was 0.12-0.15 mm. With a smaller clearance the bearings seized, while larger clearanced reduced their service life. All failed bearings had a considerable wear on one side (up to 5 mm).

The pump was run for 2000 hr in plants operating on sodium-potassium alloys, and for 7000 hr in a plant operating on sodium, at metal temperatures of about 200 °C.

During the operation of these pumps a penetration of sodium vapors inside the electric motor and their condensation on its internal surfaces were observed. After oxidation, the sodium vapors produced a thin film of sodium oxide on the winding. After combining with this film, moisture produced hydroxide on the winding which attacked the wire and led to its failure.

With the increasing operating temperature, the bearing functioning in the liquid metal becomes the weak point of all the pumps described. Several designs of pumps for various capacities and working conditions were developed which have a bearing of frozen sodium. The schematic diagram of a pump of this type is given in Fig. 3. The pump produces a head of 100 m of the liquid being handled and its capacity reaches 25 m^3/hr. The motor operates at 2960 rpm. The power of the electric motor 1 is 14 kw. Its shaft is supported at two points: in two journal-thrust bearings 4 and in two radial bearings 5. The bearing 6, which is made of frozen sodium, is in effect the third support. Thus, two metal partitions are placed between the cooling agent and the frozen sodium, which arrangement makes possible the use of water as the cooling agent. The sodium bearing suffers no wear and resists practically any temperature which is of particular importance. At the same time the frozen sodium serves as a reliable seal of the shaft.

The calculation of heat transfer in the cooling chamber is very difficult since it is not easy to calculate the heat

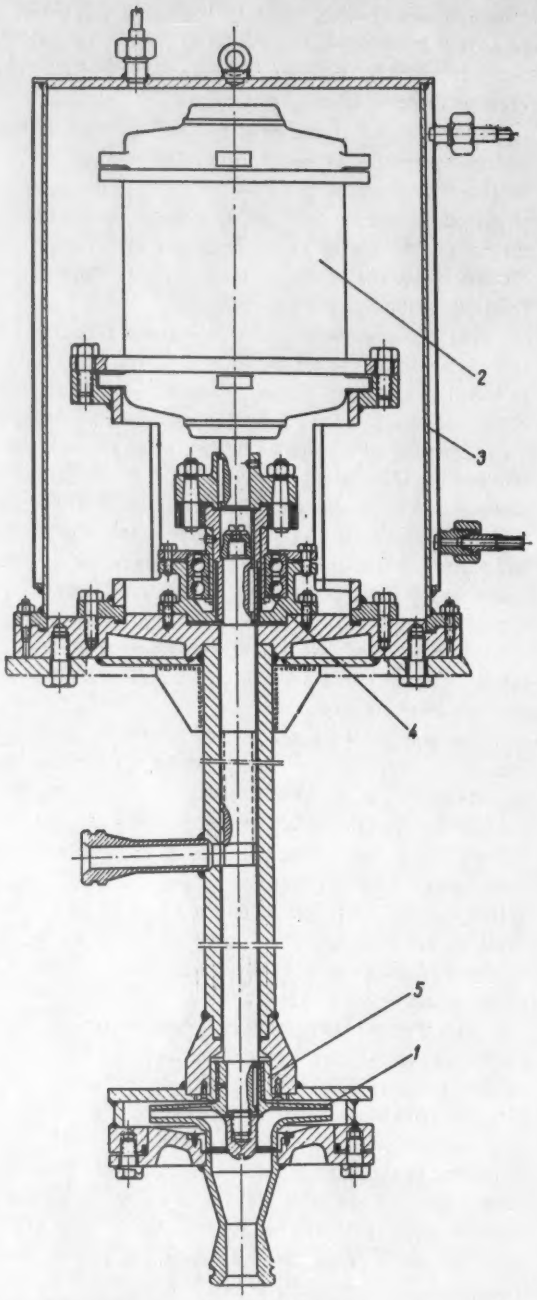

Fig. 2. Centrifugal pump with a beryllium-bronze bearing and a standard electrical motor: 1) impeller; 2) electric motor; 3) casing; 4) journal-thrust bearing; 5) sliding bearing.

flow directed upward from the housing and to take into account the complex shape of the chambers. The main shortcomings of this pump are the leakage through the seal of the housing and frequent changes of the temperature. Since at a rapid heating of the pump body the pins 8 become heated more rapidly than the nickel packing 7, the seal becomes less effective and a leakage occurs. The metal which has leaked changes in air to hydroxide which rapidly destroys the pump casing. For this reason the split seal was replaced by a welded design. The pump is started only after a prior heating of the frozen seal. When starting, first the cooling system and then the motor are switched on. A delay in starting the motor leads to a "seizure" of the shaft in the frozen seal, which makes a repeated heating necessary. If the cooling system is switched on after the pump, the liquid sodium leaks through the clearance. At the starting moment the load on the motor is usually higher than during its operating. This is explained, apparently, by the contamination of the liquid by the metal in the frozen seal during the starting period. The amount of sodium which flows out is about 1-2 g in 24 hr.

Three pumps with the frozen seal were tested. Two pumps, similar to those described above, have worked for ~ 2000 hr at temperatures of 400-500 °C and are still in operation. The seals of these two pumps are shown in Fig. 4. The third pump was tested before the other two. Its design was less satisfactory. It was dangerous to use water for cooling in this pump and, therefore, a sodium-potassium alloy was used to cool the machine. The allow was pumped through the cooling chambers by means of the electromagnetic pump and before admission was cooled in a heat exchanger. This pump was put in operation for more than 5000 hr at moderately high temperatures (400-500 °C).

We shall omit the "head-delivery" characteristic of these pumps obtained for sodium and its alloys, since they are identical with the characteristics obtained for water. On the basis of the experience obtained in the operation of the pumps described, it can be said that a pump with a frozen-sodium bearing is one of the simplest and most reliable machines as far as the pumping of sodium is concerned.

ELECTROMAGNETIC PUMPS

Among the many electromagnetic pumps known at present [1, 5-7] the most convenient for experimental operation is the ac conductive pump. These pumps require no special supply units which are, for example, needed for dc conductive pumps. In addition, they relatively easily resist temperatures of 400-600 °C, at which the use of induction pumps is practically impossible because of the absence of isolation.

The single-phase ac conductive pump (Fig. 5) takes a current of 30 amp at 220 v, and delivers up to 4 m^3/hr at a pressure of 2 kg/cm^2. The magnetic circuit of E-2 electrical steel is common to the supply transformer and the pump. PSD square wire with 4.55 mm^2 cross section was used for the primary winding, which consists of two

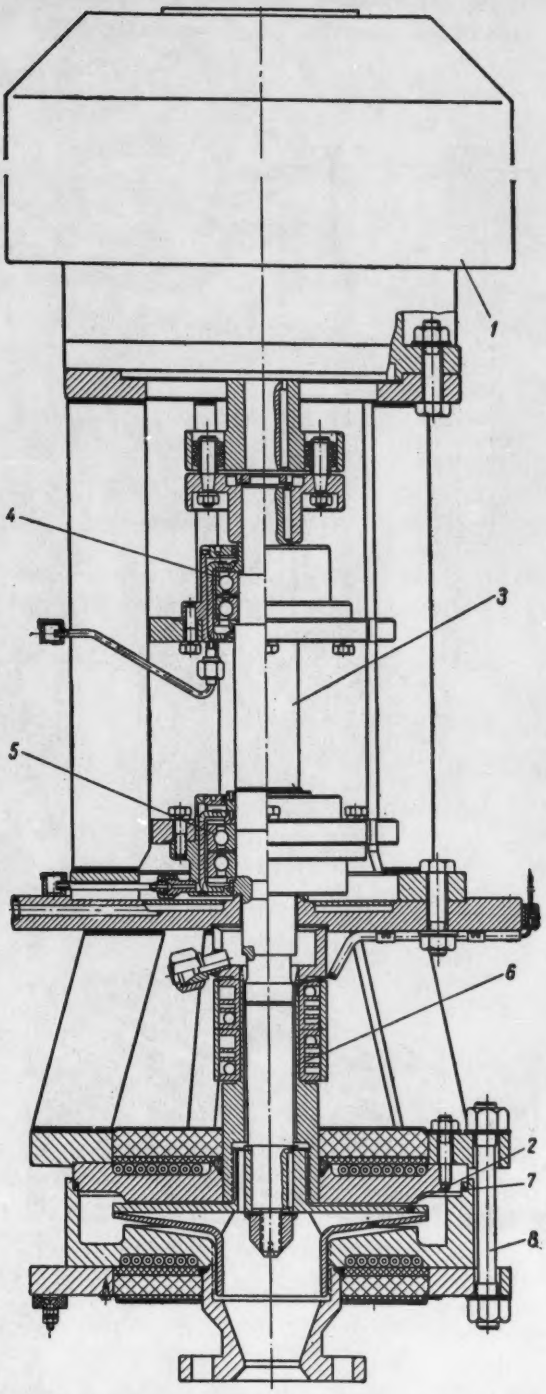

Fig. 3. Centrifugal pump with a bearing of frozen sodium: 1) electric motor; 2) impeller; 3) shaft; 4) journal-thrust bearing; 5) journal bearing; 6) bearing of frozen sodium; 7) packing; 8) pin.

coils. Each coil has 130 turns. The winding of the pump and the secondary winding of the transformer are made as a single unit from 20 x 5 mm diameter copper tubing. The tube is water cooled, which enables a greater current density and a more compact winding to be achieved. The terminals of the secondary winding are led to the electrodes of the working section, which consists of two flattened thin-walled tubes placed close to one another and connected in series. Such design of the working section makes it possible to nearly double the head produced by the pump and to compensate the reaction of the armature. The wall thickness of the tube is 0.5 mm while the material for the tubes of the working section is 1Kh18N9T steel.

The use of a common magnetic circuit, the doubling of the working section, the increased current density in the winding, etc., make possible the construction of a very compact pump. Several pumps of this type have been in operation at various plants. One pump worked for 250 hr with sodium at a temperature of 450°C, the other was in operation for more than 2500 hr on a sodium-potassium alloy at an average temperature of about 250 °C, the third pump worked for more than 3500 hr on a sodium-potassium alloy at a temperature of 40-50 °C, and the fourth for 1000 hr with sodium at a temperature of 300-400 °C. The experience obtained in the working of these pumps showed that they are simple to operate and are reliable.

The ac conductive pumps are suitable for use only at low deliveries (up to 10 m^3/hr). At higher deliveries, the use of inductive pumps with travelling magnetic fields is more advantageous. One of the pumps of this type which worked on sodium-potassium alloy is shown in Fig. 6. It consists of two flat inductors arranged above and below a channel, through which the liquid metal is pumped. The three-phase eight-pole winding of PSD wire is placed into the grooves of the inductors. Copper tubes through which water is circulated for cooling the winding are also placed into the grooves. The width of the channel is 150 mm and its height 6.1 mm in one pump, and 8.7 in the case of another. Walls are made of 1Kh18N9T steel and their thickness is 0.8 mm. Copper bars are installed in the channel on the sides of the pumps; these act as the close-circulating rings on the rotor of an asynchronous electric motor. The characteristics of the pump are given in Fig. 7 in $p = f_1(S)$ and $\eta = f_2(S)$ coordinates, where $S = 1 - Q/Q_s$ is the slip; Q is the discharge of liquid through the pump (m^3/hr); Q_s is the discharge at the metal velocity in the channel which is equal to the velocity of the field (m^3/hr); p is the pressure of the liquid (kg/cm^2); and η is the efficiency (%). This pump was working on the sodium-potassium alloy at a temperature of 150-200 °C for 300 hr. The cooling system proved unsatisfactory since it failed to provide an adequate thermal protection of the winding. In addition, the wetting of the winding, caused by the condensation of water vapors from the air, twice caused the breakdown of isolation. After some improvements this pump can be used in laboratory plants at temperatures of 200-250 °C, where a capacity of up to 30 m^3/hr is required.

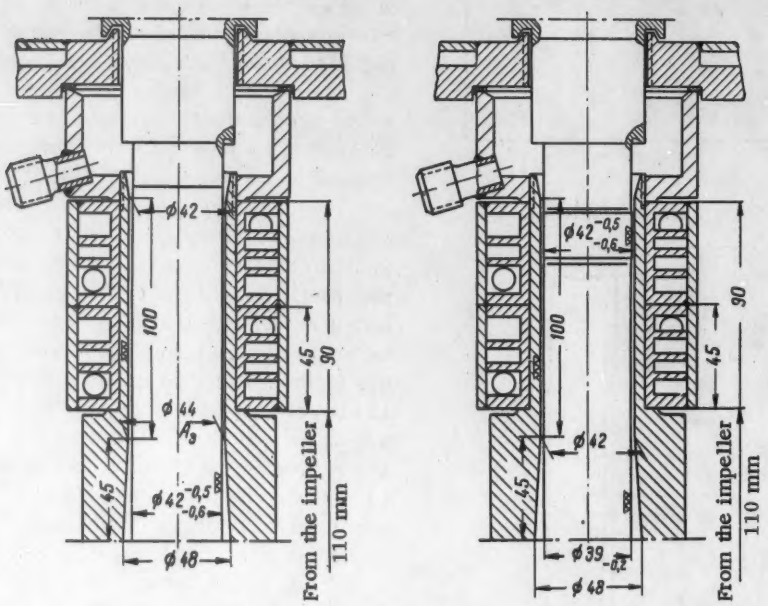

Fig. 4. Seals of frozen sodium.

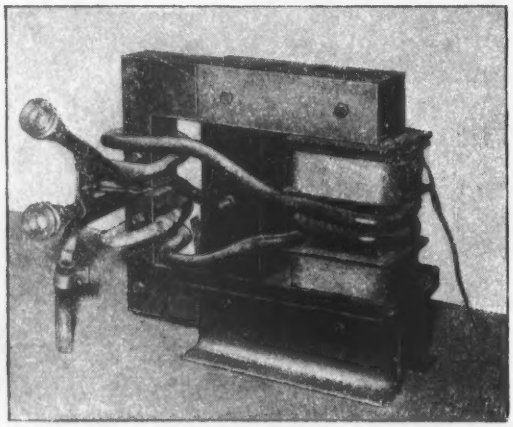

Fig. 5. Single-phase conductive electromagnetic pump.

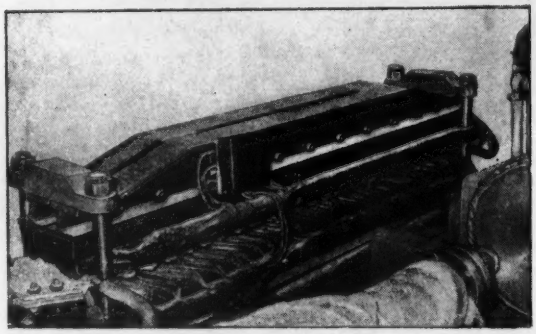

Fig. 6. Conductive electromagnetic pump.

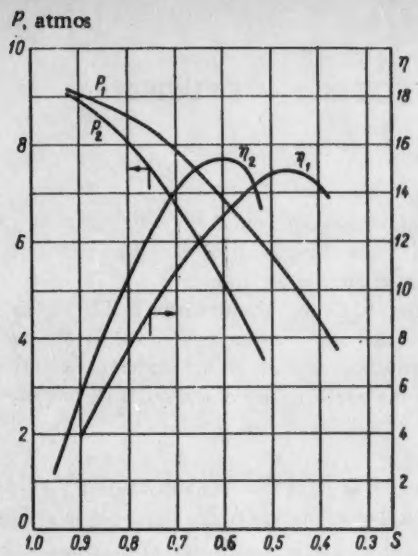

Fig. 7. Characteristics of the inductive pump.

Finally, the authors would like to emphasize the importance of the contribution of the team of designers headed by G. V. Skladnev and V. D. Rostovtsev to the development of centrifugal pumps for liquid metals. This team designed the pump illustrated in Fig. 1. The design of the pump shown in Fig. 2 is by a team headed by M. N. Ivanovskii. The designs of centrifugal pumps with frozen seal were developed by a team headed by V. I. Orlov. The ac conductive pump was designed under the guidance of N. M. Turchin. The inductive pump with the travelling magnetic field was designed and constructed by the team headed by I. A. Tyutin.

LITERATURE CITED

1. Liquid-Metal Heat Carriers [Russian translation] (ed. by A. E. Sheindlin) (IL, 1958).
2. H. Savage, Chem Eng. Progr., Symp. Ser. 50, 171 (1954).
3. P. Fortescue, J. Nuclear Energy 1, 5 (1954).
4. Voprosy Yadernoi Énergetiki No. 5, 42 (1957).
5. D. Watt, Engineering 181, 264 (1956).
6. Voprosy Yadernoi Énergetiki No. 5, 42 (1957).
7. Trudy Inst. Fiz. AN Latv SSR 8, 1956.

EFFECT OF A CYLINDRICAL CHANNEL ON NEUTRON DIFFUSION

N. I. Paletin

Original article submitted August 16, 1958

Voids in the core of a nuclear reactor have an important effect on neutron leakage from the reactor. It is important that this effect be taken into account in computing the critical mass of the reactor. It is also frequently desirable to know the effect of empty channels on the neutron distribution outside the core.

In the present paper we consider the effect of a single hollow cylindrical channel on neutron diffusion. Expressions are obtained for neutron leakage through a channel located at the center of the reactor and for the additional neutron leakage (due to the existence of the channel) in the immediate vicinity of the channel. We also consider the effect of the neutron flux distribution along a channel on the applicability of the diffusion formulas.

INTRODUCTION

The propagation of neutrons in a medium with voids depends on the number of voids per unit volume, the dimensions of the voids, and their shape.

If the distribution of neutron flux in a porous medium changes slowly in space, it may be assumed that the flux passing through any area inside the medium depends only on the gradient in the neutron distribution at a given point, that is to say, neutron diffusion theory applies. However, the coefficient of proportionality between the flux and the gradient will not be the same as in the case of a continuous medium; it will depend on the dimensions and shape of the voids and the number of voids per unit volume. The average value of this coefficient plays an important role in the effective diffusion coefficient for a porous medium. It is also obvious that any deviation from linearity in the neutron distribution will have an effect which is different than that which obtains in a continuous medium and that the criteria for the applicability of the diffusion formulas depends on the ratio between the dimensions of the void and the curvature of the neutron distribution.

The effect of voids on neutron propagation has been studied by a number of authors. For example, Behrens [1] had considered the change in neutron diffusion length in a medium with voids of arbitrary dimensions and shape for various void densities. In this work it was assumed that the voids are distributed uniformly and that the shape of the voids in such that in in a time corresponding to one mean free path the neutron does not cross the surface of the void more than twice. Using the relation $L^2/L_0^2 = \lambda^2/\lambda_0^2$, L and L_0 are the neutron diffusion lengths in the medium with voids and in the continuous medium, respectively, and λ and λ_0 are the corresponding mean free paths, this author has found an increase in the mean free path because of thepresence of voids:

$$\frac{\lambda^2}{\lambda_0^2}=\frac{L^2}{L_0^2}=1+2p+\frac{p^2\left(\frac{2a}{p\lambda}\right)}{\exp\left(\frac{2a}{p\lambda}\right)-1}+Q\frac{ap}{\lambda}. \quad (1)$$

Here p is the ratio of the void volume to the volume of matter in the unit lattice; a is the hydraulic radius of the void, given by $a=\frac{2pv}{S}$; v is the volume of matter in the unit cell; S is the surface area of the void; Q is the quantity which depends only on the shape of the void.

In the case in which the void density is low, i.e., when $s\lambda/v \ll 1$, eq. (1) assumes from the form

$$\frac{\lambda^2}{\lambda_0^2}=1+2p+\frac{ap}{\lambda}Q.$$

For some voids neutron diffusion in different directions is affected differently. For example, for a void of cylindrical shape the diffusion in the direction parallel to the cylinder axis is increased by a greater amount than in the direction perpendicular to the axis. The following expression is obtained for the direction parallel to the cylinder axis when $s\lambda/v \ll 1$ [1]:

$$\frac{\lambda_{\parallel}^2}{\lambda_0^2}=1+2p+2\frac{ap}{\lambda}. \quad (2)$$

Diffusion in a medium with cylindrical channels has also been studied by S. L. Sobolev and V. S. Fursov (1948). In this work it was assumed that the neutron density distribut on is a linear function in the direction parallel to the channel axis and constant in the direction perpendicular to the axis; a calculation was made of the additional flux in the direction parallel to the axis of the channel caused by the presence of the channel. For a single cylindrical channel of radius a, the diffusion coefficient in the parallel direction is given by the following expressions:

$$D_{\parallel}=\frac{\lambda}{3}\left[1+\frac{\pi a^2}{W}\left(1+\frac{2a}{\lambda}\right)\right]$$

(Sobolev)

$$D_{\parallel}=\frac{\lambda}{3}\left[1+\frac{\pi a^2}{W}\left(1+\frac{3\pi}{4}\frac{a}{\lambda}\right)\right] \quad (3)^{*}$$

(Fursov *)

Here W is the cross section of the unit lattice.

* The paper by V. S. Fursov contains an error and the final result differs somewhat from the formula given by Sobolev.

In all the work cited above, investigations have been made of neutron diffusion and no consideration has been given to the effect of the nonlinearity in the neutron flux distribution on leakage from the channel. The total neutron leakage from a gap has been studied for a reactor with a transverse gap [2] and the effect of this leakage on the critical mass of the reactor has been delineated. The analogous problem for a reactor with a central cylindrical channel has been solved by Davison. The results of this work are given in [3]; the "negative source" method was used in making the calculation.

The following expression is obtained for the ratio $\left(\frac{\Phi}{\partial\Phi/\partial r}\right)_{r=a}$ at the edge of the channel:

$$\left(\frac{\Phi}{\frac{\partial\Phi}{\partial r}}\right)_{r=a} = \lambda \frac{1-\frac{3}{8}(\alpha a)^2}{(\alpha a)^2\frac{a+\lambda}{a}-\frac{3\pi}{8}(\alpha a)^3}, \qquad (4)$$

where Φ is the neutron flux; a is the cylinder radius; $\alpha = \pi/H$; H is the length of the channel; $\alpha a \ll 1$.

The effect of neutron leakage through a cylindrical channel on the critical mass of a reactor has been studied in [4], but the neutron leakage has not been calculated properly.

CENTRAL CYLINDRICAL CHANNEL

We consider a central cylindrical channel of radius a in a reactor of height H (see figure). It will be assumed that the channel is thin so that the neutron flux distribution inside the reactor can be given in the form of a product $\Phi(r,z) = \Phi(z)\,\psi(r)$, where $\Phi(z)$ is of the form $\Phi(z) = \sin\alpha(z+\delta)$, and where $\alpha = \pi/H$, and δ is the extrapolated boundary.

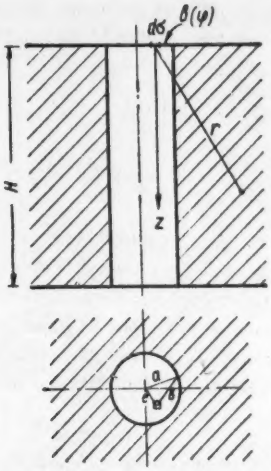

Figure for calculating the effect of a cylindrical channel on neutron difussion.

We compute the neutron leakage through one side of the channel. The neutron flux through an elementary area $d\sigma$ of the aperture in the channel, at a distance ε from the axis of the channel, is given by the expression

$$dJ = \int_0^{2\pi} d\varphi \int_{\theta_0=\operatorname{arctg}\frac{b(\varphi)}{H}}^{\pi/2} d\theta \int_{\frac{b(\varphi)}{\sin\theta}}^{\frac{H}{\cos\theta}} dr \frac{\Phi e^{-\frac{r'}{\lambda}}\cos\theta\sin\theta}{4\pi\lambda} d\sigma, \qquad (5)$$

where λ is the mean free neutron path in the material; $r' = r - b(\varphi)/\sin\theta$ gives the trajectory of the neutron in the medium; $b(\varphi) = e\cos\varphi + \sqrt{a^2 - e^2\sin^2\varphi}$. Since the channel is at the center of the reactor, we can write $\psi(r) = \text{const} = 1$ with reasonable accuracy. Expanding $\Phi(z)$ in a Maclaurin series and substituting in (5), we have

$$dJ = \int_0^{2\pi} d\varphi \int_{\theta_0}^{\pi/2} d\theta \int_{\frac{b}{\sin\theta}}^{\frac{H}{\cos\theta}} dr \sum_{n=0}^{\infty}(-1)^n\left[\frac{\Phi_0 z^{2n}}{(2n)!} + \frac{\Phi_1 z^{2n+1}}{(2n+1)!}\right]\frac{\alpha^{2n}e^{-\frac{r'}{\lambda}}\cos\theta\sin\theta}{4\pi\lambda} d\sigma,$$

where $\Phi_0 = \Phi(0) = \sin\alpha\delta$ and $\Phi_1 = \left.\frac{\partial\Phi(z)}{\partial z}\right|_{z=0} = \alpha\cos\alpha\delta$.

Now, converting from the variable r to r' we have

$$dJ = \int_0^{2\pi} d\varphi \int_{\theta_0}^{\pi/2} d\theta \int_0^{\frac{H}{\cos\theta}-\frac{b}{\sin\theta}} dr' \sum_{n=0}^{\infty}(-\alpha^2)^n \times \left[\frac{\Phi_0\left(r'+\frac{b}{\sin\theta}\right)^{2n}\cos^{2n}\theta}{(2n)!} + \frac{\Phi_1\left(r'+\frac{b}{\sin\theta}\right)^{2n+1}\cos^{2n+1}\theta}{(2n+1)!}\right] e^{-\frac{r'}{\lambda}}\frac{\cos\theta\sin\theta}{4\pi\lambda} d\sigma. \qquad (6)$$

It is convenient to remove the term with $n = 0$ from the summation in the last expression. Obviously this term gives the neutron flux for a channel in a plate of thickness H for a linear variation of flux along the channel axis. We write the expression for the neutron flux in the form

$$\left.\begin{aligned} dJ_0 = {} & \int_0^{2\pi}\int_0^{\pi/2}\int_0^{\infty}(\Phi_0+\Phi_1 r'\cos\theta)\frac{e^{-\frac{r'}{\lambda}}}{4\pi\lambda}\times \\ & \times\sin\theta\cos\theta\, dr'd\theta\, d\varphi + \int_0^{2\pi}\int_0^{\pi/2}\int_0^{\infty}\Phi_1 b\cos^2\theta\times \\ & \times\frac{e^{-\frac{r'}{\lambda}}}{4\pi\lambda} dr'd\theta\, d\varphi - \int_0^{2\pi}\int_0^{\theta_0}\int_0^{\infty}\times \end{aligned}\right\} \qquad (7\,a)$$

$$\left.\begin{aligned}&\times\left[\Phi_0+\Phi_1\cos\theta\left(r'+\frac{b}{\sin\theta}\right)\right]\frac{e^{-\frac{r'}{\lambda}}}{4\pi\lambda}\times\\&\times\cos\theta\sin\theta\,dr'd\theta\,d\varphi+\int_0^{2\pi}\int_{\theta_0}^{\pi/2}\int_{\frac{b}{\sin\theta}}^{\frac{H}{\cos\theta}}\times\\&\times\left[\Phi_0+\Phi_1\cos\theta\left(r'+\frac{b}{\sin\theta}\right)\right]\frac{e^{-\frac{r'}{\lambda}}}{4\pi\lambda}\times\\&\times\cos\theta\sin\theta\,dr'd\theta\,d\varphi.\end{aligned}\right\}\quad(7\text{ b})$$

The first integral in the right side of (7) determines the diffusion flux in the absence of a channel $(\Phi_0/4)+(\lambda/6)\Phi_0$; the second represents the additional flux due to a channel in an infinite medium; the remaining terms are corrections for the fact that the medium is finite. We denote these integrals by Y_0, Y_1, Y_2, and Y_3, respectively.

Carrying out the integration for r' and θ we have

$$Y_1=\frac{\Phi_1}{16}\int_0^{2\pi}b(\varphi)\,d\varphi,$$

$$Y_2=\frac{\Phi_1}{4\pi}\int_0^{2\pi}\frac{b^2(\varphi)}{H}\,d\varphi+0\left(\frac{b^2}{H^2}\right),$$

$$Y_3=0\left(\frac{\lambda^2}{H^2}\right).$$

Whence, to second order in b/H and λ/H we have

$$dJ_0=\frac{\Phi_0}{4}+\frac{\lambda}{6}\Phi_0+\frac{\Phi_1}{16}\int_0^{2\pi}b(\varphi)\,d\varphi-\frac{\Phi_1}{4\pi H}\int_0^{2\pi}\times\times b^2(\varphi)\,d\varphi.\quad(7')$$

The total neutron leakage through the channel is

$$J_0=\int_0^a dJ_0\,2\pi e\,de.$$

Noting that $\int_0^{2\pi}d\varphi\int_0^a 2\pi e\,de\,b(e,\varphi)=\frac{16}{3}\pi a^2 a$,

$$\int_0^{2\pi}\int_0^a b^2 2\pi e\,de\,d\varphi=2\pi^2a^4\text{†},$$

we have

$$J_0=\pi a^2\left[\frac{\Phi_0}{4}+\frac{\lambda}{6}\Phi_1+\frac{\lambda}{3}\Phi_1\frac{a}{\lambda}-\frac{\lambda}{3}\Phi_1\frac{3}{2}\frac{a}{\lambda}\frac{a}{H}\right].\quad(8)$$

We now compute the contribution due to terms characterized by $n\geq 1$ in (6):

$$dJ_1=\int_0^{2\pi}\int_{\theta_0}^{\pi/2}\int_{\frac{b}{\sin\theta}}^{\frac{H}{\cos\theta}}\times$$

$$\times\left\{\sum_{n=1}^{\infty}(-\alpha^2)^n\left[\frac{\Phi_0\cos^{2n}\theta\left(r'+\frac{b}{\sin\theta}\right)^{2n}}{(2n)!}+\right.\right.$$

$$\left.+\frac{\Phi_1\cos^{2n+1}\theta\left(r'+\frac{b}{\sin\theta}\right)^{2n+1}}{(2n+1)!}\right]\times$$

$$\left.\times\frac{e^{-\frac{r'}{\lambda}}}{4\pi\lambda}\cos\theta\sin\theta\right\}dr'\,d\theta\,d\varphi=$$

$$=\Phi_1\int_0^{2\pi}\left[\frac{b^2}{H}\sum_{n=1}^{\infty}(-1)^n\frac{\pi^{2n}}{(2n-1)(2n+1)!}+\right.$$

$$\left.+0\left(\frac{\Phi_0}{\Phi_1}\frac{b^2}{H^2}\ln\frac{b}{H}\right)+0\left(\frac{\lambda^2}{H^2}\right)\right]d\varphi\simeq$$

$$\simeq\frac{\Phi_1}{4\pi H}\left[\frac{1}{2}-\frac{\pi^2}{4}-\frac{\pi}{2}\,\mathrm{Si}(\pi)\right]\int_0^{2\pi}b^2(\varphi)\,d\varphi=$$

$$=\frac{\Phi_1a^2}{2H}\left[\frac{1}{2}-\frac{\pi^2}{4}-\frac{\pi}{2}\,\mathrm{Si}(\pi)\right],$$

where $\mathrm{Si}(\pi)=\int_0^{\pi}\frac{\sin y}{y}\,dy$.

Integrating over the cross-sectional area of the channel we have

$$J_1=\int_0^a 2\pi e\,de\,dJ_1=$$

$$=\pi a^2\frac{\Phi_1a^2}{2H}\left[\frac{1}{2}-\frac{\pi^2}{4}-\frac{\pi}{2}\,\mathrm{Si}(\pi)\right];\quad(9)$$

then the total leakage of neutrons through the channel for a sinusoidal variation of flux along the channel axis is given by the expression

$$J=J_0+J_1=\pi a^2\left[\frac{\Phi_0}{4}+\frac{\lambda}{6}\Phi_1+\frac{\lambda}{6}\Phi_1\frac{2a}{\lambda}-\right.$$

$$\left.-\frac{\lambda}{6}\Phi_1\frac{a}{\lambda}\frac{a}{H}\left(\frac{3\pi^2}{4}-\frac{3}{2}+\frac{3\pi}{2}\,\mathrm{Si}(\pi)\right)\right].\quad(10)$$

In addition to the neutron leakage through the channel, the presence of the channel causes an additional leakage of neutrons through surfaces which are close to the aperture of the channel. The neutron flux through an elementary area located at the surface of the reactor close to the channel aperture, at a distance ρ from the channel axis, is

$$J_1=\int_v\frac{\Phi(\rho,z)\,e^{-\frac{r'}{\lambda}}\cos\theta\,dV}{4\pi\lambda r^2},$$

† $\int_0^{2\pi}b^2(\varphi)\,d\varphi=2\pi a^2$ and is independent of e.

where r' gives the neutron trajectory in the material. The integration is taken over the volume of the reactor, neglecting the channel volume.

It can be shown that in the diffusion approximation this integral is

$$J_+ = \int_0^{2\pi}\int_0^{\pi/2}\int_0^{\infty} \frac{(\Phi_0+\Phi_1 r'\cos\theta)}{4\pi\lambda} e^{-\frac{r'}{\lambda}} \cos\theta\sin\theta\, dr' \times$$

$$\times\, d\theta\, d\varphi + \int_{-\arcsin\frac{a}{\rho}}^{+\arcsin\frac{a}{\rho}} d\varphi \int_0^{\pi/2} d\theta \int_{\frac{\rho\cos\varphi-\sqrt{a^2-\rho^2\sin^2\varphi}}{\sin\theta}}^{\infty} dr'\,\Phi_1 \times$$

$$\times \frac{\sqrt{a^2-\rho^2\sin^2\varphi}}{2\pi\lambda} e^{-\frac{r'}{\lambda}} \cos^2\theta. \qquad (11)$$

Corrections for the finite dimensions of the channel and the nonlinearity in the neutron flux distribution along the axis of the channel are of second order and higher in a/H and λ/H.

It is apparent that the first term on the right side of (11) is the diffusion flux in the absence of the channel $(\Phi_0/4)+(\lambda/6)\Phi_1$, while the second additional leakage through the area dσ due to the presence of the channel. The additional leakage of neutrons through the surface of the reactor close to the aperture of the channel is given by the following integral:

$$\Delta L_{ch} = \int_a^{\infty} 2\pi\rho\, d\rho \left[\int_{-\arcsin\frac{a}{\rho}}^{+\arcsin\frac{a}{\rho}} \int_0^{\pi/2} d\theta \times \right.$$

$$\left. \times \int_{\frac{\rho\cos\varphi-\sqrt{a^2-\rho^2\sin^2\varphi}}{\sin\theta}}^{\infty} dr'\,\Phi_1 \frac{\sqrt{a^2-\rho^2\sin^2\varphi}}{2\pi\lambda} e^{-\frac{r'}{\lambda}} \cos^2\theta \right].$$

The integration over ρ can be taken to infinity since the integrand falls off rapidly with increasing ρ. Carrying out the integration with respect to r' and converting from the variables ρ and φ to the variables $\sigma = \sqrt{a^2-\rho^2\sin^2\varphi}$ and $\tau = \rho\cos\varphi - \sqrt{a^2-\rho^2\sin^2\varphi}$, we have

$$\Delta L_{ch} = 2\int_0^{\infty} d\tau \int_0^{a} d\sigma \frac{\Phi_1\sigma^2}{\sqrt{a^2-\sigma^2}} \times$$

$$\times \int_0^{\pi/2} e^{-\frac{\tau}{\lambda\sin\theta}} \cos^2\theta\, d\theta = \frac{\lambda}{6}\pi a^2\Phi_1. \qquad (12)$$

In all the calculations carried out above we have assumed that the transverse distribution of neutron density is uniform close to the channel, neglecting the variation due to leakage of neutrons through the channel. We now estimate the error introduced by this assumption.

We consider an elementary area dσ at the point P on the inner surface of the channel. The neutron flux striking this area in the channel is

$$J_+ d\sigma = \int_v \frac{\Phi e^{-\frac{r}{\lambda}} \cos\theta\, dV}{4\pi\lambda r^2} d\sigma. \qquad (13)$$

(It is assumed that the polar axis is normal to the area.)

We limit outselves to the first terms in the expansion of Φ(ρ, z) in the Maclaurin series and carry out the integration over r in (13), thus obtaining the neutron angular distribution for neutrons which enter the channel through the area dσ:

$$F(P,\ \theta,\ \psi)\, d\theta\, d\psi = \frac{\sin\theta\cos\theta}{4\pi}\left\{\Phi(P) + \right.$$

$$\left. + \lambda\cos\theta\left(\frac{\partial\Phi}{\partial r}\right)_P + \lambda\sin\theta\cos\psi\left(\frac{\partial\Phi}{\partial z}\right)_P\right\},$$

where ψ is the angle formed by the radium vector r with respect to the channel axis. Carrying out the remaining integration in (13) we obtain the well-known result

$$J_+ = \frac{\Phi(P)}{4} + \frac{\lambda}{6}\left(\frac{\partial\Phi}{\partial r}\right)_P.$$

The neutron flux J_(P), which strikes the elementary area dσ from the channel side is

$$J_-(P) = \int \frac{F(P',\ \theta,\ \psi)}{\sin\theta} \frac{\cos\theta}{r^2} d\sigma =$$

$$= J_1\Phi + J_2\frac{\partial\Phi}{\partial\rho} + J_3\Phi,$$

where:

$$J_1 = \frac{a^3}{2\pi}\left\{\int_{-\frac{H}{2}}^{+\frac{H}{2}} \cos\alpha k\, dk \int_0^{\pi} \frac{(1-\cos\beta)^2 d\beta}{[k^2+2a^2(1-\cos\beta)]^2} + \int_{\frac{H}{2}}^{\frac{H}{2}+z} \cos\alpha k\, dk \int_0^{\pi} \frac{(1-\cos\beta)^2 d\beta}{[k^2+2a^2(1-\cos\beta)]^2} - \right.$$

$$- \int_{\frac{H}{2}-z}^{\frac{H}{2}} \cos\alpha k\, dk \int_0^{\pi} \frac{(1-\cos\beta)^2 d\beta}{[k^2+2a^2(1-\cos\beta)]^2} + \operatorname{tg}\alpha z \left[\int_{\frac{H}{2}}^{\frac{H}{2}+z} \sin\alpha k\, dk \int_0^{\pi} \frac{(1-\cos\beta)^2 d\beta}{[k^2+2a^2(1-\cos\beta)]^2} + \right.$$

$$\left.\left. + \int_{\frac{H}{2}-z}^{\frac{H}{2}} \sin\alpha k\, dk \int_0^{\pi} \frac{(1-\cos\beta)^2 d\beta}{[k^2+2a^2(1-\cos\beta)]^2}\right]\right\},$$

$$J_2=\lambda\frac{a^4}{2\pi}\left\{\int\limits_{-\frac{H}{2}}^{\frac{H}{2}}\cos\alpha k\,dk\int\limits_0^{\pi}\frac{(1-\cos\beta)^2\,d\beta}{[k^2+2a^2(1-\cos\beta)]^{5/2}}+\int\limits_{\frac{H}{2}}^{\frac{H}{2}+z}\cos\alpha k\,dk\int\limits_0^{\pi}\frac{(1-\cos\beta)^2\,d\beta}{[k^2+2a^2(1-\cos\beta)]^{5/2}}-\right.$$

$$-\int\limits_{\frac{H}{2}-z}^{\frac{H}{2}}\cos\alpha k\,dk\int\limits_0^{\pi}\frac{(1-\cos\beta)^2\,d\beta}{[k^2+2a^2(1-\cos\beta)]^{5/2}}+\operatorname{tg}\alpha z\left[\int\limits_{\frac{H}{2}}^{\frac{H}{2}+z}\sin\alpha k\,dk\int\limits_0^{\pi}\frac{(1-\cos\beta)^2\,d\beta}{[k^2+2a^2(1-\cos\beta)]^{5/2}}+\right.$$

$$\left.\left.+\int\limits_{\frac{H}{2}-z}^{\frac{H}{2}}\sin\alpha k\,dk\int\limits_0^{\pi}\frac{(1-\cos\beta)^2\,d\beta}{[k^2+2a^2(1-\cos\beta)]^{5/2}}\right]\right\}.$$

$$J_3=\lambda\frac{a^2}{2\pi}\left\{\int\limits_{-\frac{H}{2}}^{\frac{H}{2}}[-\alpha\sin\alpha k]\,k\,dk\int\limits_0^{\pi}\frac{(1-\cos\beta)^2\,d\beta}{[k^2+2a^2(1-\cos\beta)]^{5/2}}+\right.$$

$$+\int\limits_{\frac{H}{2}}^{\frac{H}{2}+z}[-\alpha\sin\alpha k]\,k\,dk\int\limits_0^{\pi}\frac{(1-\cos\beta)^2\,d\beta}{[k^2+2a^2(1-\cos\beta)]^{5/2}}-\int\limits_{\frac{H}{2}-z}^{\frac{H}{2}}[-\alpha\sin\alpha k]\times$$

$$\times\int\limits_0^{\pi}\frac{(1-\cos\beta)^2\,d\beta}{[k^2+2a^2(1-\cos\beta)]^{5/2}}-\operatorname{tg}\alpha z\left[\int\limits_{\frac{H}{2}}^{\frac{H}{2}+z}(-\alpha k)\cos\alpha k\,dk\times\right.$$

$$\left.\left.\times\int\limits_0^{\pi}\frac{(1-\cos\beta)^2\,d\beta}{[k^2+2a^2(1-\cos\beta)]^{5/2}}+\int\limits_{\frac{H}{2}-z}^{\frac{H}{2}}(-\alpha k)\cos\alpha k\,dk\int\limits_0^{\pi}\frac{(1-\cos\beta)^2\,d\beta}{[k^2+2a^2(1-\cos\beta)]^{5/2}}\right]\right\}.$$

Here β is the angle between the plane which passes through the channel axis and the point P, and the plane which passes through the channel axis and the point P'.

The resulting neutron flux in the channel through the area $d\sigma$ is

$$J_+-J_-=\frac{\Phi}{4}[1-4J_1-4J_3]+$$
$$+\frac{\lambda\partial\Phi}{6\partial\rho}\left(1-\frac{6}{\lambda}J_2\right).$$

In the diffusion approximation this flux is $\frac{\lambda}{3}\left(\frac{\partial\Phi}{\partial\rho}\right)_{\rho=a}$.

Whence $\left(\frac{\partial\Phi/\partial r}{\Phi}\right)_{\rho=a}=\frac{\frac{1}{4}-J_1-J_3}{\frac{\lambda}{6}+J_2}$.

Computing the mean values of the integrals J_1, J_2, and J_3 we have

$$\left(\frac{\partial\Phi/\partial\rho}{\Phi}\right)_{\rho=a}\approx\frac{(\alpha a)^2}{\lambda}\left(1+\frac{\lambda}{a}\right).$$

Because (5) is nonlinear, the neglect of the variation in the transverse distribution of neutron density results in an error:

$$\lambda\left(\frac{\partial\Phi/\partial\rho}{\Phi}\right)_{\rho=a}\simeq(\alpha a)^2\left(1+\frac{\lambda}{a}\right)\simeq\left(\frac{a}{H}\right)^2.$$

DISCUSSION OF THE RESULTS

In order to compare the results which have been obtained with the results obtained by other authors we imagine a cylindrical channel in the unit lattice cell of the system in which the cross section of the cell W is much larger than the cross section of the channel πa^2. We will compare the leakage of neutrons through the face of the cell, assuming that the neutron distribution in the directions perpendicular to the channel axis is uniform.

In the work carried out by Behrens, Sobolev, and Fursov it has been indicated that the only effect of the channel is to change the diffusion characteristics of the medium and that leakage from the cell can be expressed by the difussion formula

$$L_{\text{lat}}=-D_{\parallel}\left(\frac{\partial\Phi}{\partial z}\right)_{\text{edge}}W,$$

where $D_{\parallel}=L^2_{\parallel}\Sigma'_a$ is the diffusion coefficient; $\Sigma'_a=\Sigma_a(1-\pi a^2/W)$ is the effective cross section for neutron absorption for the medium with the channel; Σ_a is the macroscopic absorption cross section in the continuous medium.

Using this expression and (2), we find

$$D_{\parallel}=\frac{\lambda}{3}\left[1+\frac{\pi a^2}{W}\left(1+2\frac{a}{\lambda}\right)\right]$$

and

$$L_{\text{lat}}=-\frac{\lambda}{3}\left(\frac{\partial\Phi}{\partial z}\right)_{\text{edge}} W\left[1+\frac{\pi a^2}{W}\left(1+2\frac{a}{\lambda}\right)\right]. \tag{14}$$

This same result has been obtained by Sobolev.

Using (10) and (12), the neutron leakage is found to be

$$L_{\text{lat}}=\left(\frac{\Phi_0}{4}-\frac{\lambda}{6}\frac{\partial\Phi}{\partial z}\right)(W-\pi a^2)-$$
$$-\frac{\lambda}{6}\frac{\partial\Phi}{\partial z}\pi a^2\left[2+2\frac{a}{\lambda}-C\frac{a}{\lambda}\frac{a}{H}\right]+\frac{\Phi_0}{4}\pi a^2=$$
$$=\frac{\Phi_0}{4}W-\frac{\lambda}{6}W\left(\frac{\partial\Phi}{\partial z}\right)_{\text{edge}}\times$$
$$\times\left[1+\frac{\pi a^2}{W}\left(1+2\frac{a}{\lambda}-C\frac{a}{\lambda}\frac{a}{H}\right)\right],$$
$$C=\frac{3\pi^2}{4}-\frac{3}{2}+\frac{3\pi}{2}\operatorname{Si}(\pi).$$

Making use of the fact that the back flux of neutrons must vanish at the edge of the medium, we have

$$L_{\text{lat}}=-\frac{\lambda}{3}\left(\frac{\partial\Phi}{\partial z}\right)_{\text{edge}}\times$$
$$\times W\left[1+\frac{\pi a^2}{W}\left(1+2\frac{a}{\lambda}-C\frac{a}{\lambda}\frac{a}{H}\right)\right]. \tag{15}$$

Equation (15) differs from the formulas given above by the term $\sim a/H$, which takes account of the finite dimensions of the medium and the nonlinearity in the distribution of neutron flux.

If the leakage through one side of the channel is computed by means of (4), taken from [3], the following result is obtained:

$$L_{\text{ch}}=-\frac{\lambda}{3}\left(\frac{\partial\Phi}{\partial z}\right)_{\text{edge}}\pi a^2\left|2+2\frac{a}{\lambda}-\frac{3\pi^2}{4}\frac{a}{\lambda}\frac{a}{H}\right|.$$

If the "negative-source" technique is used for the calculation, the neutron leakage in the vicinity of the channel does not vary, so that the leakage from the lattice cell is

$$L_{\text{lat}}=-\frac{\lambda}{3}\left(\frac{\partial\Phi}{\partial z}\right)_{\text{edge}}\times$$
$$\times W\left[1+\frac{\pi a^2}{W}\left(1+2\frac{a}{\lambda}-\frac{3\pi^2}{4}\frac{a}{\lambda}\frac{a}{H}\right)\right]. \tag{16}$$

To terms of order $\sim a/H$ this formula coincides with all those given above and the coefficient for the a/H term is very similar to the corresponding coefficient in (15). Thus, in [3] the additional leakage near the channel is taken as the equivalent of additional leakage from the channel. In this form the result is convenient for calculating the effect of the channel on the critical mass. We can solve the reactor equation in the diffusion approximation, assuming as the boundary condition at the walls of the channel that

$$\left(\frac{\Phi}{\frac{\partial\Phi}{\partial r}}\right)_{r=a}\simeq\frac{\lambda}{(aa)^2\frac{a+\lambda}{a}-\frac{3\pi}{8}(aa)^3}$$

and keeping the boundary conditions the same at the surface of the reactor; on the other hand, if we separate the leakage through the channel and the leakage near the channel, the boundary conditions for the function Φ become much more complicated. Expressions for the correction to the critical mass due to the presence of the channel are given in [3].

It will be apparent from the analysis given above that taking account of the finite dimensions of the medium and the deviation in the neutron density distribution from linearity results in a correction term $\sim a/H$; if we can neglect this term in studying the distribution of neutrons in a medium with a channel it is possible to use the diffusion analysis if the diffusion characteristics are modified appropiately.

It can be shown that all the formulas given above apply not only for a uniform transverse neutron density distribution but also for the case in which this distribution varies in linear fashion. If there is a change in the transverse distribution of the current density from linearity the following error appears:

$$\eta\approx\frac{(\lambda+a)^2}{2}\frac{\partial^2\Phi}{\partial x^2}\frac{1}{\Phi}.$$

For $\Phi(x)=\cos\alpha_{\perp}x\quad|\eta|\approx\frac{(\lambda+a)^2\alpha_{\perp}^2}{2}.$

For $\Phi(x)=e^{\frac{x}{L_{\perp}}}\quad|\eta|\approx\frac{(\lambda+a)^2}{2L_{\perp}^2}.$

CYLINDRICAL CHANNEL WITH EXPONENTIAL LONGITUDINAL VARIATION OF NEUTRON FLUX

We have established, based on channel dimensions, criteria for using neutron diffusion theory. However, there is still another important aspect of the problem. Up to this point we have assumed that the neutron flux along the length of the channel is linear of sinusoidal. In this case the neutron flux through any cross section of the channel is determined by the regions close to this cross section, since the contribution from remote regions falls off as the third power of the distance from this cross section to the remote regions. If, however, the neutron flux along the length of the channel varies as z^3 or faster, these regions may become important and the difussion equation may no longer apply. We now analyze a case which is of practical importance, a cylindrical channel with an exponential longitudinal distribution.

In a continuous medium with an exponential flux function exp z/L, the condition $\lambda \ll L$ must be satisfied for the diffusion formulas to be valid (weak absorption). We now investigate this problem as it applies to the diffusion formulas in the case of a medium with a channel.

We calculate the neutron flux J through a cross section a a channel in a plate of thickness H with an exponential variation of flux over the plate thickness $\Phi(z) = \Phi_0 \exp z/L$. The distance from a cross section to the end of the channel in the direction of increasing flux is denoted by h.

The neutron flux through an elementary area of the channel cross section located at a distance e from the channel axis is $dJ = dJ_+ - dJ_-$, where

$$\left.\begin{aligned} dJ_+ &= \int_0^{2\pi} d\varphi \int_{\theta_0}^{\pi/2} d\theta \int_{\frac{b}{\sin\theta}}^{\frac{h}{\cos\theta}} dr \times \\ &\times \frac{\Phi_0 e^{\frac{r\cos\theta}{L} - \frac{r'}{\lambda}}}{4\pi\lambda} \cos\theta \sin\theta; \\ dJ_- &= \int_0^{2\pi} d\varphi \int_{\pi/2}^{\pi-\theta_1} d\theta \int_{\frac{b}{\sin\theta}}^{\frac{H-h}{\cos\theta}} dr \times \\ &\times \frac{\Phi_0 e^{\frac{r\cos\theta}{L} - \frac{r'}{\lambda}}}{4\pi\lambda} \cos\theta \sin\theta; \end{aligned}\right\} \qquad (17)$$

$$\theta_1 = \operatorname{arctg} \frac{b}{H-h}.$$

The remaining notation is the same as that used above. Expanding the function $\Phi(z)$ in powers of z/L we have

$$\Phi(z) = \Phi_0 \sum_{n=0}^{\infty} \left(\frac{r\cos\theta}{L}\right)^n \frac{1}{n!}.$$

The contribution in the integrals of (17) due to terms in the summation with $n = 0$ and $n = 1$ is given by (7') where in place of Φ we substitute Φ_0/L. If this part of the flux is denoted by dJ_0, we have

$$J_0 = \int_0^a dJ_0 2\pi e\, de = -\frac{\lambda\Phi_0}{3L} \times$$
$$\times \left[1 + 2\frac{a}{\lambda} - \frac{3}{2}\frac{a}{\lambda}\frac{a}{h} - \frac{3}{2}\frac{a}{\lambda}\frac{a}{H-h}\right] \pi a^2.$$

The contribution due to the remaining terms in the summation is

$$dJ_1 = \int_0^{2\pi} d\varphi \int_{\theta_0}^{\pi/2} d\theta \int_{\frac{b}{\sin\theta}}^{\frac{h}{\cos\theta}} dr \times$$
$$\times \frac{\Phi_0 \sum_{n=2}^{\infty} \frac{1}{n!}\left(\frac{r\cos\theta}{L}\right)^n e^{-\frac{r'}{\lambda}}}{4\pi\lambda} \sin\theta\cos\theta -$$
$$- \int_0^{2\pi} d\varphi \int_{\pi/2}^{\pi-\theta_1} d\theta \int_{\frac{b}{\sin\theta}}^{\frac{H-h}{\cos\theta}} dr \times$$
$$\times \frac{\Phi_0 \sum_{n=2}^{\infty} \frac{1}{n!}\left(\frac{r\cos\theta}{L}\right)^n e^{-\frac{r'}{\lambda}}}{4\pi\lambda} \sin\theta\cos\theta.$$

In the second term on the right, under the integral sign we convert from the variable θ to $\vartheta = \pi - \theta$ and in both terms we convert from the variable r to $r' = r - b/\sin\theta$. Then, carrying out the integration and limiting ourselves to second-order terms in a/h, λ/h, a/(H − h), and λ (H − h), we have

$$J_1 = \int_0^a dJ_1 2\pi e\, de =$$
$$= -\frac{\Phi_0\lambda}{3L}\left\{\frac{3}{4}\frac{a}{\lambda}\frac{aL}{h^2} - \frac{3}{4}\frac{a}{\lambda}\frac{aL}{(H-h)^2} + \frac{3}{2}\frac{a}{\lambda}\frac{a}{h} + \right.$$
$$+ \frac{3}{2}\frac{a}{\lambda}\frac{a}{H-h} + \frac{3}{4}\frac{a}{\lambda}\frac{a}{L}\left[Z\left(\frac{h}{L}\right) - \right.$$
$$\left.\left. - Z\left(-\frac{H-h}{L}\right)\right]\right\} \pi a^2,$$

where

$$Z(y) = \int_{-\infty}^{y} \frac{e^t}{t}\, dt - \frac{e^y}{y} - \frac{e^y}{y^2}.$$

Adding J_0 and J_1 and noting that $\Phi_0/L = (\partial\Phi/\partial z)_{z=0}$, we have

$$J = -\frac{\lambda}{3}\frac{\partial\Phi}{\partial z}\left\{1 + 2\frac{a}{\lambda} + \frac{3}{4}\frac{a}{\lambda}\frac{aL}{h^2} - \right.$$
$$- \frac{3}{4}\frac{a}{\lambda}\frac{aL}{(H-h)^2} + \frac{3}{4}\frac{a}{\lambda}\frac{a}{L}\left[Z\left(\frac{h}{L}\right) - \right.$$
$$\left.\left. - Z\left(-\frac{H-h}{L}\right)\right]\right\} \pi a^2.$$

It can be shown that the additional neutron flux in the neighborhood of the channel is

$$\mathcal{J} = -\frac{\lambda}{3}\frac{\partial\Phi}{\partial z}\pi a^2 + 0\left(\frac{a^2L^2}{h^4} e^{\frac{h}{L}}\right).$$

In order to obtain agreement with the formulas obtained by Behrens and Sobolev, the following conditions must be satisfied:

$$\frac{a}{h} \ll 1, \quad \frac{a}{H-h} \ll 1 \quad \text{и} \quad \frac{a}{L} Z\left(\frac{h}{L}\right) \ll 1.$$

For large values of h/L, $Z\left(\frac{h}{L}\right) \approx \frac{2e^{\frac{h}{L}}}{\left(\frac{h}{L}\right)^3}$ and the last condition becomes $\frac{aL^2}{h^3} e^{\frac{h}{L}} \ll 1$.

In conclusion the author wishes to thank P. E. Stepanov for valuable discussions of the problems considered here.

LITERATURE CITED

1. D. Behrens, Proc. Phys. Soc. 62A 607 (1949).
2. J. Chernick and J. Kaplan, J. Nuclear Energy 2, 41 (1955).
3. Peshkhagen, Proceedings of the International Conference on the Peaceful Uses of Atomic Energy, Geneva (1955) [in Russian] (Izd ANSSSR, 1958) 5 p. 309.
4. E. Critoph and R. Pearce, J. Nuclear Energy 4, 455 (1957).

DETERMINATION OF CRITICAL MASS AND NEUTRON FLUX DISTRIBUTION BY MEANS OF PHYSICAL MODELS

V. A. Dmitrievskii and I. S. Grigorev

Original article submitted November 18, 1958

The design of nuclear reactors, especially new reactors, requires experimental measurements in order to obtain accurate values of the pertinent parameters. In the present paper we present a new method for the preliminary determination of the critical mass of a reactor and the neutron flux distribution; this method is based on the use of physical models. In carrying out these experiments use is made of a model of the reactor which does not contain fissionable material. The "working" channels in the model are filled with a neutron absorber whose cross section simulates the absorption cross section for neutrons in the fissionable material. The production of fast fission neutrons is simulated by means of a neutron source which is moved along the channels. The distribution of thermal neutrons is measured by means of detectors which are sensitive to thermal neutrons. If the source strength and the absolute value of the neutron flux are known, it is possible to find the critical mass of the reactor.

This method has been checked in a reactor with uranium hexafluoride. The value of the critical mass found experimentally was found to be in good agreement with the value obtained when the reactor was started up.

The proposed method can also be useful in preliminary investigations of reactor designs, the choice of optimum lattice parameters, etc. The technique is extremely simple and does not require fissionable material or high neutron fluxes.

BRIEF DESCRIPTION OF THE METHOD

We consider a model of a reactor: the geometric dimensions, construction materials, and moderator are the same as in the reactor being investigated. We fill the channels of the model with a neutron absorber which plays the role of the fissionable material. It is desirable that the energy dependence of the neutron absorption cross section for the material used to simulate the actual material be approximately the same as in the actual material.

In such a model, using a neutron source, it is possible to reproduce completely the neutron flux distribution in the actual reactor. We first group the channels of the model which contains the absorber into individual cells. In a reactor in the critical state, each such cell is a local source of neutrons. The number of fast neutrons emitted by one cell characterized by the coordinate $\vec{r}$ in a time $\perp$ is

$$N_r(\vec{r}) = \eta \Phi_0 \psi(\vec{r}) \Sigma t, \qquad (1)$$

where: η is the number of fast fission neutrons emitted by the nucleus in each absorption of a thermal neutron; Φ_0 is the thermal neutron flux at the center of the core; $\psi(\vec{r})$ is a dimensionless flux distribution function normalized to unity; Σ is the macroscopic neutron absorption cross section in the fissionable material (per unit cell).

In order to simulate the actual emission of fast neutrons we can place a source of fast neutrons in each cell of the channel. If the strength of the source is Q neut./sec, and if it emits $N_m(\vec{r})$ neutrons, the dwell time of the source in the cell is given by

$$\tau(\vec{r}) = \frac{N_m(\vec{r})}{Q}. \qquad (2)$$

In order to determine the thermal neutron flux distribution we place thermal neutron indicators in the model (for example, indicators made from dysporosium). Let us suppose that the half life of the indicator is much larger than the time during which it is irradiated. Under these conditions the activity of the detector will be independent of whether or not it is activated by a number of sources simultaneously (as is the case in an actual reactor), or by a single source which is successively moved to all cells (as is the case in the model). The validity of this assertion follows from the fact that the neutron flux at any point in the reactor can be given as the superposition of fluxes from each individual source.

The strength of the source at different points in the reactor varies in proportion to the thermal neutron flux $\Phi(\vec{r})$. Sources of different power can be simulated by keeping the source at a given cell of a channel for an appropriate length of time $\tau(\vec{r})$, proportional to the flux:

$$\tau(\vec{r}) = \tau_0 \psi(\vec{r}). \qquad (3)$$

In order to carry out this procedure the thermal neutron flux distribution must be known beforehand. We can use any preliminary distribution (for example, we can move the source through the channels uniformly). Then, from the activity of the thermal neutron indicators, the distribution is determined to a first approximation. By using the distribution which is found in each successive try it is then possible to determine the true distribution. As will be seen below, the successive approximations converge rather rapidly. The convergence of the successive approximations in systems of this kind has been studied in [1] in connection with the calculation of the critical mass of a reactor.

We now show that the model can be used to determine the critical mass. Each element of the reactor is a source of neutrons, emitting $N_r(\vec{r})$ fast neutrons in a time t. Equating the number of fast neutrons emitted by the elementary volumes of the reactor N_r and the model N_m, we have

$$\eta \Phi_0 \psi(\vec{r}) \Sigma t = Q \tau_0 \psi(\vec{r}). \quad (4)$$

Whence, η is given by

$$\eta = \frac{Q\tau_0}{\Phi_0 \Sigma t}. \quad (5)$$

The numerator of this expression is the number of fast neutrons emitted in a time t by a cell of fissionable material located at the center of the reactor, while the denominator is the number of thermal neutrons absorbed. In the model the same processes occur in a time $\tau_1 + \tau_2 + \ldots = \sum_i \tau_i$, equal to the total time of the experiment.

Suppose that the strength of the source Q is known and that the indicators, by their activity A, allow us to determine the absolute value of the integrated thermal neutron flux

$$\Phi t = \frac{A}{B}, \quad (6)$$

where 1/B is a coefficient of proportionality which takes account of the geometry of the experiment and the counting efficiency. Then, combining (5) and (6) we can compute the value

$$\eta = \frac{BQ\tau_0}{A\Sigma}. \quad (7)$$

Depending on the materials which are used and the geometric dimensions of the system, the quantity η may be larger than or equal to unity; (5) is the neutron balance condition. As a consequence of leakage of neutrons from the system and absorption in the slowing-down process, the number of thermal neutrons absorbed by an elementary cell cannot be larger than the number of fast neutrons emitted by the cell. It can be shown that the model is equivalent to a real critical system in which the fissionable material, having a macroscopic absorption cross section Σ, emits η fast neutrons per absorption of a thermal neutron. In particular, if U^{235} is used, the reactor will be supercritical if the value $\eta < 2.07$ is found experimentally and subcritical if $\eta > 2.07$.

By performing experiments with different amounts of absorbing material and plotting the curve of the function $\eta = f(\Sigma)$, using the point of intersection of this function with the line $\eta = 2.07$, it is possible to determine Σ_{crit}, i.e., the critical mass for the reactor.

A single experiment is sufficient for estimating the critical mass. This follows from the fact that the function $\eta = f\left(\frac{1}{\Sigma}\right)$ is approximately a straight line which intersects the ordinate axis at a point close to unity. For example, in the simplest case, an infinitely large reactor of pure U^{235} ($\varphi = 1$), the function is completely linear; from the condition $k_\infty = 1$ we have

$$\eta = \frac{k_\infty}{f} = 1 + \beta \frac{1}{\Sigma}.$$

Here f is the thermal utilization coefficient and β is a coefficient which depends on the lattice parameters and the properties of the moderating material.

The difficulty of determining the critical mass of a reactor lies in the fact that in computing η it is necessary to know both the strength of the source Q and the absolute value of the thermal neutron flux (the quantity B). Generally speaking, the measurement of each of these quantities is independent and involves a rather complicated experimental procedure. However, since we are not interested in these quantities individually but only in their product QB, this difficulty may be circumvented by means of the following experiment. We consider a sphere of radius R filled by an ideal (nonabsorbing) moderator. At the center of this sphere we place a source of strength Q. If the radius of the sphere is large compared with the moderating length, through the surface of the sphere there will pass a thermal neutron flux given by $Q/4\pi R^2$. The saturation activity of the thermal neutron detector located at the surface of the sphere is

$$A' = \frac{Q}{4\pi R^2} \frac{B}{\lambda}, \quad (8)$$

where λ is the decay constant of the indicator.

Taking account of (8), the expression for η becomes

$$\eta = \frac{A'}{A} \cdot \frac{4\pi R^2 \lambda \tau_0}{\Sigma}. \quad (9)$$

Thus, in order to compute η only the relative activity of the indicator need be measured.

EXPERIMENTAL VERIFICATION OF THE METHOD

In order to verify this method experimentally a simple reactor model was built. The moderator and neutron reflector in this model are ordinary water. A diagram of the model is shown in Fig. 1. The reactor model is an aluminum tank filled with water with 37 aluminum tubes which comprise a cylindrical core 52 cm high and 25 cm in radius. Inside the aluminum tubes are inserted tubes of thick paper on which are deposited a boron carbide power. The boron simulates the U^{235} for absorption of thermal neutrons. The neutron source is a Po - α - B source with a strength of 3×10^6 neut./sec. The neutron flux indicators are plates of dysprosium oxide.

Since the half life of dysprosium $T_{1/2} = 139.2$ min [2], the total irradiation time is at least 30 min (approximately $0.2\ T_{1/2}$). The thermal neutron flux distribution is first assumed to be uniform. Each channel is divided vertically into ten equal zones and each of the 370 cells obtained in this way is occupied by the source for 5 sec.

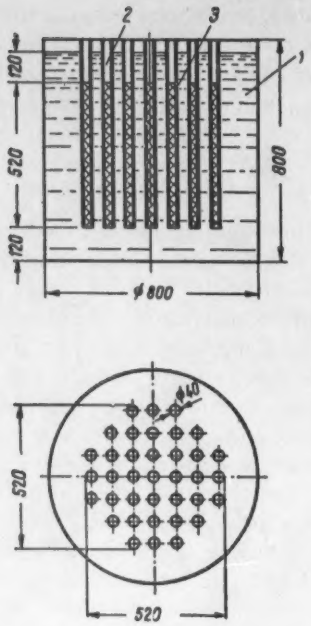

Fig. 1. Diagram of the model of a water reactor: 1) water; 2) channels in the core (the lattice spacing is 80 mm); 3) layer of boron carbide. The dimensions are given in mm.

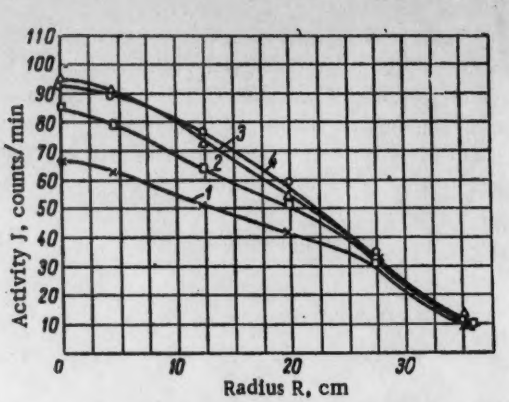

Fig. 2, Distribution of indicator activity over the radius of the model.

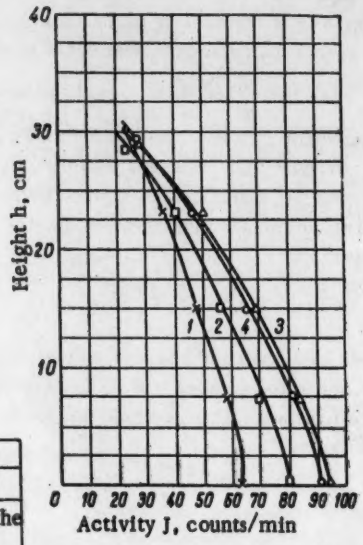

Fig. 3. Distribution of indicator activity over the height of the model.

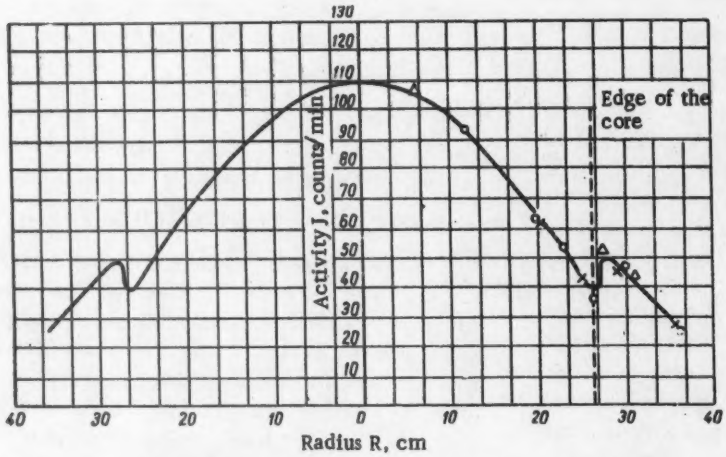

Fig. 4. Distribution of indicator activity over the radius of the model corresponding to an absorber concentration equal to 18 g of boron carbide in the channel. Δ, ×, O are the values obtained in three independent experiments.

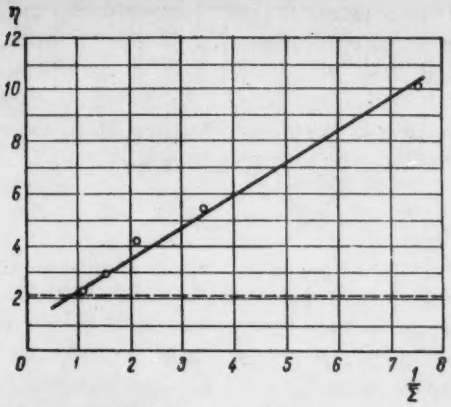

Fig. 5. The function $\eta = f(1/\Sigma)$. In the scale taken here unity on the abscissa axis corresponds to an absorbent concentration of 19.2 g of boron carbide in the channel.

The distribution of indicator activity (proportional to the thermal neutron flux) found in the first experiment is shown in Figs. 2 and 3 (Curve 1). Then, maintaining the total activation time, the dwell time of the source is changed in each cell in accordance with the previously obtained distribution. As a result of these successive approximations, further distribution curves are obtained for the thermal neutron flux (2, 3, and 4). It is apparent from the figures that Curves 3 and 4 are essentially the same.

Thus, the successive approximations converge to a limiting distribution corresponding to the distribution of thermal neutron flux in the system being studied.

For purposes of illustration, in Fig. 4 is shown the measured thermal neutron flux distribution corresponding to a concentration of 18 g of boron carbide in the channel, which is equivalent to 324 g of U^{235}. The distribution is typical of the thermal neutron flux distribution for reactors of this type.

To determine the dependence of the quantity η on $1/\Sigma$, distribution curves were plotted corresponding to concentrations of 2.52, 5.5, 9.0, 12.6, and 18 g of boron carbide in the channel. In each case the value of η was computed from (7). The value of the coefficient B was determined from the activation of the indicators in a known neutron flux.

The function $\eta = f\left(\frac{1}{\Sigma}\right)$ is shown in Fig. 5. The experimental points lie on a straight line which intersects the ordinate axis at a point close to unity. As has been indicated above, the intersection of the lines $\eta = f\left(\frac{1}{\Sigma}\right)$ and $\eta = 2{,}07$ [3] yields the value of $1/\Sigma_{crit}$. For the model described here the critical mass of U^{235} is approximately 13 kg.

MODEL EXPERIMENTS ON A REACTOR WITH A PRESSURIZED-GAS FUEL

It is of interest to verify the model method using a model for a reactor whose critical mass is known exactly. An experiment of this kind was carried out with a model with a pressurized gas fuel [4].

Before the experiments were carried out, all 148 working channels of the reactor were replaced by channels with a layer of boron carbide. The experiment was carried out three times with different amounts of absorbing material. The macroscopic absorption cross section of the boron carbide deposited on the paper was determined by measurements of the transmission of a monochromatic neutron beam.* The values of Σ reduced to a temperature of 343°K are 0.85, 1.33, and 2.06 cm^2, equivalent, respectively, to pressures of 500, 785, and 1210 mm Hg of gaseous uranium hexafluoride containing 90% U^{235} at a temperature of 350°K. (It is assumed that the temperature of the neutron gas is 50° higher than the temperature of the moderator.)

Because of the absence of a Po - α - B neutron source of adequate strength in these experiments use was made of a Po - α - Be source, with a mean neutron energy estimated as 4.4 Mev. It can be shown that the difference in the fission neutron spectrum from the neutron spectrum of the source which was used does not introduce any significant error in the determination of the critical mass. There was some inconvenience in carrying out the experiments because of the large number of channels (148). Because of the geometric symmetry of the reactor it was possible to limit the coverage of the source to thirty seven channels ($^1/_4$ of the total number). In the computations using (9) appropriate corrections were made for this procedure.

In computing the values of η it is necessary to know the source strength Q and the absolute magnitude of the thermal neutron flux (the coefficient B). To determine the product of these quantities use was made of a spherical shell of radius R = 30 cm which was filled with heavy water. The sphere was placed in a metal jacket, the inner walls of which were lined with sheet cadmium. At the center of the sphere was placed the source being investigated. The saturation activity of the indicators located at the surface of the sphere is [cf. (8)]

$$A' = \xi \frac{BQ}{\lambda 4\pi R^2}. \qquad (10)$$

The coefficient ξ is introduced to take account of the neutrons which are not slowed down.

Neglecting the absorption in the heavy water, we can obtain the magnitude of ξ [5]. For the sphere which was used and the Po - α - Be source, this coefficient is found to be 0.607.

Thus, the calculation formula (9) assumes the final form:

$$\eta = \frac{\frac{1}{4} A' \lambda 4\pi R^2 \int \tau \, dV}{\Sigma \xi f_{B'} \int A \, dV}, \qquad (11)$$

* This work was carried out at our request by Yu. Ya. Konakhovich.

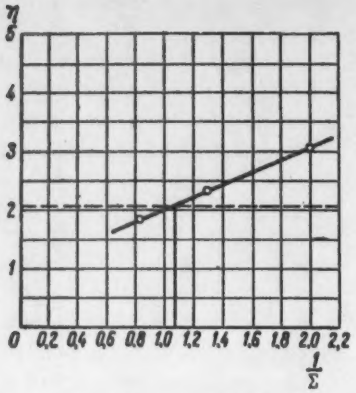

Fig. 6. The function $\eta = f(1/\Sigma)$ for a reactor model with gaseous UF_6. In the scale used here unity of the abscissa axis corresponds to an absorbent concentration equivalent to a pressure of 1000 mm.

where the ratio of τ_0/A is equal to the dwell time of the source in the central cell of the core to the activity of the indicator, which is equivalent to the ratio of the corresponding integrals over the total volume of the model. The coefficient $1/4$ takes account of the fact that the source extends over only $1/4$ of the total number of channels. The coefficient $f_B = 1.026$ is the Bothe correction for the distortion of the neutron field by the probe.

In three experiments with different amounts of absorbing material the following values were obtained for η:

$$\eta = 3.04; \quad \eta = 2.3 ; \eta = 1.8.$$

The dependence of η on $1/\Sigma$ is shown in Fig. 6.

From the point of intersection of the line $\eta = f(1/\Sigma)$ and the line $\eta = 2.07$, the value found for the critical pressure of $P_{crit} = 935$ mm Hg, whereas the true value of the critical pressure as determined by starting up the reactor is 1018 mm Hg. The agreement is good.

CONCLUSION

The use of models makes it possible to find the thermal neutron flux distribution and to estimate the critical mass of a reactor using enriched uranium of low density. The possibility of applying the method to other reactors is limited by the possibility of finding neutron absorbers whose properties can simulate those of fissionable materials being used. This technique may also be found valuable for solving a number of related problems in neutron physics.

LITERATURE CITED

1. A. Thompson, J. Appl. Phys. 22 1223 (1951).
2. A. N. Nesmeyanov, A. V. Lapitskii, and N. P. Rudenko, Production of Radioactive Isotopes [in Russian] (Goskhimizdat, Moscow, 1954).
3. D. Hughes and R. Schwartz, Neutron Cross Sections, BNL-325 (U.S. Government Printing Office, 1958).
4. I. K. Kikoni, V. A. Dmitrievskii, et al., Atomnaya Énergiya 5, 294 (1958).†
5. I. Sneddon, The Fourier Transform [Russian translation] (IL, 1955).

† Original Russian pagination. See C.B. translation.

HEAT OF FORMATION OF UBe_{13}

M. I. Ivanov and V. A. Tumbakov

Original article submitted November 25, 1958

When a mixture of beryllium power and finely dispersed uranium, prepared by the decomposition of its hydride, was heated, a substance was obtained which consisted in the main of UBe_{13} and a small quantity of free beryllium. From the difference between the heat of solution of UBe_{13} and of the corresponding mixture of its components, the heat of formation $(-\Delta H^0_{298})UBe_{13}$ was determined. After corrections for impurities were allowed for, the heat of formation was found to be 39.3 ± 3.8 kcal/mole.

No data on the heat of formation of UBe_{13} is available. We determined it from the difference between the heat of solution of the prepared UBe_{13} and the heat of solution of the mixture of initial components of the same composition as the substance prepared. The calorimetric apparatus and the method of measurements have been described earlier [1]. For the heat unit we took the gram-calorie and as a criterion for the accuracy we took the probable experimental error.

Starting materials. The uranium was used in lumps form and the beryllium (electrolytic) in powder form. The surface oxides on the uranium were removed by means of electropolishing in H_3PO_4. The content and assumed phase composition of impurities in uranium and beryllium are given in Table 1. On the basis of this data we determined the phase composition of the uranium and beryllium used in our experiments.

Preparation and identification of UBe_{13}. The UBe_{13} was prepared by heating a mixture of beryllium powder and finely dispersed uranium in an electric furnace in an atmosphere of pure hydrogen (620 mm Hg) at 1300 ± 50°C for 1.5 hr. When the heating was completed, hydrogen was pumped off from the reaction space at the temperature of 600 °C. The mixture (34% wt. beryllium) was kept in a BeO crucible placed in a quartz ampoule with a water-cooled, ground lid. The cooled product was ground in a jasper mortar in a chamber filled with purified argon.

Table 1. Content of impurities in uranium and beryllium, and their assumed phase composition.

Impurity	Content, % wt.			
	in uranium	compound	in beryllium	compound
Carbon	$6\cdot10^{-2}$	UC	$11\cdot10^{-2}$	Be_2C
Oxygen	$9\cdot10^{-3}$	UO	$7\cdot10^{-2}$	BeO
Nitrogen	$5\cdot10^{-3}$	UN	$6\cdot10^{-3}$	Be_3N_2
Silicon	$3{,}6\cdot10^{-2}$	U_3Si	$9\cdot10^{-3}$	Si
Iron	$1{,}4\cdot10^{-2}$	U_6Fe	$1{,}4\cdot10^{-2}$	Fe
Manganese	$3\cdot10^{-3}$	U_6Mn	$1\cdot10^{-3}$	Mn
Nickel	$6\cdot10^{-4}$	U_6Ni	—	—
Magnesium	$<1\cdot10^{-3}$	Mg	$2{,}3\cdot10^{-3}$	Mg
Copper	$9\cdot10^{-4}$	UCu_5	$2{,}8\cdot10^{-3}$	Cu
Chromium	—	—	$<3\cdot10^{-3}$	Cr
Aluminum	—	—	$7\cdot10^{-3}$	Al
Boron	$5\cdot10^{-4}$	UB_2	—	—

The analysis of the prepared substance by means of x-ray powder method showed that it consisted of one phase only, i.e., UBe_{13} with the lattice constant a = 10.236 ± ±0.001 kX. According to [2] the lattice constant of UBe_{13} is a = 10.235 ± 0.001 kX, and this value is in close agreement with our results. According to [3] a = 10.26 kX and according to [4] a = 10.3489 ± 0.0001 kX.

It was found by means of metallographic investigations that the substance obtained consisted in the main of UBe_{13}; there were minute traces of another phase along the grain boundaries of UBe_{13}, but it could not be identified. To determine the content of uranium and beryllium in the substance prepared (taking into account uranium and beryllium with the impurities indicated in Table 1) we determined:

1. The quantity of oxygen which combines with the uranium and beryllium or with the prepared UBe_{13} when they are ignited until constant weight is attained. The uranium and the prepared UBe_{13} were ignited in air at 800 °C, and the beryllium was ignited at 800°C for eight hrs in air and then at 1300°C in oxygen.

2. The amount of gas (consisting mainly of hydrogen) which evolves when uranium, beryllium, or UBe_{13} is dissolved in a solvent of the same composition as used in the experiments on the determination of the heat of solution, i.e.: 600 ml HCl (A. R., sp. gr. 1.78); 400 ml H_3PO_4 (A. R., sp. gr. 1.39); 0.25 g Na_2SiF_6 (pure); 0.12 g $CuSO_4 \cdot 5H_2O$ (A. R.).

The method of measuring the amount of gas evolved differed from the method described previously [1] only in so far as, for convvenience, air from the thin-wall glass bulb with the substance under analysis and from the glass vessel was pumped off and not displaced by carbon dioxide before they were sealed.

The results on the determination of the increase in weight due to oxidation and of the amount of gas evolved on the dissolution of uranium, beryllium, and UBe_{13} are given in Table 2.

The beryllium content in the prepared UBe_{13} was 33.60 ± 0.09 % wt. as determined from the increase in

weight on ignition, and 33.62 ± 0.06% wt. as determined from the amount of gas evolved. The mean beryllium content is 33.61 ± 0.05% wt.

Impurities which were present in the initial uranium and beryllium could react with uranium, beryllium, or with each other during the preparation of the alloy. Unfortunately, it was not possible either by direct experimental determination or by calculation (in view of the absence of data on the free energy of formation for the most important compounds taking part in the reactions) to evaluate the amount of impurities in the alloy. Therefore, the following assumptions were made:

1. impurities do not take part in reactions;

2. only the uranium impurities react with beryllium, for instance $UC + 15Be = Be_2C + UBe_{13}$;

3. only the beryllium impurities react with uranium, for instance $Be_2C + 1\frac{1}{13}U = UC + \frac{2}{13}UBe_{13}$.

Results of the determination of heat of prepared UBe_{13} and of the mixture of initial components. The heat of solution of the prepared UBe_{13} was found to be 3631.0 ± 4.1 cal/g (7 determinations). The heat of solution of the mixture of uranium and beryllium (33.61% wt. Be) was found to be 3737.5 ± 5.1 cal/g (six determinations). The difference is 106.5 ± 8.6 cal/g. The error in this difference also includes the experimental error in the determination of the components of the alloy.

The difference between the heat of solution of the mixture and the heat of solution of the substance prepared (10,650 ± 860 cal per 100 g of alloy) constitutes the heat of reactions which take place between the components of the alloy during its formation (standard conditions).

For the determination of the heat of formation of UBe_{13} in accordance with assumptions 2) and 3), it is necessary to know the heat of formation of the impurities. The values which we assumed are given in Table 3.

It follows from the data in Table 3 and from the assumptions 1), 2), and 3) of possible reactions, that the heat of formation $(-\Delta H^0_{298})UBe_{13}$ is equal to 39.3 ± 3.1; 38.6 ± ±3.1; and 40.0 ± 3.1 kcal/mole, respectively.

Since the impurities present in the initial metals react to a certain extent with uranium and beryllium in the course of the preparation of the alloy, the heat of formation of UBe_{13} when calculated without taking these reactions into account may have a maximum systematic error of ±(40.0 - 38.6)/2 = 0.7 kcal/mole. Therefore, for the heat of formation $(-\Delta H^0_{298})UBe_{13}$, we accepted the value of 39.3 ± 38 kcal/mole.

Errors in the determination of the heat of formation of UBe_{13}. The largest error in the determination of the heat of formation of UBe_{13} is caused by an inaccurate determination of the uranium and beryllium contents in the alloy. A 0.01% error in the determination of beryllium results in a systematic error of approximately 1% in the determination of the heat of formation of UBe_{13}.

The fact that in the process of alloy preparation the contaminations which are present in the components of the alloy may react with these components, with intermetallic compounds formed, or with each other, has no effect on the results of our determinations (Table 2). For analysis by means of ignition this statement is obvious. The results of the determination by means of dissolution are affected only by the following reaction (out of the reactions in which impurities take part)

$$UC + 15\,Be = Be_2C + UBe_{13},$$

because different amounts of gasses are evolved depending on whether the compounds on the left hand side or on the right hand side of the above equation are dissolved. Experiments, however, showed that, when UC was dissolved in the solvent which we used, 0.83 moles of gas (calculated as ideal gas) was formed per 1 mole of dissolved UC. Since this value is nearly 1 mole, the analysis of the alloy by means of dissolution, as well as the analysis by means of ignition, gives correct results.

The systematic error in both methods of analysis depends on the variation in the relative content of impurities, this variation being caused by the evaporation of beryllium or some impurities as well as by the introduction of new im-

Table 2. Results of ignition and dissolution

Substance	Mean increase in weight due to oxygen per 1 mg of substance, mg	No. of determinations	Amount of gas formed on the dissolution of 1 mg of the substance (mm at 299°K in a system of 565.5 cm³ volume)	No. of determinations
U	0,18070±0,00017	6	0,2735±0,0002	5
Be	1,77031±0,00113	3	3,6552±0,0057	5
UBe_{13}	0,71474±0,00023	5	1,4105±0,0005	5

Table 3. The values of the heat of formation of impurities in the uranium, beryllium and alloy as assumed for the calculation of the heat of formation of UBe_{13}

Substance	$-\Delta H^0_{298}$	Basis
UC	40 000	[5]
UO	135 000	[7]
UN	68 000	[8]
BeO	147 000	[9]
Be_2C	8 000	Approximate, from $\Delta F^0_{2400^0K} = -7830$ cal for Be_2C [6]
U_3Si	40 000	By analogy with ΔH^0_{298} for $ThSi_2$ [10]
U_6Fe	20 000	Arbitrary, but the order of magnitude of ΔH^0_{298} for intermetallic compounds has been taken into account.
U_6Mn	20 000	The same

purities in the course of alloy preparation. The evaporation of beryllium in the course of alloy preparation is most probable. However, under the experimental conditions in our determinations the amount of beryllium which evaporated did not exceed 0.4% wt. Calculations show that this would result in a systematic error of < 0.01%.

As regards the introduction of new impurities into the alloy in the course of its preparation, the most likely impurity is oxygen. The analysis of the alloy by means of melting under vacuum in a platinum vessel in a graphite crucible showed that the total content of oxygen in the alloy was 0.05% wt., but the calculations based on the weight of the sample and the content of oxygen in the individual components of the sample gave an oxygen content equal to 0.03% wt. The difference is within the limits of the experimental error of the determination of oxygen in the alloy and in the components of the sample. If we also consider that according to calculations the appearance of 1% oxides (of uranium or beryllium) during the preparation of the alloy changes our value of the heat of formation of UBe_{13} by only slightly more than 1%, it becomes clear that a difference of 0.02% wt. of oxygen introduced no error in the determination of the heat of formation of UBe_{13}. No other impurities could contaminate the alloy during the preparation process since the sample was heated in a crucible made of pure beryllium oxide (for luminophores) in an atmosphere of very pure hydrogen. The alloy was ground in a chamber filled with purified argon.

The authors wish to thank N. T. Chebotarev for the x-ray analysis, T. S. Men'shikov for the metallographic analysis,and V. T. Kharlamov and A. I. Lebedev for the determination of oxygen in the alloy and its components.

LITERATURE CITED

1. M. I. Ivanov, V. A. Tumbakov, and N. S. Podolskaya. Atomnaya Énergiya 5, 166 (1958).*
2. N. Baenzieger and R. Rundle, Acta Cryst. 2, 258 (1949).
3. W. Koehler, I. Singer, and A. Coffinberry, Acta Cryst. 5, 394 (1952).
4. R. Buzzard, J. Research Natl. Bur. Standards 50, No. 63 (1953).
5. Nuclear Reactors, Collection III [Russian translation] (IL, Moscow, 1956) p. 96.
6. Nuclear Reactors, Collection III [Russian translation] (IL, Moscow, 1956) p. 83.
7. J. Katz and E. Rabinowitch, Chemistry of Uranium [Russian translation] (IL, Moscow, 1954), p. 244.
8. O. Kubashewski and E. Evans, Thermochemistry in Metallurgy [Russian translation] (IL, Moscow, 1954) p. 290.
9. O. Kubashewski and E. Evans, Thermochemistry in Metallurgy [Russian translation] (IL, Moscow, 1954) p. 250.
10. D. Robins and J. Jenkins, Acta Met. 3, 598 (1955).

* Original Russian pagination. See C.B. translation.

RADIOLYTIC REDUCTION OF Am (VI) AND Am (V)

A. A. Zaitsev, V. N. Kosyakov, A. G. Rykov, Yu. P. Sobolov, and G. N. Yakolev

Original article submitted November 17, 1957

We obtained the rate constants of the radiolytic reduction of AmO_2^{2+} in perchloric, sulfuric, and nitric acids by determining the radiation yield of the reducing products. These values, combined with data on hydrogen peroxide yield, make it possible to evaluate the consumption of hydrogen radicals in the over-all reduction reaction. A mechanism is proposed for the radiolytic reduction of AmO_2^{2+} and AmO_2^{+}. The expression for the rate of AmO_2^{+} reduction makes it possible to calculate the yields of hydrogen peroxide and hydrogen radicals in the solutions investigated.

Simultaneously with the preparation of the higher oxidation states of americium, Am (VI) and Am (V) [1-4], it was established that Am(VI) and Am (V) in aqueous solutions are spontaneously reduced at a rate of about 4 and 2 % per hour, respectively. This process is caused by reducing agents formed during radiolytic decomposition of water by the action of Am^{241} α radiation.

In the first investigations on the kinetics of americium autoreducation [3-5], it was established that the rate of this reaction was directly proportional to the total americium concentration and did not depend on the Am (VI) or Am (V) concentration. However, a more detailed investigation [6] showed that this was true only in the case of Am (VI).

A study of the radiolytic reduction of Am (VI) and Am (V) is also quite valuable in the radiation chemistry of aqueous solutions, where the action of strongly ionizing radiation has been studied comparatively little.

EXPERIMENTAL

Americium. The americium isotope Am^{241} with a half life of 461.3 years was used in this work [7]. Spectral analysis showed practically complete absence of impurities (< 1%).

Reagents. In all cases the reagents used without preliminary purification were "chemically pure" grades. The water was doubly distilled from acidified potassium permanganate solution. The sulfuric and nitric acids were also distilled before use. The reaction of chlorine ions with silver nitrate was used to check that the nitric acid did not contain chlorine. The perchloric acid was distilled at 30 mm Hg. Sodium perchlorate was prepared by neutralizing sodium carbonate with perchloric acid and purified by recrystallization from water and alcohol.

Radiometric analysis. The total americum concentration in solution was determined radiometrically by the Am^{241} α radiation in a slit chamber with a counting coefficient of $4.85 \cdot 10^{-6}$.

Am (V) preparation. Am (III) hydroxide was washed with distilled water and dissolved in hot 40% potassium carbonate solution. Ozone was passed through the solution for 30-40 min at 80-90°C. After ozonization, the suspension of the double carbonate of Am (V) and potassium was heated for about 30 minutes on a water bath. The precipitate was separated by centrifuging and traces of Am (III) removed by washing with 40% potassium carbonate solution and then water. The Am (V) and potassium double carbonate obtained was dissolved in 0.1 M perchloric acid and reprecipitated from 40% potassium carbonate solution.

Am (VI) preparation. The aqueous suspension of Am (V) and potassium double carbonate was placed in an ozoniation vessel. The water was removed by evaporation on a water bath in a stream of ozone. The dry, black residue was dissolved with 0.1 M perchloric acid and the solution again evaporated in a stream of ozone.

Autoreduction of Am (V) and Am (VI). The Am (V) and potassium double carbonate or Am (VI) perchlorate was dissolved in the appropriate acid and transferred to a prismatic quartz or cylindrical glass cell, which was then placed in a thermostatted holder. The temperature in the cell was maintained with an accuracy of ± 0.2°C. An SF-4 spectrophotometer was used for measuring the optical density of solutions. As analytical bands we chose the absorption bands with wavelengths 992-997 mμ for Am (VI), 715-718 mμ for Am (V) and 809-815 mμ for Am (III). The absorption spectra of Am (VI) and Am (III) in all the solutions investigated were first plotted. The absorption spectrum of Am (V) was practically independent of the solution composition.

Accumulation of hyrdogen peroxide in Am^{241} solutions. Am (III) hydroxide or Am (V) and potassium double carbonate was dissolved in 0.1 or 0.1 M sulfuric acid containing Ti (IV) sulfate. The titanium concentration was 0.5 g/liter. The hydrogen peroxide was determined by the absorption of the titanium complex at wavelengths of 400, 450, and 470 mμ. The Am (III) and Am (V) concentrations were determined by the absorption of the solution at 811 and 717 mμ. Ti (IV) and the Ti (IV) peroxide complex have no absorption at 811 and 717 mμ.

The hydrogen peroxide concentration was culculated from the relation obtained by preliminary calibration:

$$[H_2O_2]\ (\mu M) = 456D_{400} = 644D_{450} = 950D_{470},$$

where D is the optical density at the given wavelength.

RESULTS AND THEIR DISCUSSION

Radiolytic reduction on Am (VI) and Am (V) in perchloric and sulfuric acid solutions. Figures 1 and 2 show typical curves of americium reduction in 2.0 M $HClO_4$ and 0.2 M $HCLO_4$ + 1.0 M Li_2SO_4. Beside the change in the Am (VI), Am(V),and Am (III) concentrations, the figures show the change in the mean valence state (N) of americium, which was determined from the relation:

$$N = \frac{6[AmO_2^{2+}] + 5[AmO_2^{+}] + 3[Am^{3+}]}{[Am]_{tot.}}.$$

At perchloric acid concentrations above 2 M and sulfuric acid concentrations above 1 M,the main process producing a change with time in the Am (VI), Am (V),and Am (III) concentrations was the disproportionation of Am (V). However, the mean valence state did not change as a result of the disproportionation and its decrease with time was due to reduction only.

As Figures 1 and 2 show, in the initial period a linear decrease in the Am (VI) concentration and an increase in the Am (V) concentration was observed; the Am (III) concentration remained constant in this period. When a considerable amount of Am (V) had accumulated in the solution,the rate of Am (VI) reduction fell and the Am (III) concentration started to increase. After the disappearance of Am (VI), the reduction of pentavalent americium proceeded at a rate depending on its concentration. The mean valence state changed linearly with time until the practically complete reduction of Am (VI). The rate at which Am (VI) reacted with the reducing agents formed as a result of radiolysis was much greater than the rate at which these agents were formed; therefore, as long as Am (VI) was present in the solution all the reducing agents were consumed. For the period when Am (VI) reduction proceeded at a constant rate,

$$-\frac{d[AmO_2^{2+}]}{dt} = \frac{d[AmO_2^{+}]}{dt} = k_\alpha [Am]_{tot.}$$

while

$$\frac{d[Am^{3+}]}{dt} = 0.$$

Then

$$-\frac{dN}{dt} = -\frac{1}{[Am]_{tot.}} \frac{d}{dt}(6[AmO_2^{2+}] + 5[AmO_2^{+}] + 3[Am^{3+}]) = -\frac{1}{[Am]_{tot.}} \frac{d[AmO_2^{2+}]}{dt} = k_\alpha.$$

The values of k_α, calculated from the slope of the linear sections of the curves of the mean valence state changes, are given in Table 1, which also gives the values of the initial reduction yield $G_{Am_2^{2+}}$. The constant k_α is related to the yield G by the expression

$$G = \frac{T_{1/2}}{0{,}693 Q_\alpha} k_\alpha = 103{,}4 k_\alpha,$$

where $T_{1/2}$ is the half life of Am^{241} (in hours); Q_α is the energy emitted in one decay act (in electron volts).

Hall and Markin [8] observed an analogous decrease in the reduction constant in the same acids. However, the values for k_α in Table 1 are higher than those of the corresponding constants obtained by these authors. The strong effect of solution composition on the reduction rate cannot be explained by complex formation as was proposed earlier [9]. As the reduction rate is determined by the rate of reducing agent formation, a change in the rate constant of Am (VI) reduction is due only to changes in the radiolytic yield of reducing products.

Table 1. Rate constant and yield of radiolytic reduction of AmO_2^{2+}

Composition and concentration of solution, mole/liter	$k_\alpha \cdot 10^2$ (hr^{-1})	$G_{AmO_2^{2+}}$, ions/100 ev
0.2 $HClO_4$	4.04	4.18
2.0 $HClO_4$	3.20	3.31
4.0 $HClO_4$	3.20	3.31
6.0 $HClO_4$	3.40	3.52
2.0 $HClO_4$ + +4.0 $NaClO_4$	3.81	3.94
4.0 $NaClO_4$ + +2.0 $NaClO_4$	3.55	3.67
0.1 H_2SO_4	4.04	4.18
1.0 H_2SO_4	2.85	2.95
2.0 H_2SO_4	2.50	2.59
4.0 H_2SO_4	2.02	2.09
6.0 H_2SO_4	1.80	1.86
10.0 H_2SO_4	2.20	2.28
0.2 $HClO_4$ + +1.0 Li_2SO_4	3.15	3.26
0.2 $HClO_4$ + +2.0 Li_2SO_4	2.54	2.63

One of the products of water decomposition under the action of α radiation is hydrogen peroxide. Its radiation yield was determined in Am (III) solutions in 0.1 and 1.0 M H_2SO_4 and was found to be 1.18 ± 0.12 and 0.69 ± 0.05 molecules of hydrogen peroxide per 100 ev. A comparison of these values with those for the yield of Am (VI) reduction in the corresponding acids showed that the reduction of Am (VI) was produced only partially (~50%) by hydrogen peroxide. The remaining part was apparently reduced by hydrogen atoms which exist in the form of HO_2 radicals in the air-saturated solution.

Am (VI) and Am (V) solutions were also analyzed for free hydrogen peroxide content. No hydrogen peroxide was found in the presence of Am (VI) in solution. The curve for hydrogen peroxide accumulation in a sulfuric acid solution of Am (V) is shown in Fig. 3. As this figure shows, free hydrogen peroxide appeared in the solution towards the end of Am (V) reduction.

By using the value we obtained for the rate constant of the reaction of AmO_2^{+} with hydrogen peroxide in 0.1 M $HClO_4$, we may determine how much of the hydrogen peroxide accumulating in the solution is consumed in the observed radiolytic reduction of Am (V).

For the calculation,we assumed that the rate constant of the reaction of Am_2^{+} with hydrogen peroxide in 0.1 M H_2SO_4 was equal to the rate constant of this reaction in 0.1 M $HClO_4$. Such an assumption presumable should not introduce large errors. The results of such a calculation are given in Table 2. As Table 2 shows, the hydrogen

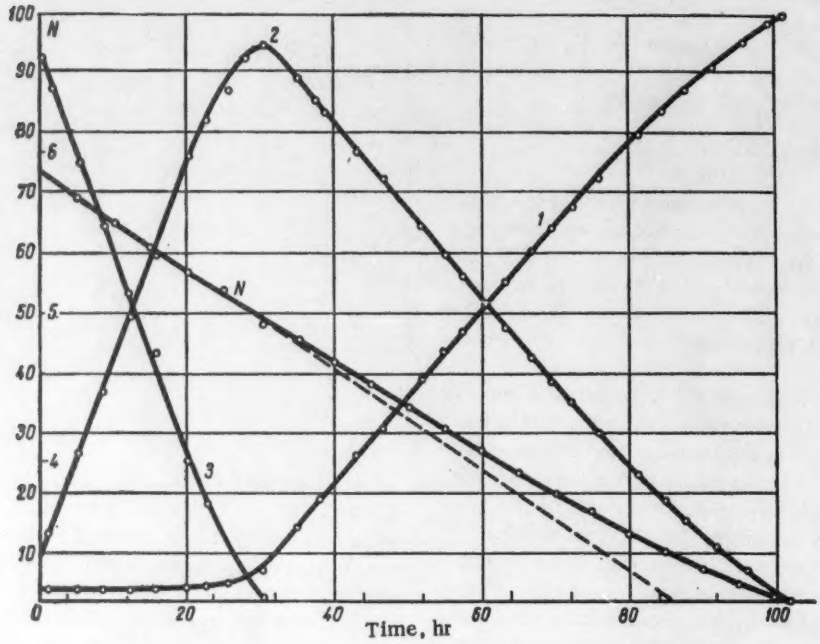

Fig. 1. Radiolytic reduction of americium in 2.0 M $HClO_4$ ($[Am]_{tot} = 5.19$ mM): 1) Am (III); 2) Am (V); 3) Am (VI).

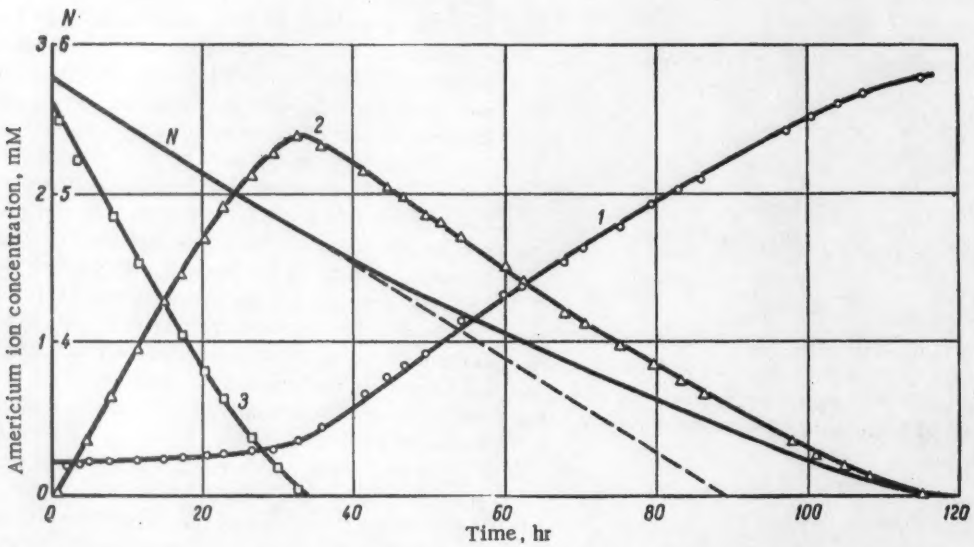

Fig. 2. Radiolytic reduction of americium in 0.2 M $HClO_4$ + 1.0 M Li_2SO_4 ($[Am]_{tot} = 2.79$ mM): 1) Am (III); 2) Am (V); 3) Am (VI).

Table 2. Observed and calculated rate of AmO_2^+ reduction in 0.1 M H_2SO_4 ($k = 14.8$ mole^{-1} · liter · hr^{-1})

Time, hr	Concentration		Rate of AmO_2^+ reduction, mole · liter^{-1} · hr^{-1} · 10^6		$\frac{1}{v_5}/\frac{v_5}{\%}$
	AmO_2^+, mM	H_2O_2, μM	observed*	calculated**	
42	1.72	26	92	0.66	0.7
44	1.54	30	88	0.82	0.9
46	1.37	33	86	0.67	0.8
48	1.19	36	86	0.63	0.7
50	1.03	40	83	0.61	0.7
52	0.86	44	80	0.56	0.7
54	0.71	56	79	0.59	0.7
56	0.55	84	73	0.68	0.9
58	0.42	130	60	0.81	1.4
60	0.31	208	51	0.96	1.9
62	0.22	286	43	0.93	2.2
64	0.14	370	31	0.77	2.5

* $v_5 = \frac{d\,[AmO_2^+]}{dt}$.

** $v_5' = k[AmO_2^+]\,[H_2O_2]$.

peroxide accumulating in the solution hardly participates in Am (V) reduction.

Keeping in mind the scheme for the oxidation–reduction potentials of Am [10]:

$$Am^{3+} \xrightarrow{1.74v} AmO_2^+ \xrightarrow{1.60v} AmO_2^{2+}$$
$$\underbrace{\qquad\qquad\qquad}_{1,69\,v}$$

and considering that the value of the constant for the reaction of Am (V) with hydrogen peroxide is small, we may put forward the following hypothesis:

Am (V) is reduced only by HO_2 radicals.

Am (V) may be oxidized to Am (VI) by OH radicals and this reaction competes with that of hydrogen formation; hydrogen peroxide is consumed only in Am (VI) reduction.

The kinetics of the radiolytic reduction of AmO_2^{2+} and AmO_2^+ in aqueous, air-saturated solutions may be explained by the following reactions:

$$H_2O \longrightarrow\!\!\!\!\!\!\vee\!\!\!\!\!\!\vee\!\!\!\!\!\!\vee\!\!\!\!\!\!\longrightarrow H + OH; \quad (1)$$
$$H + O_2 = HO_2; \quad (2)$$
$$OH + OH \xrightarrow{k_3} H_2O_2; \quad (3)$$
$$AmO_2^{2+} + HO_2 \xrightarrow{k_4} AmO_2^+ + O_2 + H^+; \quad (4)$$
$$AmO_2^{2+} + H_2O_2 \xrightarrow{k_5} AmO_2^+ + HO_2 + H^+; \quad (5)$$
$$AmO_2^+ + 2HO_2 + 2H^+ \xrightarrow{k_6} Am^{3+} + 2O_2 + 2H_2O; \quad (6)$$
$$AmO_2^+ + OH \xrightarrow{k_7} AmO_2^{+} + OH^-. \quad (7)$$

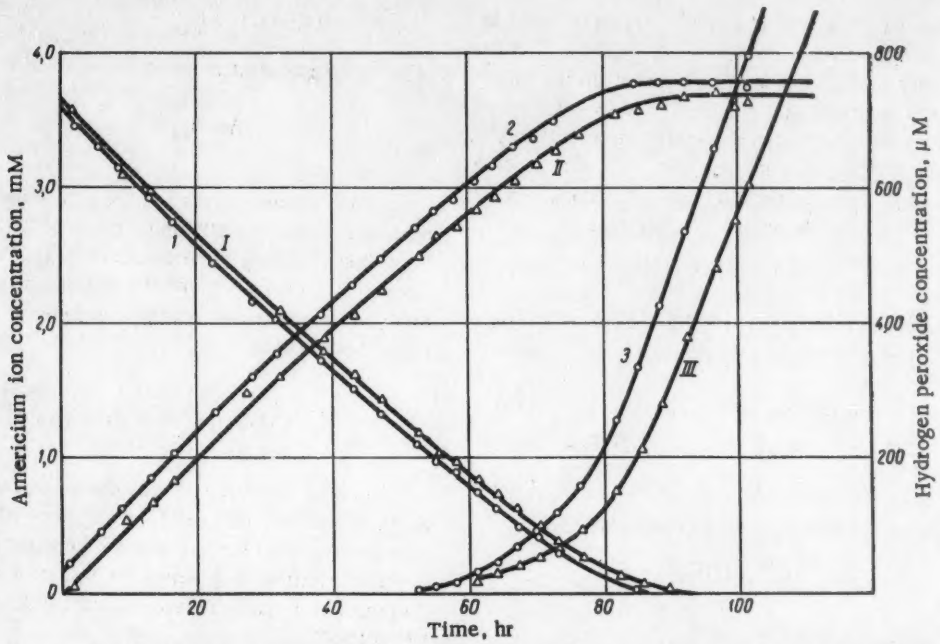

Fig. 3. Radiolytic reduction of Am (V) and hydrogen peroxide accumulation in 1.0 M H_2SO_4. First experiment ($[Am]_{tot} = 3.76$ mM): 1) change in Am (V) concentration; 2) change in Am (III) concentration; 3) hydrogen peroxide accumulation. Second experiment ($[Am]_{tot} = 3.64$ mM): I) change in Am (V) concentration; II) change in Am (III) concentration; III) hydrogen peroxide accumulation.

In the initial period of AmO_2^{2+} reduction when the concentration of AmO_2^+ is low, the kinetics of the whole process would be determined by reactions (1-5):

$$-\frac{d[AmO_2^{2+}]}{dt} = k_4[AmO_2^{2+}][HO_2] + \\ + k_5[AmO_2^{2+}][H_2O_2]; \quad (8)$$

$$\frac{d[H_2O_2]}{dt} = k_3[OH]^2 - k_5[AmO_2^{2+}][H_2O_2] = 0; \quad (9)$$

$$\frac{d[HO_2]}{dt} = r_H[Am]_{tot.} + k_5[AmO_2^{2+}][H_2O_2] - \\ - k_4[AmO_2^{2+}][HO_2] = 0; \quad (10)$$

$$\frac{d[OH]}{dt} = r_{OH}[Am]_{tot.} = 2k_3[OH]^2 = 0, \quad (11)$$

where r_H and r_{OH} are the rate constants of the formation of H and OH radicals under the action of Am^{241} radiation.

Combining (8-11) we have

$$-\frac{d[AmO_2^{2+}]}{dt} = (r_H + r_{OH})[Am]_{tot.} = k_\alpha[Am]_{tot.}, \quad (12)$$

where $k_\alpha = (r_H + r_{OH})$.

From (11) it follows that the radiolytic yield of hydrogen peroxide formation equals half the yield of OH radicals, so

$$k_a = r_H + 2r_{H_2O_2}.$$

When AmO_2^+ accumulates in the solution, reactions (6) and (7) start to have an effect and this leads to a decrease in the reduction rate of AmO_2^{2+} and an increase in the Am^{3+} concentration.

When only AmO_2^+ and Am^{3+} are present in the solution, the main reactions will be (1 - 3) and (5 - 7). Reaction (4) may be ignored as the concentration of AmO_2^{2+} formed by reaction (7) is much less than the concentration of AmO_2^+, and AmO_2^{2+} cannot compete with AmO_2^+ for HO_2 radicals to an appreciable extent. In this case

$$-\frac{d[AmO_2^+]}{dt} = k_6[AmO_2^+][HO_2]^2 + \\ + k_7[AmO_2^+][OH] - k_5[AmO_2^{2+}][H_2O_2]; \quad (13)$$

$$\frac{d[AmO_2^{3+}]}{dt} = k_7[AmO_2^+][OH] - \\ - k_5[AmO_2^{2+}][H_2O_2] = 0; \quad (14)$$

$$\frac{d[OH]}{dt} = r_{OH}[Am]_{tot.} - 2k_3[OH]^2 - \\ - k_7[AmO_2^+][OH] = 0; \quad (15)$$

$$\frac{d[HO_2]}{dt} = r_H[Am]_{tot.} + k_5[AmO_2^{2+}][H_2O_2] - \\ - 2k_6[AmO_2^+][HO_2]^2 = 0, \quad (16)$$

hence

$$-\frac{d[AmO_2^+]}{dt} = \frac{r_H}{2}[Am]_{tot.} + \\ + \frac{r_{OH}}{2}[Am]_{tot.}\frac{[AmO_2^+]}{[AmO_2^+] + \frac{2k_3}{k_7}[OH]_{st}}, \quad (17)$$

where $[OH]_{st}$ is the stationary concentration of OH radicals.

Writing (17) in the form

$$-\frac{d[AmO_2^+]}{dt} = \frac{r_H}{2}[Am]_{tot.} + \\ + \frac{r_{OH}}{2}[Am]_{tot.}\frac{[AmO_2^+]}{[AmO_2^+] + c} \quad (18)$$

and integrating it, we obtain a relation of Am (V) concentration to time:

$$[AmO_2^+] = [AmO_2^+]_0 - \frac{k_\alpha}{2}[Am]_{tot.}t + \\ + \beta_1 \ln\frac{[AmO_2^+]_0 + \beta_2}{[AmO_2^+] + \beta_2}, \quad (19)$$

where $k_\alpha = r_H + r_{OH}$; $\beta_1 = \frac{r_{OH}}{k_\alpha}c$; $\beta_2 = \frac{r_H}{k_\alpha}c$.

When the difference between $[AmO_2^+]_0$ and $[AmO_2^+]$ is small, the term in (19) containing the logarithm of the ratio is close to zero and the AmO_2^+ concentration changes practically linearly with respect to time. As AmO_2^+ is reduced, the last term in (19), which allows for the relation of the reduction rate to AmO_2^+ concentration, begins to have an effect.

The constants β_1 and β_2 may be determined by rearranging (19) to the form

$$\beta_1 \ln\{[AmO_2^+] + \beta_2\} = x - A, \quad (20)$$

where $x = \frac{k_\alpha}{2}[Am]_{tot.}t + [AmO_2^+]$; $A = [AmO_2^+]_0 + \\ + \beta_1 \ln\{[AmO_2^+]_0 + \beta_2\}$,

or as the exponential function

$$[AmO_2^+] = \frac{e^{x/\beta_1}}{e^{A/\beta_1}} - \beta_2. \quad (21)$$

All the values included in the expression for x are determined experimentally and a graph of (21) may be plotted from them. Taking three values of x, related by the expression $x_3 = (x_1 + x_2)/2$ and the corresponding values of the AmO_2^+ concentration, $[AmO_2^+]_i$, we obtain the constant β_2 by the equation

$$\beta_2 = \frac{[AmO_2^+]_1[AmO_2^+]_2 - [AmO_2^+]_3^2}{[AmO_2^+]_1 + [AmO_2^+]_2 - 2[AmO_2^+]_3}. \quad (22)$$

Knowing the value of the constant β_2, we may plot the graph of equation (20) and, from the slope of the line obtained, determine the value of the constant β_1. Figure 4 shows the relation $\ln\{[AmO_2^+] + \beta_2\}$ to $x = k_\alpha/2[Am]_{tot} \cdot t + [AmO_2^+]$ for one of the experiments (0.2 M $HClO_4$ + 1.0 M Li_2SO_4).

The linear dependence obtained indicates that (19) and, hence, our initial hypotheses are confirmed by the experimental results.

Knowing the values of constants β_1 and β_2 we may determine the values of the constants r_H and r_{OH} and the

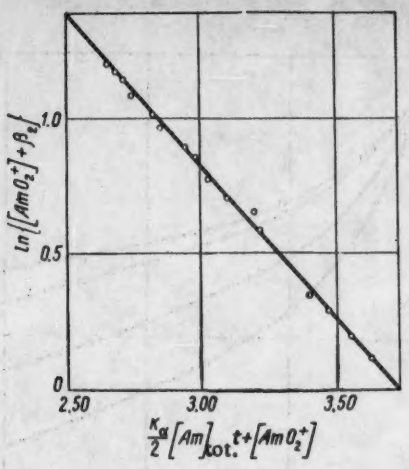

Fig. 4. Relation of $\ln\{[Am(V)]+\beta_2\}$ to $\frac{k_\alpha}{2}\times$ $\times[Am]_{tot.}t+[Am(V)]$ for 0,2 *M* $HClO_4$+ +1,0 *M* Li_2SO_4: $[Am]_{tot.}=3,19$ mM; $\frac{k_\alpha}{2}=1,58\cdot10^{-2}$ hr^{-1}; $\beta_2=0,90$ mM.

yields of hydrogen and OH radicals (using the relation between r_i and G_i). Actually

$$\beta_1+\beta_2=\frac{r_{OH}}{k_\alpha}c+\frac{r_H}{k_\alpha}c=\frac{r_{OH}+r_H}{k_\alpha}c=c. \quad (23)$$

Substituting the value $c=\beta_1+\beta_2$ in the expression for β_1 and β_2, we obtain

$$r_{OH}=\frac{\beta_1}{\beta_1+\beta_2}k_\alpha;\quad r_H=\frac{\beta_2}{\beta_1+\beta_2}k_\alpha. \quad (24)$$

If one considers that $r_{H_2O_2}=r_{OH}/2$, then having determined the constants k_α, β_1, and β_2, we may calculate the values of the hydrogen peroxide and hydrogen radical yields for various solutions (Table 3). The values given for the hydrogen peroxide yield for 0.1 and 1.0 M H_2SO_4 agree well with the values for $G_{H_2O_2}$ obtained by measuring the accumulation of hydrogen peroxide in Am^{3+} solutions. This agreement confirms the accuracy of the mechanism proposed for the reduction of AmO_2^+.

Table 3. Yields of hyrogen peroxide and hydrogen radicals in sulfuric and perchloric acid solutions.

Composition and concentration of solution, mole/liter	$G_{H_2O_2}$, molecules/100 ev	G_H, molecules/100 ev
0.1 H_2SO_4	1.16±0.04	1.86±0.11
1.0 H_2SO_4	0.54±0.04	1.87±0.07
0.2 $HClO_4$+ +1.0 Li_2SO_4	0.78±0.04	1.73±0.08
0.2 $HClO_4$+ +2.0 Li_2SO_4	0.81±0.04	1.01±0.02
2.0 $HClO_4$	1.15±0.03	1.02±0.09
2.0 $HClO_4$+ +4.0 $NaClO_4$	0.56±0.02	2.82±0.04

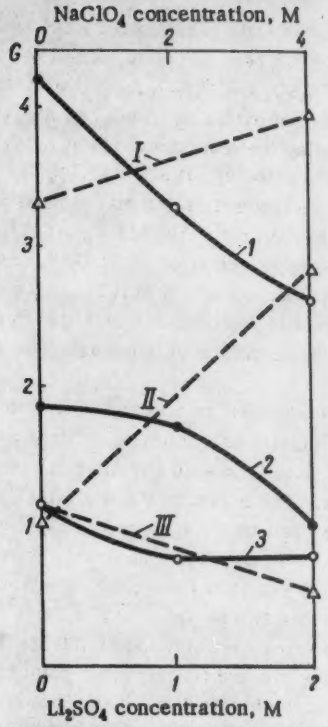

Fig. 5. Changes in the reduction yield of AmO_2^{2+} and partial yields of hydrogen peroxide and hydrogen radicals in relation to sulfate and perchlorate ion concentrations:

1 – $G_{Am(VI)}$ (0,2 *M* $HClO_4$+*n M* Li_2SO_4) $n=0, 1, 2$;
2 – G_H (0,2 *M* $HClO_4$+*n M* Li_2SO_4) $n=0, 1, 2$;
3 – $G_{H_2O_2}$ (0,2 *M* $HClO_4$+*n M* Li_2SO_4) $n=0, 1, 2$;
I – $G_{Am(VI)}$ (2 *M* $HClO_4$+*n M* $NaClO_4$) $n=0,4$;
II – G_H (2 *M* $HClO_4$+*n M* $NaClO_4$) $n=0,4$;
III – $G_{H_2O_2}$ (2 *M* $HClO_4$+*n M* $NaClO_4$) $n=0,4$.

Figure 5 presents curves of the change in reduction yield of AmO_2^{2+} and partial yields of hydrogen peroxide and hydrogen radicals in relation to the lithium sulfate and sodium perchlorate concentrations at constant acidity. The values obtained for $G_{H_2O_2}$ and G_H for 0.1 H_2SO_4 were taken for the point corresponding to 0.2 M $HClO_4$ (Li_2SO_4 concentrations were equal to zero). Such a substitution is justified as the reduction yields of AmO_2^{2+} in 0.2 M $HClO_4$ and 0.1 M H_2SO_4 were practically the same (see Table 1).

As Fig. 5 shows, the increase in Li_2SO_4 concentration led to a decrease in the reduction yield of AmO_2^{2+} due to the decrease in the hydrogen peroxide and hydrogen radical yields. The fall in hydrogen peroxide yield with an increase in Li_2SO_4 or H_2SO_4 concentration and the related decrease in the reduction yield of AmO_2^{2+} (see Tables 1 and 3) may be explained by the occurrence of the following reactions in sulfuric acid solutions:

$$OH + HSO_4^- = OH^- + HSO_4 \quad (25)$$

or

$$OH + H_2SO_4 = H_2O + HSO_4, \quad (26)$$

which compete with the reaction OH + OH = H_2O_2, and lower the hydrogen peroxide yield. The HSO_4 radical or the peracids H_2SO_4 and $H_2S_2O_8$ formed with its participation are capable of oxidizing AmO_2^+ to AmO_2^{2+} and even further decreasing the reduction yield of AmO_2^{2+}. The formation of the peracids H_2SO_5 and $H_2S_2O_8$ during the γ irradiation of sulfuric acid solutions has been proved experimentally by Daniels, Lion, and Weiss [11]. A certain increase in the reduction yield of AmO_2^{2+}, observed in 10 M H_2SO_4 in comparison with 6 M H_2SO_4 was apparently due to the direct action of radiation on H_2SO_4 molecules, which led to the formation of reducing agents of the SO_2 type.

The reduction yield of americium in concentrated (9 and 12 M) perchloric acid solutions differed from the reduction yield in sulfuric acid and more dilute perchloric acid solutions. The reduction yield of AmO_2^{2+} in 9 M $HClO_4$, which was first ~2.9, decreased rapidly (Fig. 6). With an increase in the total americium concentration and, consequently, the radiation dose, the reduction yield decreased more sharply. No reduction of AmO_2^{2+} in 12 M $HClO_4$ was observed over a period of 300 hr. This phenomenon is extremely interesting from the point of view of stabilization of the higher valence states of americium. The very slow reduction or the complete absence of reduction of americium in concentrated perchloric acid is probably related to the radiolytic decomposition of perchloric acid. M. Cottin [12] showed that the action of

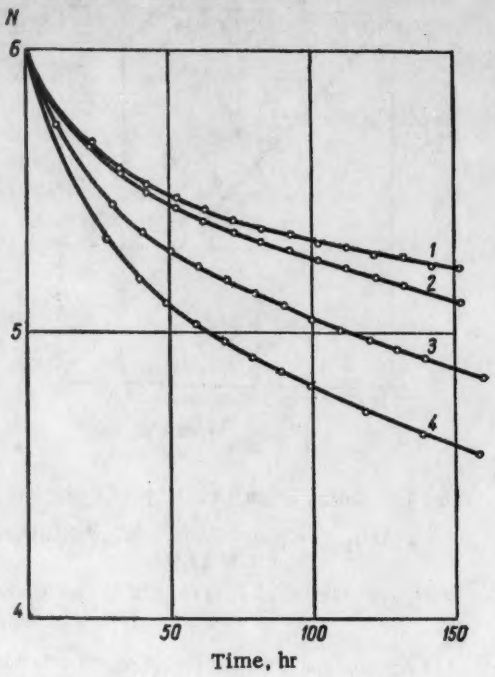

Fig. 6. Change in mean valence state (N) of americium in radiolytic reduction in 9.0 M $HClO_4$. Americium concentration, mM: 1) 4.69; 2) 4.60; 3) 3.83; 4) 2.02.

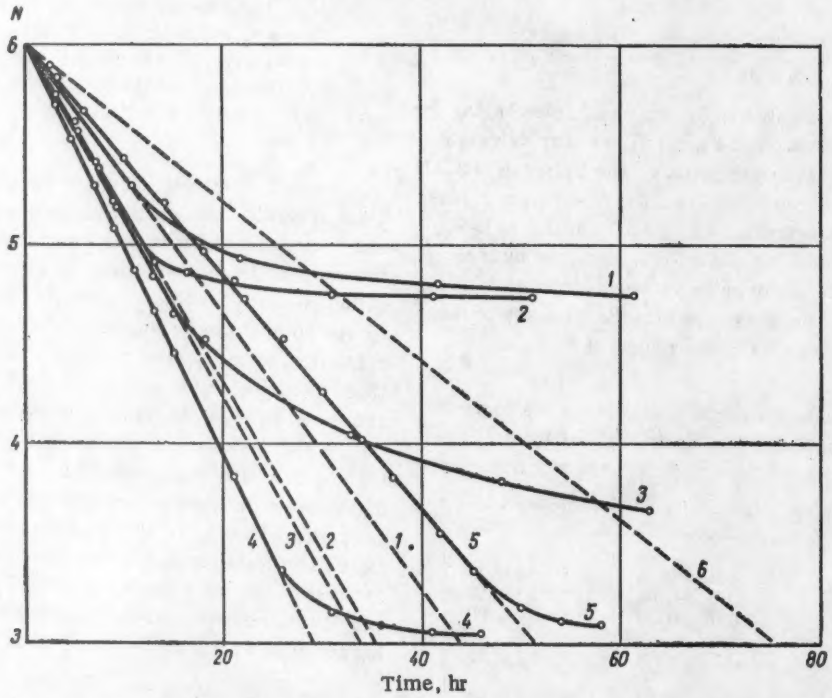

Fig. 7. Change in the mean valence state (N) of americium in radiolytic reduction in nitric acid: 1) 0.5 M HNO_3; 2) 3.0 M HNO_3; 3) 6.0 M HNO_3; 4) 9.0 M HNO_3; 5) 14.3 M HNO_3; 6) 0.2 M $HClO_4$.

γ radiation on concentrated perchloric acid solutions gave Cl_2 and ClO_2. One may also suppose that the action of Am^{241} radiation also caused the formation of chlorine and chlorine dioxide, which hindered the reduction of Am (VI) and Am (V). Such a supposition was confirmed by the following observations: the optical density of Am^{3+} solutions in 12 M $HClO_4$ increased rapidly in the short wavelength region of the spectrum ($\lambda < 500$ mμ) and this may have been caused by the formation of Cl_2 and ClO_2 as they absorb in this region of the spectrum.

The effect of temperature on the reduction rate of AmO_2^{2+} was studied in 4.0 M $HClO_4$ + 2.0 M $NaClO_4$ solution. The values of the reduction yields of Am_2^{2+} in 4.0 M $HClO_4$ + 2.0 M $NaClO_4$ solution for 25, 50, and 75°C are given below:

Temperature	$G_{AmO_2^{2+}}$
°C	ions/100 ev
25	3.67
50	4.07
75	15.9*

* Initial value of reduction yield of AmO_2^{2+}.

The reduction yield of AmO_2^{2+} at 75° C decreases with a decrease in Am (VI) concentration. From the increase in the reduction rate of AmO_2^{2+} with temperature, and also from the dependence of the reduction rate on AmO_2^{2+} concentration, one may assume that with an increase in temperature, AmO_2^{2+} is reduced by water as the radiolytic reduction should not depend strongly on temperature. This hypothesis could be confirmed conclusively by investigations using the longlived isotope of americium Am^{243}.

Radiolytic reduction of Am (VI) and Am (V) in nitric acid solutions. The curves of the change in the mean valence state of americium in relation to nitric acid concentration are shown in Fig. 7. The linear sections of the curves correspond to the Am (VI) content of the solution and this indicates that the general kinetic rules governing the radiolytic reduction of AmO_2^{2+} (observed in perchloric and sulfuric acid solutions) are also obeyed in the case of nitric acid.

However, the reduction yield of Am (VI) in nitric acid is a factor of approximately 1.5-2 higher than the maximum yield obtained in 0.2 M $HClO_4$ and 0.1 M H_2SO_4 and, in contrast to that obtained in perchloric and sulfuric acid solutions, increases with an increase in the nitric acid concentration (with the exception of 14.3 M HNO_3 where the reduction yield of AmO_2^{2+} decreased). The values obtained for the rate constants and reduction yields of AmO_2^{2+} in nitric acid solutions are given below:

HNO_3 concentration, M	$k_\alpha \cdot 10^2$, (hr^{-1})	G AmO_2^{2+} ions/100 ev
0.5	6.9	7.1
3.0	8.6	8.9
6.0	8.7	9.0
9.0	10.3	10.6
14.3	5.8	6.0

In contrast to Am (VI), Am (V) was reduced very slowly in nitric acid and its reduction rate decreased with a decrease in AmO_2^+ concentration. The maximum reduction rate of AmO_2^+ was ~1% per hour in 0.5 M HNO_3 and 0.8% per hour in 3.0 M HNO_3. No hydrogen peroxide was detected in the nitric acid solutions.

The change in the character of the radiolytic reduction of AmO_2^{2+} and AmO_2^+ in nitric acid as compared with that in perchloric and sulfuric acids seems to indicate that in nitric acid solutions the reduction is produced by secondary products, formed by the action of radicals on nitric acid. The total yield of such secondary products (in equivalents) is greater than the total yield of reducing products of water radiolysis and this leads to an increase in the reduction rate of AmO_2^{2+}. On the other hand, the secondary products obtained are weak reducers relative to AmO_2^+.

A similar increase in reduction rate of Ce (IV) in nitric acid was explained by the formation of nitrite ions [13]. We tested the reducing action of nitrite ions on AmO_2^+. It was found that the addition of sodium nitrite in an amount ten times greater than that of AmO_2^{2+} did not result in an acceleration of the very slow radiolytic reduction of AmO_2^+ in 1.0 M HNO_3. In contrast, AmO_2^{2+} ions were effectively reduced by nitrite. The different behavior towards nitrite ions apparently explains the different character of the reduction of AmO_2^{2+} and AmO_2^+ in nitric acid solutions.

LITERATURE CITED

1. L. Werner and I. Perlman, J. Am. Chem. Soc. 73, 495 (1951).
2. S. Stephanou, J. Nigon, and R. Penneman, J. Chem. Phys. 21, 42 (1953).
3. G. Hall and P. Herniman, J. Chem. Soc. (1954) 2214.
4. L. Asprey and S. Stephanou, AECD-924 (1950).
5. S. Gunn, UCRL-2541 (1954).
6. G. N. Yakovlev, A. A. Zaitsev, V. N. Kosyakov, A. G. Rykov, and Yu. P. Sobolev, Coll.: Isotopes and Radiation in Chemistry [in Russian] (Izd. AN SSSR, 1958) p. 326.
7. G. Hall and T. Markin, J. Inorg. and Nuclear Chem. 2, 202 (1956).
8. G. Hall and T. Markini, J. Inorg. and Nuclear Chem. 4, 296 (1957).
9. G. N. Yakovlev and V. N. Kosyakov, "Investigations in the fields of geology, chemistry, and metallurgy," Reports of the Soviet Delegation to the International Conference on the Peaceful Use of Atomic Energy (Geneva, 1955) [in Russian] (Izd. AN SSSR, 1955) p. 237.
10. R. A. Penneman and L. B. Asprey, "Chemistry of nuclear fuel," Reports of Foreign Scientists to the International Conference on the Peaceful Use of Atomic Energy (Geneva, 1955) [in Russian] (Goskhimizdat, 1956) p. 475.
11. M. Daniels, J. Lion, and J. Weiss, J. Chem. Soc. (1957) 4388.
12. M. Cottin, J. Chim. Phys. 53, 903 (1956).
13. G. Challenger and B. Masters, J. Am. Chem. Soc. 77, 1063 (1955).

CHARACTERISTIC FEATURES OF THE MINERALOGY OF URANIUM

V. I. Gerasimovskii

Original article submitted October 4, 1958

The following characteristic features of the mineralogy of uraniun are discussed in the article: 1) all known uranium and uranium-bearing minerals contain oxygen; 2) uranium in minerals is present only in the tetra- and hexavalent states; 3) the bulk of the uranium in the earth's crust is concentrated in nonuranium minerals in the form of isomorphous replacement of other elements (thorium, zirconium, rare-earth elements, etc.); 4) the conditions under which uranium and uranium-bearing minerals are formed differ; 5) radioactivity is one of the most characteristic properties of uranium minerals.

Uranium occurs in various modes in the earth's crust. The uranium in the earth's crust forms chemical compounds (minerals), it appears isomorphously as ions in the crystalline structures of many nonuranium minerals, is present in the disseminated state (in an adsorbed form on the surface of crystals and grains of minerals composing rocks), and in the dissolved state (in liquid inclusions of minerals and in the intergranular solutions of rocks).

The most characteristic features of the mineralogy of uranium are as follows:

All known uranium and uranium-bearing minerals* contain oxygen. Uranium is an element of high chemical activity, which is confirmed by the absence of native uranium in nature; paragenetic associations with phosphorus, arsenic, vanadium, silicon, titanium, niobium, tantalum, rare-earth elements, thorium, calcium, copper, and other elements, as well as oxygen, are characteristic of uranium. Under natural conditions, uranium reacts with a large number of elements forming numerous uranium and uranium-bearing minerals.

Uranium minerals differ widely with respect to chemical composition. More than 100 uranium minerals are known at present. They are usually divided into the following groups: oxides, hydroxides (simple and complex), silicates, carbonates, sulfate-carbonates, sulfates, phosphates, arsenates, vanadates, and molybdates.

Of the uranium-bearing minerals, the most important with respect to uranium content are those included in complex oxides of titanium, niobium, tantalum (titanates, titanotantaloniobates), silicates of zirconium, thorium, and rare-earth elements, phosphates, etc.

Uranium in minerals is present only in the tetra- and hexavalent states. In primary uranium and uranium-bearing minerals of different origin (magmatic, pegmatitic, hydrothermal, and sedimentary), uranium is mainly tetravalent or less frequently, tetra- and hexavalent; the latter is usually present in lesser amounts. In minerals formed in the zone of oxidation uranium is always hexavalent, but it enters these minerals as the complex cation $[UO_2]^{2+}$, not as the ion U^{6+}. Because of the relatively large radius of the $[UO_2]^{2+}$ ion, its isomorphous introduction into the crystalline structures of nonuranium minerals is difficult; this limits the isomorphous dissemination of hexavalent uranium in other minerals. This explains the extensive development of various secondary uranium minerals in the zone of oxidation.

The bulk of the uranium in the earth's crust is present in uranium-bearing minerals as isomorphous replacements of certain elements in them (thorium, zirconium, rare-earth elements, calcium, etc.). In these minerals the uranium content sometimes reaches considerable amounts, particularly in minerals included in the group of complex titanium, niobium, and tantalum oxides.

The isomorphous introduction of tetravalent uranium in minerals containing thorium, zirconium, and rare-earth elements is due to the fact that their ionic radii are of similar dimensions (in A): $U^{4+} = 1.05$; $Th^{4+} = 1.10$; $Ce^{4+} = 1.02$; $Ce^{3+} = 1.18$; $Y^{3+} = 1.06$; $Zr^{4+} = 0.87$; $Ca^{2+} = 1.06$. Since there is less uranium than thorium, zirconium, rare-earth elements, or calcium in the earth's crust, it is often disseminated within the minerals of these elements.

In minerals of the oxide group, for example in thorianite and its varieties, uranium replaces thorium isomorphously. It was recently shown [1] that there is a continuous isomorphous transition series from uraninite $(U^4_{1-x}U^6_x) \cdot O_{2+x}$ to thorianite (ThO_2). These minerals have identical cubic structures of the fluorite type.

In minerals of the complex titanium, niobium, and tantalum oxide group, uranium is usually present in the composition of minerals which contain more niobium than tantalum and a considerable amount of rare-earth elements or calcium, the rare-earth elements of the yttrium group being present to a far greater extent than those of the cerium group. In these minerals uranium isomorphously replaces, probably, rare-earth elements of the yttrium group for the most part and, possibly, calcium also. The ionic radii of these elements and tetravalent uranium are almost the same and, moreover, the rare-earth elements of the yttrium group in these minerals predominate to a considerable extent over the cerium group. The replacement of

*Minerals in which uranium isomorphously replaces other elements.

the rare-earth elements of the yttrium group by uranium may be schematically represented in the form $U^{4+}Ti^{4+} \rightarrow \rightarrow Y^{3+}Nb^{5+}$. Titanium is always present in the composition of uranium-bearing minerals of the complex oxide group.

In phosphates, uranium isomorphously replaces thorium (in monazite), rare-earth elements of the yttrium group (in xenotime) and, probably, calcium (in apatite). In xenotime, yttrium isomorphously replaces uranium, possibly according to the system $U^{4+}Ca^{2+} \rightarrow 2Y^{3+}$. Calcium is usually present in xenotimes containing uranium.

In silicates, uranium isomorphously replaces thorium (in thorite and its varieties), rare-earth elements (in orthite), and zirconium (in zircon and its varieties); in the latter case, uranium, in all probability, replaces not only zirconium but also rare-earth elements, which are often present in considerable amounts in some of the varieties of zircon (up to 15.89% TR_2O_3).

It should be mentioned that a considerable part of the uranium present in the earth's crust is not concentrated in uranium and uranium-bearing minerals, but occurs in a disseminated state; this was first pointed out by V. I. Vernadskii [2].

The conditions of formation of uranium and uranium-bearing minerals are very dissimilar. They originate from very varied processes of mineral formation: magmatitic, pegmatitic, hydrothermal, sedimentary, metamorphic, and also from weathering processes in the supergene zone. The paragenetic associations of uranium and uranium-bearing minerals are also very different.

As a result of the magmatic process, uranium-bearing and, less frequently, uranium minerals are usually formed. These include: silicates (orthite, zircon, thorite, sphene), phosphates (xenotime, monazite, apatite), oxides (thorianite, possibly uranium oxides and complex oxides-brannerite, minerals of the pyrochlore group, euxenite-polycrase, fergusonite, etc.). Minerals included in the oxides and complex oxides are rarely found in magmatic rocks, the amounts being very small. Although widely distributed, uranium-bearing minerals of the silicate and phosphate group do not form large accumulations and their uranium content is low.

In minerals of magmatic origin, the uranium is primarily tetravalent and isomorphously replaces thorium, zirconium, rare-earth elements, and calcium.

In pegmatites, the bulk of the uranium is not concentrated in uranium minerals, which are represented mainly by uraninite and its varieties, but in uranium-bearing minerals. Of the latter, the minerals of the complex oxide group, particularly titanotantaloniobates, are the most widely distributed.

In uranium and uranium-bearing minerals, the uranium is usually tetravalent, but often tetra- and hexavalent. Tetravalent uranium isomorphously replaces thorium, rare-earth elements, calcium, and zirconium.

Pegmatites containing uranium-bearing and uranium minerals are generally associated with acid rocks and are most widely distributed over the Precambrian shields of Canada, Brazil, Scandinavia, Africa, Australia, and India. According to Page's data [3], in the majority of cases, uranium-bearing and uranium minerals are correlated with pegmatites rich in potash feldspar; within the pegmatites, they are correlated with zones rich in perthite. The paragenetic associations of uranium-bearing and uranium minerals in pegmatites are very varied.

At the present time uranium ores are extracted from the Bancroft (Ontario) pegmatites only; these are composed of microcline, acid plagioclase, and quartz. Uraninite, uranothorite, fluorite, zircon, sphene, pyrite, pyrrhotine, and calcite are found in these pegmatities [4].

The hydrothermal process is characterized by the presence of a small number of uranium minerals. In deposits of hydrothermal origin only uranium oxides (uraninite and pitchblende†) are widely distributed; small amounts of complex oxides (davidite) and silicates (coffinite) occur. In uraninite and pitchblende, thorium and rare-earth elements of hydrothermal origin are generally absent or are found in small amounts (usually not more than 1%), whereas uraninite from pegmatites contains up to 12.24% TR_2O_3 and up to 14% or more ThO_2. V. I. Vernadskii [2] was the first to indicate that although the geochemical fate of uranium and thorium in pegmatites is the same, only uranium is characteristic of the hydrothermal process. At the same time he also noted the absence of thorium in the composition of pitchblende of hydrothermal origin. The separation of uranium and thorium in the late magmatic stage could be due to the oxidation of tetravalent uranium to the hexavalent form, which was removed by hydrothermal solutions separating from tetravalent thorium.

In uraninite and pitchblende, uranium is tetra- and hexavalent, the tetravalent form being generally predominant if these minerals have not undergone exogenic modification. Hexavalent uranium in uraninite and pitchblende is formed by the oxidation of tetravalent uranium as a result of radioactive decay; it is possible that it entered into the composition of these minerals at the time of formation.

The paragenetic associations of uranium oxides (uraninite and pitchblende) in deposits and ore occurrences of hydrothermal type are very varied. Uranium oxides are almost always found together with sulfides, quartz, and carbonates. One of the most interesting mineral associations is uranium-nickel-cobalt-silver-bismuth: often called the arsenide association. Nickel, cobalt, and iron arsenides, and also native bismuth and silver, frequently copper and silver sulfides, etc., are characteristic of uranium deposits of this type. Of the uranium minerals, pitchblende is found. The mineralization sequence for the Eldorado deposit (Canada) is as follows [5]: hematite–quartz;

† Uranium oxides found as crystals are included in uraninite; cryptocrystalline, usually collomorphic, compact, nodular, sinter, and botryoidal aggregates are included in pitchblende.

pitchblende–quartz; quartz–nickel and cobalt arsenides; copper sulfides–chlorite; carbonates–native metals (silver, bismuth).

The second, most widely distributed mineral association in uranium deposits and ore occurrences of the hydrothermal type is that of uranium oxides with sulfides (the sulfide type of deposits). It is very varied and the following subtypes may be distinguished:

1. The association of pitchblende with ordinary sulfides, pyrite (sometimes marcasite), sphalerite, galena, and chalcopyrite. Pyrite is usually the most widely distributed of these. Of the vein minerals, quartz is characteristic (often chalcedonic and jaspery); carbonates and fluorite sometimes occur. The uranium deposits in France, Portugal, and other countries may be mentioned by way of example [6].

2. The association of pitchblende with molybdenum is one of the most widely distributed in uranium hydrothermal deposits of the USSR. Pyrite, arsenopyrite, blende, galena, chalcopyrite, marcasite, calcite, quartz, ankerite, manganocerite, chlorites, hydromicas, and fluorite are found in paragenesis with pitchblende and molybdenite [7].

The joint occurrence of pitchblende and amorphous molybdenite (jordisite) is known in the Marysville deposit (Utah), where pitchblende is found together with pyrite, magnetite, hematite, quartz, chalcedony, fluorite, and adularia. Here, the secondary minerals of molybdenum-umohoite (uranium molybdate) and ilsemanite–are found, in addition to the primary molybdenum mineral jordisite [8].

3. The association of pitchblende with galena has been established in deposits in the USSR. The pitchblende and galena are accompanied by the following minerals: molybdenite, sphalerite, tetrahedrite, pyrargyrite, chalcopyrite, marcasite, and also calcite, sericite, flourite, albite, quartz, chlorite, etc., [7].

4. The association of pitchblende with sphalerite has been found in deposits in the USSR. Pitchblende and sphalerite are found together with galena, molybdenite, chalcopyrite, chlorite, quartz, calcite, fluorite, etc., [7].

5. The association of pitchblende with sulfides is very widely distributed in certain deposits in the USSR. The following minerals are found in association with pitchblende: native copper, bismuth and silver, goethite, hematite, chalcopyrite, bornite, chalcosite, covellite, marcasite, sphalerite, galena, tennantite, molybdenite, calcite, and, occassionally, quartz, chlorite, dolomite, barite, etc., [7].

6. The association of uraninite with gold. This association is found in the Chihuahua deposit (Mexico) and the deposits of the Central City region (Colorado). In the Chihuahua deposit the uranium mineralization (uraninite) is found in veins composed of quartz and calcite with a very slight feldspar content. The ore minerals are: uraninite, pyrite, native gold, and a small amount of magnetite. In the deposits of the Central City region [9] pitchblende is found in association with native gold and sulfides (pyrite, sphalerite, chalcopyrite, enargite) in quartz veins containing carbonates.

7. The association of pitchblende with silver is found in the deposit of the Boulder Batholith region (Montana). Here pitchblende is observed together with argentite, pyrite, galena, sphalerite, and chalcopyrite; the vein minerals are microcrystalline quartz, chalcedony, calcite, and siderite [10].

8. The association of uraninite with nickel and cobalt sulfides is known in the Shinkolobwe (Belgian Congo) deposit [11]. Here sulfides are widely distributed: cattierite (CoS_2), nickelcattierite, vaesite (NiS_2), cobalt-vaesite and siegenite (nickel-bearing linnaeite). The usual accessory minerals are: pyrite, chalcopyrite, and molybdenite; gold is found. Carbonates (magnesite, dolomite) have developed to a considerable extent in the deposit. Of the other nonore minerals, quartz and chlorite should be mentioned. According to the data of G. Derriques and G. Vaes, the deposition of the mineral associations in the deposit took place in the following order: first stage–formation of magnesite, second stage–separation of uraninite, third stage–deposition of molybdenite, monazite, and chlorite (selenium being associated with this stage), fourth stage–deposition of sulfides, cobalt, and nickel (vaesite, cattierite, and their varieties), fifth stage–formation of dolomite and chalcopyrite.

The association of pitchblende with hematite, which is the most widely distributed ore mineral (third type) is also characteristic of deposits of hydrothermal types. Sulfides–the most usual of which are pyrite, chalcopyrite, and galena–are nearly always present, but in slight amounts. The vein minerals are calcite, quartz, and chlorite. This type includes the uranium deposits in the region of Beaver Lodge Lake, located north of Lake Athabaska (Saskatchewan) [12, 13].

The joint occurrence of uraninite and nenadkevite, which are probably of hydrothermal origin (fourth type), is of great interest. Nenadkevite [14] is found in zones of sodium metasomatism of the iron-uranium deposit in paragenetic association with brannerite, yttrosphene, uraninite, uranium-bearing malacon, and apatite.

Davidite is probably included in the uranium minerals of the hydrothermal type. Its association with other minerals (fifth type) is very unusual and is little characteristic of deposits of the hydrothermal type. For example, the davidite from Radium Hill (Australia) is present in intimate association with rutile, ilmenite, hematite and, less frequently, magnetite; this close association is also found with the nonore minerals, namely quartz and biotite [15].

Of the uranium minerals, coffinite is found–although rarely–in hydrothermal deposits.

Other paragenetic associations for uraninite and pitchblende, as well as those mentioned for uranium minerals, are known in hydrothermal deposits.

During the process of formation of sedimentary rocks, only an insignificant part of the uranium enters into the

uranium minerals. The uranium minerals of sedimentary origin include pitchblende and coffinite. Pitchblende is widely distributed, and in sedimentary rocks is usually associated with organic matter, iron sulfides (pyrite, marcasite), less frequently with copper, lead and zinc sulfides, phosphates, and sometimes with vanadium, molybdenum, etc.

An association with vanadium (montroseite, roscoelite), sulfides of iron (pyrite, marcasite), copper (chalcopyrite, bornite, chalcosite, and covellite), lead (galena), carbonates (calcite, dolomite), and also with organic matter is characteristic of the pitchblende of sedimentary deposits, for example the Colorado Plateau (USA) [16].

Coffinite is widely known only on the Colorado Plateau. For example, in the Ambrosia Lake deposit (New Mexico), one of the largest uranium deposits in the USA, uranium is represented by coffinite and is closely associated with asphaltitic matter [17].

As in magmatic rocks, the bulk of the uranium in sedimentary rocks is present in a disseminated state. The distribution of uranium in sedimentary rocks is not uniform It is correlated to organic matter, calcium phosphates, clay minerals, iron and manganese hydroxides. The association of disseminated uranium with organic matter, in which it is often concentrated, is particularly characteristic. As far back as 1934, V. I. Vernadskii wrote, with regard to this problem, that the concentration of uranium by organic matter is the exceptional fact in its geological history [2].

It is now generally recognized that the organic matter of sediments concentrates uranium within itself. Uranium-bearing marine black shales are well known in the USA, Sweden, and other countries [18, 19]. Uranium is found in coal and petroleum products as uranium-bearing bitumens (asphaltites).

According to the representations of contemporary investigators [20, 21], the concentration of uranium by organic matter takes place as a result of the formation of uranium oxides (pitchblende), the sorption of uranium—in all probability as the uranyl ion (UO_2)—and the formation of organic complexes of uranium (uranium humates and fulvates, and melanoidines containing uranium), in which the uranium is probably present in the hexa- and tetravalent states. In coal, the bulk of the uranium is sometimes present as oxides closely associated with pyrite [22].

As a result of the decomposition of organic matter under reducing conditions, hydrogen sulfide is formed which, together with the carbon of the native organic matter, assists the reduction of hexavalent uranium to the tetravalent form and precipitates the latter as finely divided uranium oxide (pitchblende). In deposits of sedimentary origin, pitchblende is usually accompanied by pyrite.

Uranium is concentrated in marine sedimentary rocks containing phosphorites, According to one representation, uranium is introduced in calcium phosphates by the isomorphous replacement of their calcium [23, 24]; another opinion is that it is introduced as a result of sorption [25]. Uranium minerals are not formed in phosphate rocks, even when they have a high uranium content.

It should be noted that a new uranium mineral, ningyôite—$CaU^{4+}(PO_4)_2 \cdot nH_2O$—has been found in Japan, in the lacustrine deposits of NingyoTogé [26].

An important role in the accumulation of uranium in sedimentary rocks is played by sorption processes, both at the time these rocks were formed (syngenetic deposits) and after their formation, as a result of epigenetic ore-formation.

Monazite deposits are included in uranium-bearing sedimentary rocks. For example, Indian monazite contains 0.2-0.46% U_3O_8 and 5-11% ThO_2. A variety of monazite, called cheralite, containing 4-6% of U_3O_8 and 19-32% ThO_2, was found there.

The behavior of uranium during metamorphic processes has been poorly studied. Uraniun oxides: uraninite, pitchblende, and brannerite, which are present in association with thucolite, are found in metamorphic deposits of uranium minerals. The uranium-bearing conglomerates of Witwatersrand (South Africa), Blind River (Canada), etc., are examples of metamorphic deposits.

In the Witwarersrand deposits, uraninite is found together with thucolite, or without it, in gold-bearing conglomerates consisting of quartz pebbles cemented with fine-grained quartz, sericite, and chlorite. Pyrite, pyrrhotite, galena, sphalerite, chalcopyrite, pentlandite, cobaltite, linnaeite, and arsenopyrite are also found in the conglomerates. Thucolite is a mixture of solid hydrocarbons, uraniumoxide, and other minerals [27].

In the uranium-bearing conglomerates of the Blind River region [28] the uranium minerals (brannerite, uraninite, pitchblende) are present in the matrix cementing the conglomerate and consisting of quartz grains, sericite, chlorite, and pyrite (up to 15%). The latter is present in intimate association with the uranium minerals, together with which thucolite is sometimes found as well. Pyrrhotine, galena, sphalerite, chalcopyrite, molybdenite, marcasite, and cobaltite are also found in the uranium-bearing conglomerates.

As a result of weathering processes numerous secondary uranium minerals—which are particularly varied in the zone of oxidation—are formed in the supergene zone from primary uranium minerals, principally uraninite and pitchblende.

In the minerals of the zone of oxidation the uranium is usually hexavalent and, in the form of the uranyl group $(UP_2)^{2+}$, plays the part of a bivalent cation.

Uranium black (oxides), hydronasturan and ianthinite (hydroxides), lermontovite (phosphate), and moluranite (molybdates) are examples of secondary uranium minerals formed in the zone of cementation. In uranium minerals formed in this zone the uranium is tetra- and hexavalent, the latter usually predominating over the tetravalent form.

The composition of the uranium minerals in the supergene zone and their paragenetic associations are determined mainly by the composition of the primary ore and vein minerals and the adjoining strata, in which the uranium mineralization is present, and also the climate, relief, tectonics, hydrogeological conditions, etc.

The paragenetic associations of the uranium minerals of the zone of oxidation are very varied. They may be divided into two main types.

Uranium phosphates and arsenates are characteristic of the first type. They are usually formed in the zone of oxidation of deposits, the primary ores of which contain a considerable amount of sulfides (particularly pyrite). As a result of the decomposition of the sulfides, the solutions in the zone of oxidation acquire a sulfate character; in consequence, conditions are produced for the solution and transfer of uranium from the zone of oxidation of uranium deposits and also for the formation of secondary minerals—often of very varied composition—in them. Zonality is sometimes observed in the distribution of uranium minerals in the zone of oxidation of uranium deposits. A clearly expressed vertical zonality—pitchblende, uranium black, uranium arsenates, uranium phosphates, uranium silicates, uranium-bearing hyalite, etc.—was investigated and described [29] by way of the example of one of the deposits with a well-developed zone of oxidation.

Three stages of development of the zone of oxidation are usually distinguished: the initial, middle, and final [30]. The role of the (SO_4^{2-}) ion in the water of the zone of oxidation in the final stage of its development is negligible, and the (CO_3^{2-}) and (SiO_3^{2-}) ions become very important. In the upper level of the zone of oxidation, oxidizing processes are usually present in the final stage of its development, as opposed to the middle and lower levels, and uranium silicates instead of uranium phosphates and arsenates are, therefore, formed in it, as a result of the increase in the pH of the solutions.

The second type of zone of oxidation of hydrothermal uranium deposits is characterized by the development of uranium silicates and hydroxides. It is usually observed in the zone of oxidation of deposits in which sulfides are either absent or are present in very small amounts, and where there is a considerable amount of carbonates in the vein minerals. Under these conditions, the water circulating in the zone of oxidation has a hydrocarbonate character and a neutral or weakly alkaline reaction. Even in the presence of appreciable amounts of sulfides, if the bulk of the vein minerals of the deposit or the adjoining strata is composed of carbonates, the water circulating in the zone of oxidation does not acquire a sulfate character, which, as in the case of the first type, favors the formation of uranium phosphates and arsenates.

The hydrocarbonate character of the water in the zone of oxidation is due to the formation of uranium hydroxides and silicates. The reaction of alkaline carbonate solutions in the zone of oxidation, usually with strongly oxidized uranium minerals, uraninite and pitchblende, leads to the dissolution of these minerals, with the formation of uranyl-carbonate complexes. When the latter hydrolyze, uranyl hydroxides are formed. In hydrocarbonate water, which often has an alkaline character, a small amount of dissolved silica is always present [30]; the latter reacts with the uranyl ion, leading to the formation of uranyl silicates throughout the whole oxidation zone. The Shinkolobwe deposit may be mentioned as an example of a uranium deposit with a zone of oxidation containing uranium silicates and hydroxides. A considerable development of uranium hydroxides and silicates is observed in this deposit.

Intermediate types as well as the two main types of mineralization of the zone of oxidation of hydrothermal deposits are observed. Minerals of both the uranium phosphate and uranium silicate group are found in these intermediate types. Uranium deposits and ore occurrences of hydrothermal origin are known, in the zone of oxidation of which the uranium mineralization consists of one or two minerals of the phosphate or silicate group, for example parsonsite (the deposit at Lacheaux, France); autunite and torbernite (in a number of regions in France); torbernite and metatorbernite; uranophane; kasolite; etc. Moreover, uranium minerals are absent in the zone of oxidation of certain uranium deposits. In these deposits the uranium is present only in the disseminated state, being sorbed by Fe, Mn, and Si hydroxides. This is observed in deposits the primary ores of which contained only a small amount of sulfides with a good deal of ferruginous carbonates.

Taking into account the intermediate types of associations of uranium minerals, the following mineralogical types are sometimes distinguished in the zone of oxidation: hydroxide-silicate, true silicate, silicate-micaceous, true micaceous, micaceous-limonite, and true-limonite [31].

Uranium vanadates (carnotite and tyuyamunite) are sometimes widely developed in the zone of oxidation of uranium deposits and ore occurrences of sedimentary origin. One of the most important regions with this type of mineralization is the Colorado Plateau [16, 32, 33]. If the composition of the primary uranium ores includes a considerable amount of vanadium, only uranium vanadates are found in the secondary uranium minerals. Rauvite is found in weakly oxidized vanadium and uranium-bearing ores; the highly oxidized types of these ores contain carnotite and tyuyamunite. A local preponderance of tyuyamunite over carnotite is sometimes observed, this being due to the high calcium content in the adjoining sedimentary rocks.

In the zone of oxidation of pegmatites, because of their low sulfide content and high content of minerals containing alkalies, the water is unlikely to have a sulfate character; uranium hydroxides and silicates are, therefore, the most widely developed secondary uranium minerals in such cases and carbonates, phosphates (autunite), etc. are far less frequent.

In certain uranium deposits secondary uranium minerals may be absent if the primary ores contain a considerable amount of sulfides. If the sulfide contents are high (pyrite and marcasite), conditions are produced for the intense dis-

solution and transport of uranium beyond the limits of the deposits. Silicon hydroxide (opal), iron and manganese hydroxides, and also aluminohydrosilicates are usually uranium sorbents in the oxidation zone.

Regenerated uranium black, formed by the reduction of hexavalent uranium transported to the zone of cementation from the zone of oxidation by aqueous solutions, is very characteristic of the zone of cementation. Sedimentary uranium black, formed by the oxidation of tetravalent uranium in the zone of cementation and the lower part of the zone of oxidation, is also distinguished. In addition to uranium black, the hydrated products of uranium oxides, known as hydropitchblende, are found.

In the zone of cementation, and possibly also at the boundary between the zones of cementation and oxidation, the minerals ianthinite and lermontovite [34] are found with a limited distribution.

The determination of the forms in which uranium is transferred and deposited, particularly during the formation of deposits of hydrothermal and sedimentary origin, is of great importance in the geochemistry of uranium.

In magmatic and pegmatitic processes of mineral formation, the history of uranium (probably the tetravalent form) is the same as for thorium, zirconium, and the rare-earth elements, while in pegmatites it is the same as for niobium and tantalum.

During the hydrothermal process, uranium is separated from zirconium, thorium, rare-earth elements, niobium, tantalum, and titanium. Minerals of these elements are not characteristic of deposits of hydrothermal origin. During the hydrothermal process the bulk of the uranium is concentrated in the form of uranium oxides—pitchblende and, to a lesser extent, uraninite.

Varying opinions exist with regard to the forms in which uranium is transferred and deposited during the hydrothermal process. The majority of investigators [23, 34] consider that uranium is transferred in the hexavalent state by hydrothermal solutions and, very probably, in the form of carbonate complexes—possible as $[UO_2(CO_3)_3]^{4-}$.

According to A. G. Betekhtin, uranium is transferred in the tetravalent state; according to the data of V. V. Shcherbina and others [35], it is transferred in the tetra- or hexavalent state, depending on the conditions.

As is now recognized by the majority of investigators, in hydrothermal solutions bivalent iron, sulfide sulfur, and organic matter may be precipitants of hexavalent uranium with the formation of uranium oxides. This opinion is supported by experimental investigations [35, 36].

Particularly active attention is paid to iron as a reducer of hexavalent uranium because in many uranium deposits hematization of the adjoining rocks is observed, as a result of which the latter acquire a red color of varying shade. Amphiboles, pyroxenes, chlorites, carbonates, sulfides, and other minerals—both vein minerals and those of the rocks adjoining the uranium mineralization—may be a source of bivalent iron. The reduction of uranium by iron may be represented as follows: $U^{6+} + Fe^{2+} \rightarrow U^{4+}$ (uranium oxides) + Fe^{3+} (hematite).

The precipitation of hexavalent uranium from hydrothermal solutions may be due to the decomposition of uranyl-carbonate complexes as a result of a reduction in the alkalinity of uranium-bearing solutions and a lowering of their CO_3^{2-} ion concentration (removal of CO_2).

In the case of transfer of uranium in the tetravalent form, its precipitation from hydrothermal solutions as oxides is explained primarily by the change in the pH of the solutions as a result of their reaction with the adjoining rocks.

The forms of transfer and deposition of uranium in the supergene zone have been investigated more closely than for other zones. In this zone, uranium is most probably transferred as carbonate complexes of the type $Na_4[UO_2 \cdot (CO_3)_3]$, colloidal hydroxide solutions (sols) with the composition $[UO_2(OH)_2]_n$, and organic complexes (humates, fulvates, and melanoidines) [21].

The sulfate form of uranium transfer is evidently only of very limited importance within the limits of the zones of oxidation and cementation of uranium deposits and ore occurrences, because a 0.1 N solution of UO_2SO_4 is stable at a pH < 4.25.

The conditions for the precipitation of uranium in the supergene zone can vary widely. They have recently been examined very thoroughly by V. V. Shcherbina [37].

The conditions under which uranium is precipitated during the formation of sedimentary deposits vary. The precipitation of uranium on the bottom of water basins (syngenetic deposition of uranium) or from subsurface water in sedimentary rocks (epigenetic deposition of uranium) takes place principally from soluble complex carbonates or organic complexes of the uranium humate type, and possibly sols of uranium hydroxide, etc.

The precipitation of uranium takes place by the sorption of uranium by organic and inorganic sorbents, as a result of isomorphous replacements (for example, the replacement of calcium by uranium in phosphates) and the formation of uranium minerals. The precipitation of uranium is due to the change in the pH of the solutions, the lowering of the redox potentials, and the associated reduction processes under the influence of organic matter, sulfides, bivalent iron, etc. The reduction of hexavalent uranium to the tetravalent form is undoubtedly of great importance in the precipitation of uranium. This is confirmed by the fact that, as is well known, in deposits of sedimentary origin, uranium is nearly always found together with organic matter and sulfides (pyrite, etc.).

Radioactivity is one of the most characteristic properties of uranium minerals. As a result of the spontaneous decay of uranium a whole series of radioactive elements are formed, the end products of the decay being lead and helium. The radioactive decay of uranium is accompanied by the liberation of charged α and γ particles and gamma escape. This allows uranium minerals to be detected readily by means of radiation meters and also

makes it possible to determine the isotopic composition of their lead and establish their absolute geological age.

Another characteristic property of minerals containing uranium, their luminescence in ultraviolet rays, is used for detecting many of these minerals. The artificial-luminescent method is employed for detecting nonluminescent uranium minerals.

The data given indicate the great variety of uranium-bearing and uranium minerals. This is because of the high chemical activity of uranium, its ability to react with a large number of elements (and different valence forms of these elements as well). The crystallochemical characteristics of uranium also play an important role: it replaces isomorphously such elements as zirconium, thorium, rare earths, and calcium, leading to the formation of a large number of uranium-bearing minerals; in the zone of oxidation, many independent uranium minerals are formed since the uranium in this zone is present as the $(UO_2)^{2+}$ ion, which cannot enter the crystalline structure of other elements isomorphously since the ionic radius is too great.

The diversity of paragenetic associations of uranium minerals, particularly in hydrothermal deposits and the zone of oxidation, is also determined by their chemical properties which are due to the different forms of transfer and deposition of uranium.

In hydrothermal deposits associations of uranium oxides are particularly varied; this is probably also the result of the fact that uraninite and pitchblende are generally formed at the end of the hydrothermal process and are, therefore, superimposed on previously formed associations of minerals.

Of the uranium minerals, paragenetic associations of uranium oxides—uraninite and pitchblende—which are produced by different processes of mineral formation are of particular interest. In magmatic processes, uranium oxides (uraninite) are rarely formed, and only in very small amounts; they are, therefore, seldom found in pegmatites. This is probably explained by the unfavorable conditions for the formation of uranium minerals, principally by the quantitative preponderance of zirconium, thorium, and rare-earth elements over uranium, as a result of which uranium isomorphously replaces the above-mentioned elements in their minerals. The bulk of the uranium in pegmatites is accumulated in complex oxides of titanium, niobium and tantalum (titanotantaloniobates).

In the hydrothermal process the bulk of the uranium is combined as uranium oxides (pitchblende, less frequently uraninite), the characteristic feature of which is its paragenetic association with carbonates and sulfides of iron, copper, lead, molybdenum, etc., and sometimes with nickel and cobalt arsenides, often with iron oxides (hematite) as well, i.e., minerals which are not typical of magmatic and pegmatitic origin. The extensive distribution of uranium minerals—pitchblende and uraninite—in hydrothermal deposits is probably explained by the fact that zirconium, thorium, and rare earths, i.e., those elements which are isomorphously replaced by uranium, are not characteristic of the hydrothermal process.

In deposits of sedimentary origin, the uranium oxides (pitchblende) alone of the uranium minerals are widely distributed; these are usually found in close association with organic matter and frequently with sulfides, which indicates the formation of pitchblende from aqueous solutions in a reducing medium.

In both sedimentary and magmatic rocks uranium isomorphously enters the crystalline structure of other minerals and is present in the disseminated state. In this condition, uranium is readily leached from rocks and is of great interest because it is probably one of the most important sources for the formation of the uranium mineralization of industrial deposits.

LITERATURE CITED

1. S. Robinson and A. Sabina, Am. Mineralogist 40, 624 (1955).
2. V. I. Vernadskii, Outlines of Geochemistry [in Russian] (Gorgeonefteizdat, 1934).
3. Z. Page, Econ. Geol. 45, 12 (1950).
4. Z. Kelly, Canad. Mining J. 77, 87 (1956).
5. K. Donald, Canad. Mining J. 77, 77 (1956).
6. M. Rubo, The Geology of Atomic Raw Materials [in Russian] (Gosgeoltekhizdat, 1956) p. 270.
7. A. I. Tishkin, G. A. Tananaeva et al., "Paragenetic associations of hydrothermal uranium minerals in uranium deposits of the Soviet Union," Report No. 2741, presented to the Second Internation Conference on the Peaceful Use of Atomic Energy (Geneva, 1958).
8. G. V. Walker and F. V. Osterwald, Documents of the International Conference on the Peaceful Use of Atomic Energy [Russian translation] (Gosgeoltekhizdat, 1958) p. 337
9. T. Sims, Econ. Geol. 51, 739 (1956).
10. G. Becraft, Econ. Geol. 51, 362 (1956).
11. G. G. Derriques and G. F. Vaes, The Geology of Atomic Raw Materials [Russian translation] (Gosgeoltekhizdat, 1956) p. 323.
12. B. MacDonald and J. Kermeen, Canad. Mining J. 77, 80 (1956).
13. S. Robinson, Canad. Mining and Metallurg. Bull. 45, 204 (1956).
14. V. A. Polikarpova, Atomnaya Énergiya No. 3, 132 (1956).‡
15. "Ore occurrences of uranium and thorium in Australia," The Geology of Atomic Raw Materials [Russian translation] (Gosgeoltekhizdat, 1956) p. 302.
16. A. D. Weeks, Documents of the International Conference on the Peaceful Use of Atomic Energy. 6 [Russian translation] (Gosgeoltekhizdat, 1956) p. 609.
17. R. Zitting, Mines Mag. 47, 53 (1957).
18. "Uranium deposits in the USA," The Geology of Atomic Raw Materials [Russian translation] (Gosgeoltekhizdat, 1956) p. 220.

‡ Original Russian pagination. See C. B. Translation.

19. P. F. Kerr, "Uranium deposits in the USA," The Geology of Atomic Raw Materials [Russian translation] (Gosgeoltekhizdat, 1956) p. 220.
20. I. A. Berger and M. Jewel, "Uranium deposits in the USA," The Geology of Atomic Raw Materials [Russian translation] (Gosgeoltekhizdat, 1956) p. 220.
21. S. M. Manskaya, T. V. Drozdova, and M. P. Emel'yanova, Geokhimiya No. 4, 10 (1956).
22. Z. A. Nekrasova, "The problems of the forms of occurrence of uranium in certain coals," Report No. 2082, presented to the Second International Conference on the Peaceful Use of Atomic Energy (Geneva, 1958).
23. V. I. McKelvy, D. L. Everhard, and R. M. Garrels, The Geology of Atomic Raw Materials [Russian translation] (Gosgeoltekhizdat, 1956) p. 25.
24. I. G. Chentsov Atomnaya Énergiya No. 5, 113 (1956). ‡
25. E. V. Rozhkova, E. G. Razumnaya, M. B. Serebryakova, and O. V. Shcherbak, "The role of sorption in uranium concentration in sedimentary deposits," Report No. 2059, presented to the Second International Conference on the Peaceful Use of Atomic Energy (Geneva, 1958).
26. H. Katayama, "Genesis of the uranium deposit in tertiary sediments in the Ningyô-Tôgé area, western Japan," Report No. 1356, presented by the Japanese Delegation to the Second International Conference on the Peaceful Use of Atomic Energy (Geneva, 1958).
27. W. Liedenberg, Trans. Proc. Geol. Soc. Africa 58, 101 (1955).
28. F. Joubin and H. Donald, Canad. Mining J. 77, 84 (1956).
29. V. G. Melkov, Atomnaya Énergiya No. 1, 83 (1956).‡
30. S. S. Smirnov, The Oxidation of Sulfide Deposits [in Russian] (United Scientific and Technical Press, USSR, 1936) p. 40.
31. G. S. Gritsaenko, L. N. Belova, R. V. Getseva, and K. T. Savel'eva, "Mineralogical types of zones of oxidation of hydrothermal uranium and sulfide-uranium deposits of the USSR," Report No. 2155, presented to the Second International Conference on the Peaceful Use of Atomic Energy (Geneva, 1958).
32. Ya. V. Izakhsen, The Geology of Atomic Raw Materials [Russian translation] (Gosgeoltekhizdat, 1956) p. 396.
33. R. F. Fisher, The Geology of Atomic Raw Materials, [Russian translation] (Gosgeoltekhizdat, 1956) p. 374.
34. V. G. Melkov and L. Ch. Pukhal'skii, Prospecting of Uranium Deposits [in Russian] (Gosgeoltekhizdat, 1937).
35. R. P. Rafal'skii, "Experimental investigations of the conditions of transfer and deposition of uranium by hydrothermal solutions," Report No. 2067, presented to the Second International Conference on the Peaceful Use of Atomic Energy (Geneva, 1958).
36. G. B. Naumov and K. I. Tobelko, Geokhimiya No. 4, 24 (1956).
37. V. V. Shcherbina, Geokhimiya No. 6, 493 (1957).

‡ Original Russian pagination. See C. B. translation.

CYCLOTRON WITH A MAGNETIC FIELD TRAVELING IN THE RADIAL DIRECTION

E. G. Komar

Original article submitted January 6, 1959

In this paper we consider the design of a cyclotron with a magnetic field which travels in the radial direction; a machine of this kind had been proposed by the author. By means of circular windings which are fed by ac generators it is possible to produce one or more concentrated magnetic fields which travel in the radial direction in the gap.

Two versions are proposed. In the first, the traveling wave is the field in which the particles are accelerated. In the second, the traveling wave is superimposed on the usual fixed magnetic field and acceleration takes place by virtue of the combined fields. The spatial distribution of the field in the wave makes it possible to obtain a stability region ($1 > n > 0$) which is displaced in the radial direction with the radial velocity of the particles. A stability region is also obtained in the case in which the absolute value of the magnetic field of the acceleration region increases in the radial direction.

In principle the system proposed here makes it possible to build cyclotrons with energies as high as desired. In spite of the cyclic-action characteristics of the acceleration, because of the improved focusing there is reason to believe that the mean intensity can be larger than that which is obtained in the fm cyclotron.

Typical calculations are given for accelerators of various energies. These calculations indicate that the weight and size of these accelerators may be much smaller than other accelerators of the same energy.

GENERAL CONSIDERATIONS

The cyclotron proposed here differs from the conventional cyclotron in that the particles are accelerated by a magnetic field which moves out radially from the center of the machine. A method for obtaining a magnetic wave of this kind is shown in Fig. 1. (Only one wave of the field is shown but there may be more than one.)

The velocity of the wave v_r must be such that during the entire acceleration process the particles are located in a section of the field in which the condition $0 < n < 1$ is satisfied. For this condition to obtain, the radial component of the particle velocity (determined by the accelerating voltage) and the radial velocity of the wave must be the same.

In this accelerator the magnetic field can be increased as the wave approaches the terminal radius without any deterioration of the vertical focusing. Thus, it is possible to keep the frequency of the accelerating voltage constant in the region in which the particles become relativistic; that is to say, a cyclotron of this kind can be designed for energies as high as desired.

It should be noted that it is also possible to choose values of n which provide higher instantaneous intensities than can be obtained with the conventional cyclotron or with the fm cyclotron.

The intensity can be increased because in the central part of the accelerator (where the field is small) the air gap can be rather large; the gap is reduced as the energy is increased. In this accelerator, as in the fm cyclotron, the particles are accelerated in bunches; however, the average density can be higher because of the better magnetic focusing. It is obvious that the average intensity will be several orders of magnitude higher than that which can be obtained in a synchrotron.

POSSIBLE DESIGNS

In Fig. 2 is shown a diagram of one of three possible designs of the magnet for an accelerator of this type. The vacuum chamber is located between two disks of conical shape and is made from sheet iron with radial laminations; the disks are also used as pole pieces and magnetic conductors. The disks consist of separate sectors with laminations as shown in Fig. 2. On the surfaces of the disks, which face each other, are circular concentric windings.

The windings can be supplied in various ways. For example, the windings can be divided into several groups, separated in appropriate fashion, and supplied from a three-

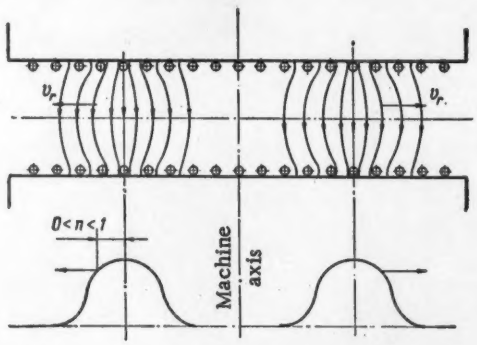

Fig. 1. Diagram of a scheme for obtaining a magnetic field which travels in the radial direction by means of special circular conductors located on the surfaces of the magnetic pole pieces.

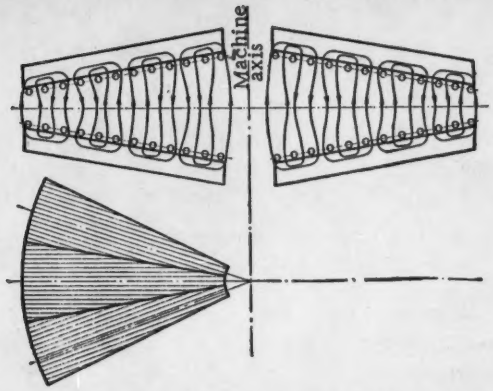

Fig. 2. A possible design of the magnet for the accelerator. Several concentric waves of the magnetic field are shown (multiple system). Below is shown a diagram of the radial laminated pole pieces.

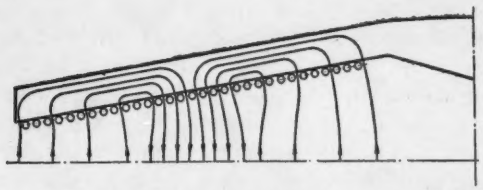

Fig. 3. Design with one magnetic wave in which the lines of force are closed through the gap twice.

phase line; then, as in ordinary electrical machinery, it is possible to produce a magnetic field (Fig. 2) which is displaced in the radial direction with a velocity which depends on the frequency and the spacing of the windings. The lines of force are closed through the laminated disks. The system acts as a multipole system and, since the disks are relatively thin, there is a considerable reduction in the weight of the magnetic path.

In Fig. 3 is shown another version of the machine. In this case, there is only one magnetic wave. The lines of force are closed through the air gap (Fig. 3) or through a special yoke located at the periphery of the accelerator (Fig. 4).

The versions shown in Figs. 3 and 4 require the use of special commutation systems; these can be realized easily by means of gas rectifiers. In order to reduce the reactive component of the power, it is possible to store the magnetic energy of the wave as it moves from one point to another.

In the accelerator proposed here the air gap can be very small (approximately 5-10 cm at maximum radius).

The field intensity is a maximum at the terminal radius and can be chosen to take advantage of the magnetic properties of the iron and the flexibility in the location of the windings; using conventional steels it is feasible to produce a field of the order of 20,000 oe.

Since the velocity of the magnetic wave is limited, the energy increment per turn must be of the order of hundreds or thousands of volts. Although a relatively high chamber vacuum is required for this voltage there is a significant reduction in the power required from the radio-frequency generator and the complexity of the accelerating systems.

In low-energy accelerators it is convenient to use dees. In large machines acceleration can be realized by means of special sectored electrodes placed in the space between the magnetic disk sectors (Fig. 5). It is also expedient to separate the disks for convenience in locating the vacuum pumps.

The design of this machine involves great difficulty from the point of view of the injection system. In the present paper we do not consider in detail the injection of particles into the moving magnetic field. In small and intermediate accelerators the central portion of the machine can be a conventional cyclotron, as is shown schematically in Fig. 6. In this case, winding A produces the field for the starting cyclotron while winding B produces the traveling magnetic wave.

Particle injection can be realized in other ways; in particular it is possible to use a linear accelerator, a synchrontron, or an fm cyclotron.

The analysis of a cyclotron in which a traveling magnetic field is superimposed on a fixed magnetic field must be carried out separately. In this case the magnetic conductor of the accelerator is the same as that of the cyclotron or fm cyclotron (Fig. 7). The pole pieces, which may be parts of the vacuum chamber, are made from laminated iron. The weight of the magnet in this design is of the same order of magnitude as in the conventional cyclotron and fm

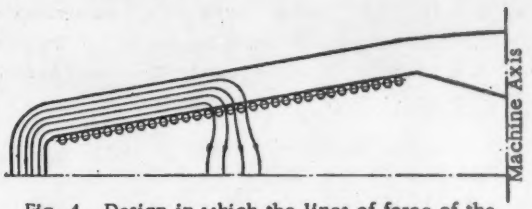

Fig. 4. Design in which the lines of force of the magnetic wave pass through the air gap once and are closed through a special yoke at the periphery.

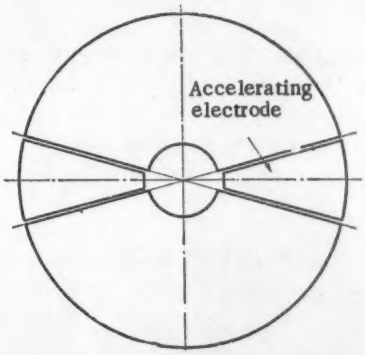

Fig. 5. Diagram showing the arrangement of the accelerating electrodes.

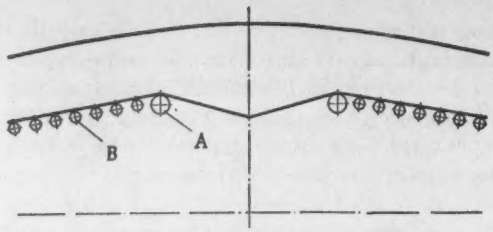

Fig. 6. A possible scheme of injection for the accelerator: (A) Winding of the central injection cyclotron; (B) Windings which provide the traveling magnetic field.

cyclotron, but the technique described here makes it possible to obtain very high energies.

Because of the specific features of the design which uses a cyclotron with a fixed field we consider this machine separately below.

RELATIONS BETWEEN THE BASIC PARAMETERS AND APPROXIMATE CALCULATIONS FOR A MACHINE WITHOUT A FIXED MAGNETIC FIELD

In order for the frequency of rotation of the particles to remain fixed, so that the frequency of the accelerating voltage can remain constant, the field intensity at all radii must be

$$H = H_0\left(1+\frac{W}{E_0}\right), \qquad (1)$$

where H_0 is the field intensity at the beginning of acceleration ($W = 0$), If W_m is the energy at the terminal radius (the nominal energy of the machine) and H_m is the maximum field intensity (terminal radius), the initial intensity of the field is given by

$$H_0 = \frac{H_m}{1+\frac{W_m}{E_0}}.$$

The radius of the particle orbit for given values of the kinetic energy and magnetic field (proton) in cm is

$$r = \frac{\sqrt{W(W+2E_0)}}{300H}, \qquad (2)$$

where W is the kinetic energy of the particle (ev), E_0 is the rest energy of the particle (ev), and H is the field intensity (oe). Replacing H by its value from (1) we have

$$r = \frac{\sqrt{W(W+2E_0)}}{300H_0\left(1+\frac{W}{E_0}\right)},$$

$$\frac{dr}{dW} = \frac{E_0^2}{300H_0}\frac{1}{\sqrt{W(W+2E_0)}(W+E_0)^2}.$$

Whence, the helix spacing is

$$\Delta_r = u\frac{dr}{dW} = \frac{uE_0^2}{300H_0}\frac{1}{(W+E_0)^2\sqrt{W(W+2E_0)}}, \qquad (3)$$

where u is the energy obtained by the particle per turn.

The period of rotation of the particle is

$$T = \frac{2\pi r}{v} = \frac{2\pi r}{c}\frac{1}{\sqrt{1-\left(\frac{E_0}{W+E_0}\right)^2}},$$

where v is the particle velocity (cm/sec); c is the velocity of light (cm/sec).

The radial velocity component of the particle is

$$v_r = \frac{\Delta r}{T} = \frac{uc}{600\pi H_0 r}\left(\frac{E_0}{W+E_0}\right)^3. \qquad (4)$$

It follows from (4) that the velocity of the magnetic wave in the central part of the accelerator must be much greater than at the final orbit. In Table 1 are shown various parameters for accelerators of different energy. In calculating these parameters the following values have been assumed: $H_0 = 20{,}000$ oesteds, gap size $\delta = 7.5$ cm, magnetizing—current frequency $f = 50$ cps.

In calculating the weight of the active iron the thickness of the disk has been taken as 15 cm. In these calculations no account has been taken of the weight of the other parts of the machine, which, in large accelerators, can be quite appreciable (the upper disk must be supported in position by a rather complicated bridge-type construction).

In this design it can be shown that it is necessary to have a larger gap between the pole pieces than has been assumed in the calculations; thus, the power may be greater than indicated. For a 100 Mev accelerator the reactive power is computed for a design in which the windings are supplied directly from the ac line. The system used to provide the traveling field is similar to that used in three-phase electrical machinery. For a 1 Bev accelerator, the calculation has been carried out for the case in which the power is supplied directly from the ac line and for the case in which the power is provided through a commutating system without storage of the magnetic energy of the individual sections of the excitation windings. For the 10 Bev machine, the figures given here indicate the power only for the case in which the switching system is used without storage of the magnetic energy.

The power requirements have not been calculated for the largest machine (50 Bev). A machine of this type is feasible only if a system of magnetic energy storage is used.

The numbers given in Table 1 indicate that a machine of this type is fearible from the point of view of economy.

In Table 2 are shown values of the magnetic field strength and magnetic field velocities at various radii of a cyclotron with a final energy of 100 Mev; in Table 3 are shown the same parameters for a 1 Bev cyclotron.

For the 100 Mev machine, the accelerating voltage U has been taken as 115 v; for the 1 Bev machine a value of 1540 v has been used.

The radial velocities of the magnetic field shown in Tables 2 and 3 and the corresponding values of the accelerating voltage refer to the design in which the accelerating

Table 1.

Final energy, Mev	Terminal orbit radiu, cm	Field intensity in the gap at the beginning of acceleration, oe	Particle rotational frequency, Mc/sec	Weight of the iron, tons	Required power, kva	
					total power, required without switching	supply for two waves without energy storage
100	74	18 000	27.6	4	37 000	—
1 000	284	9 750	14.5	60	550 000	108 000
10 000	1810	1 720	2.64	2 400	—	750 000
50 000	8500	367	0.56	53 000	—	—

Table 2.

W, Mev	H, oe	r, cm	v_r, m/sec
10	18 200	25.2	38.7
20	18 400	39.3	24.2
40	18 800	49.1	18.2
60	19 150	53.3	14.1
80	19 500	67.7	11.9
100	20 000	74	10.1

Table 3.

W, Mev	H, oe	r, cm	v_r, m/sec
15	9 800	57.3	422
50	10 200	101.5	214
100	10 800	137.5	136
300	12 900	209	54
500	14 900	244	28.9
1000	20 000	284	10

Table 4.

r, cm	W, Mev	H, oe	$\left(\frac{dH}{dr}\right)_1$	$\left(\frac{dH}{dr}\right)_2$	v_r, m/sec	u, b for v_r=const= =100 m/sec	s, cm	l, cm	I, amp
0	0	8 600	—	—	—	—	61.2	—	—
76	20	8 750	—	—	595	437	—	—	—
113	50	9 100	8.7	40	365	705	58	58	131 000
155	100	9 550	10	31	230	1 130	55	—	—
213	200	10 300	24.3	24.2	127	2 050	51	—	—
276	500	13 200	61	24.1	48.7	5 340	39.8	39.8	107 000
305	800	15 900	108	26.2	24.9	10 400	33	—	—
318	1000	17 700	167	27.8	17.1	15 200	29.7	—	—
327	1200	19 600	250	30	12.5	20 850	27	—	—
332	1350	21 000	415	31.8	10	26 100	25	25	224 000

voltage remains constant. However, if the amplitude of the accelerating field can be varied during the course of an acceleration cycle it then becomes possible to keep the velocity of the traveling wave constant at all radii. This results in a considerable simplification in the construction of the circular excitation windings.

In order to avoid unnecessary complications in this analysis, the accelerating voltages have been determined without taking account of the voltages required to compensate for the emf of the induced field. It can be shown that a magnetic wave traveling in the radial direction produces an induced electric field which opposes the accelerating field. In order to compensate for the induced electric field the accelerating voltage must be larger than has been indicated above.

RELATIONS BETWEEN THE BASIC PARAMETERS AND APPROXIMATE CALCULATIONS FOR A MACHINE WITH A FIXED MAGNETIC FIELD

Equations (1)-(4) also apply for the machine in which the traveling wave is superimposed on the fixed magnetic field (cf. Fig. 7). A is shown in the figure, the laminated pole pieces can be fabricated in such a way that the gap becomes smaller at larger acceleration orbits. This reduction in gap size must be such that the field intensity as a function of energy is given by (1).

In Fig. 8 is shown a magnetic field intensity curve for a magnet with a diameter of approximately 700 cm.

In order to provide focusing, the traveling wave must be superimposed in such a way that there is a circular zone characterized by $0 < n < 1$. The superposition of the traveling wave on the fixed magnetic field is shown graphically in Fig. 9. A current I flows through the circular group of conductors of width l starting at the radius r_1. By means of a special switching system the radius associated with this group is increased, corresponding to the increase in the radius of the circle which defines the outer edge of the magnetic flux produced by the group of conductors.

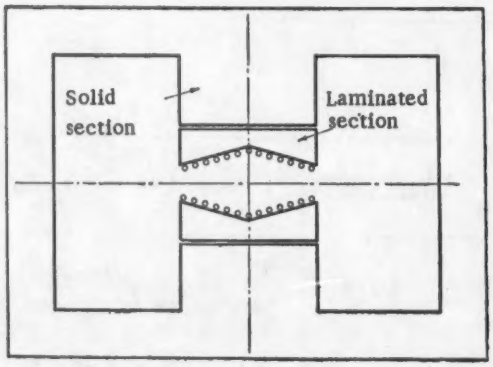

Fig. 7. Design of a cyclotron in which a megnetic field traveling in the radial direction is superimposed on the fixed magnetic field produced by the Ushaped magnet.

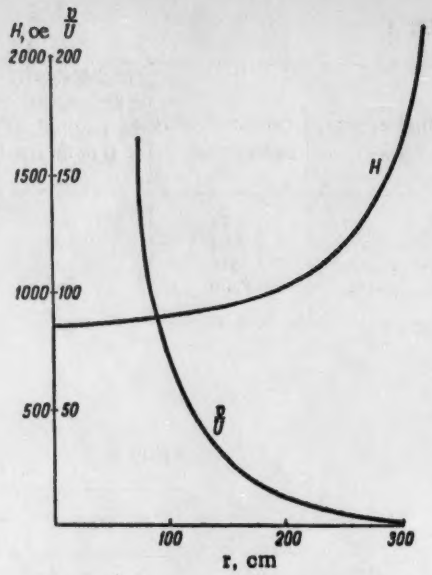

Fig. 8. Intensity curves for the magnetic field and the ratio of the velocities of the wave to the accelerating voltage for a cyclotron with a fixed magnetic field with a pole diameter of approximately 700 cm.

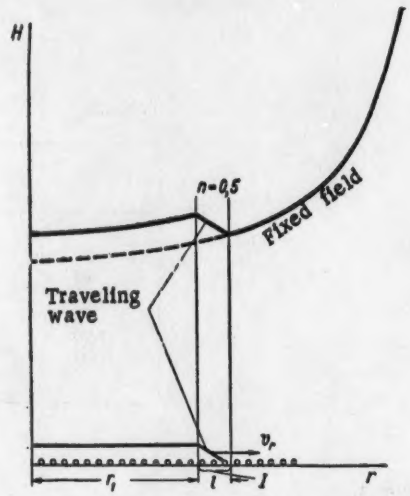

Fig. 9. Diagram showing the superposition of the traveling magnetic wave on the fixed field of cyclotron.

The resultant of the fixed flux on the variable flux produces a circular zone in which n has the required values.

If $(dH/dr)_1$ and $(dH/dr)_2$ are the absolute values of the radial derivatives of the magnetic field for the fixed flux and the total intensity in the circular zone, the total value of the current flowing through the windings in the

cross section of the circular zone of width l is

$$I = 0{,}8\delta_1 l\left[\left(\frac{dH}{dr}\right)_1 + \left(\frac{dH}{dr}\right)_2\right], \qquad (5)$$

where δ_1 is the gap size for a given value of the radius r.

The electromotive force produced by the traveling wave of magnetic flux in the group of conductors of width l can be computed from the following formula:

$$E = 2\pi r \frac{I}{0{,}8\,\delta_1} v_r \cdot 10^{-8} = 12{,}3r \frac{I}{\delta_1} v_r \cdot 10^{-8} \quad .$$

In Table 4 are shown results obtained by an approximate calculation for a machine with a magnet having a pole diameter of approximately 700 cm.

The power required for the circular windings in this version (no magnetic energy storage and wave velocity of the order of 100 m/sec) is 2-3 kva. This power is proportional to the repetition frequency (intensity).

The accelerating voltage given in Table 4 is computed for a fixed wave velocity. Actually it is more convenient to start from the fact that the power required by ring windings is constant over a cycle. In this case the wave velocity must gall off gradually as the orbit radius increases. As in the preceding calculations, no account has been taken of the induced electric field.

CONCLUSION

In this description of the proposed machine we have stressed general operating principles, possible designs, and typical calculations. The results would seem to indicate the justification of further work in the development of systems of this kind.

MULTIGROUP ANALYSIS OF AN ATOMIC POWER PLANT REACTOR ON THE "STRELA" HIGH-SPEED ELECTRONIC COMPUTER

V. A. Chuyanov

Original article submitted April 24, 1959

The multigroup method described in [1, 2] was used to calculate the effective fission factor and neutron flux for a model of a homogeneous reactor of an atomic power plant when the load was assumed to be near the critical value. In the radial direction the reactor was regarded as a three-zone model, the end reflectors were accounted for by the introduction of effective additions in height. It was assumed that the fission neutrons were monoenergetic (with an energy of 2 Mev); resonances in the cross sections were accounted for by the resonance escape probability coefficient. The equations for all the neutron groups, except for the thermal neutron group, were obtained by integrating the age equation over the lethargy interval for the investigation. The effective multiplication factor and spatial-energy distribution of the neutron flux were computed by the method of successive approximations. The difference equations for such neutron group were solved by the method of difference factorization.

In order to solve the problem indicated (as well as other, similar problems), a program was written for the "Strela" electronic computer. The calculation of a single value of the effective multiplication factor when all the neutron fluxes were obtained required about 6.5 min (for a five-group variant for the calculation with 100 points along the radius). In order to obtain an accuracy of 0.01% for k_{eff}, 9 iterations were required. The rate of convergence of the successive approximations are shown in Fig. 1; the results of the calculation of k_{eff} as a function of the number of groups used in the analysis (from 2 to 20 groups) are shown in Fig. 2. In these calculations the number of points along the radius was equal to 100.

In order to determine the influence of the particular method of grouping, the calculations were made in the six-group approximation. It turned out that dividing into groups approximately equal in size (in neutron age units) had only a weak effect on the value of k_{eff}. The thermal neutron flux distribution Φ obtained with varying numbers of the groups used in the analysis is shown in Fig. 3.

In comparing the value $k_{eff} = 1.0751$ obtained in the present paper with the value $k_{eff} = 1.023$ quoted in [1], it must be remembered that different models for the reactor were adopted (in [1] a two-zone model was used), and that the value given for k_{eff} in [1] was obtained after accounting for a number of small effects by perturbation theory.

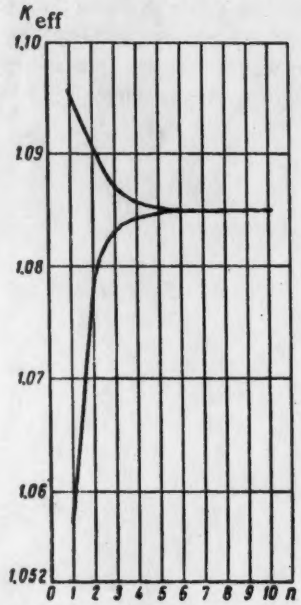

Fig. 1. Dependence of the upper and lower limits of $k_{eff}(r)$ on the number of iterations n (15 groups, 15 reference points along the radius).

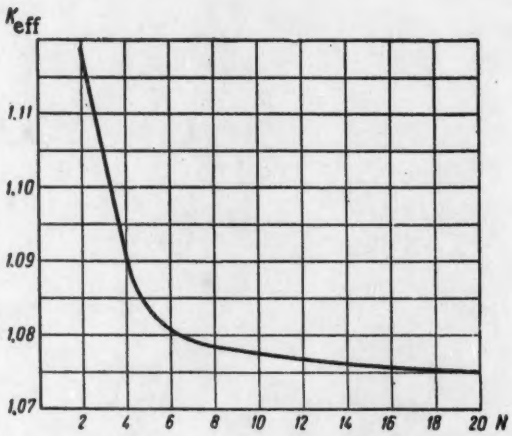

Fig. 2. Dependence of k_{eff} on N, the number of groups used in the analysis.

Reactor Zone Characteristics

	Zone I (r=0—52 cm)	Zone II (r=52—77 cm)	Zone III (r=77—147 cm)
Multiplication factor*	1.3938	0	0
Slowing-down length, cm	15.467	18.644	17.974
Thermal-neutron diffusion length, cm	8.2039	42.732	54.138

* Determined in the twenty-group approximation.

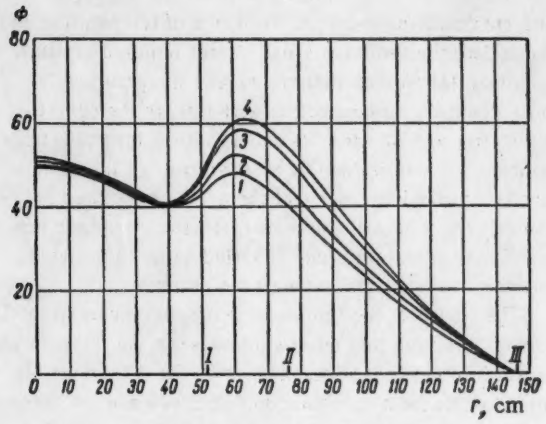

Fig. 3. Thermal neutron flux distribution: 1, 2, 3, 4) calculations with 2, 3, 5, and 20 groups, respectively; I, II, III) reactor-zone boundaries.

In the present instance accounting for the greater (by a factor of 1.5-2) absorption of thermal neutrons in the reflector in comparison with the case considered in [1] led to a reduction in the maximum of thermal neutron distribution.

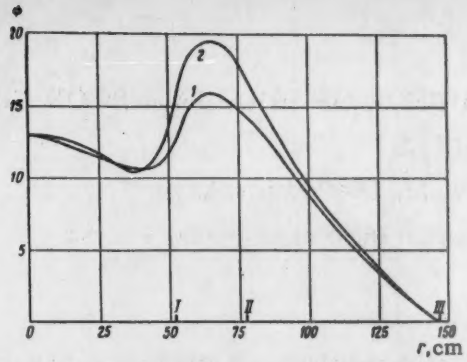

Fig. 4. Spatial distribution of the thermal neutron flux: 1) from the data of the present paper (20 groups); 2) from the data of [1]; I, II, III) reactor-zone boundaries.

The characteristics of the reactor zones are shown in the table, where for all three zones an effective reactor height H_{eff} = 223.2 cm was assumed (Fig. 4).

Comparison with the theoretical and experimental thermal neutron density distribution along the reactor radius given [3] and [4] is unfortunately unfeasible, since these refer to different load and operating conditions for the reactor.

The author gratefully acknowledges E. S. Kuznetsov for suggesting and guiding the present study, G. I. Marchuk for valuable pointers in evaluating the results, and O. K. Turchaninov for assisting in the computer operations and in the organization of the paper.

LITERATURE CITED

1. G. I. Marchuk, Atomnaya Énergiya No. 2, 11 (1956).*
2. G. I. Marchuk, Coll.: The Physics and Heat Engineering of Reactors [in Russian] (Supplement No. 1 to the journal Atomnaya Énergiya, 1958) p. 7.*
3. D. I. Blokhintsev and N. A. Nikolaev, "Reactor design and theory," Reports of the Soviet Delegation to the International Conference on the Peaceful Uses of Atomic Energy (Geneva, 1955) [in Russian] (Izd. AN SSR, 1955) p.3.
4. D. I. Blokhintsev, M. E. Minashin, and Yu. A. Sergeev, Atomnaya Énergiya No. 1, 24 (1956).*

* Original Russian pagination. See C.B. Translation.

INFLUENCE OF IRRADIATION ON THE MAGNETIC PROPERTIES OF FERRITES

N. M. Otel'yanovskaya

Original article submitted January 6, 1959

Research on the influence of irradiation on the magnetic properties of ferrites has been a subject of great interest with the application of these as memory storage units in equipment operating under irradiation. This problem has been treated in rather few papers [1-3].

Ferrites of the ZK-210 type, in the form of toroids, were procured by the authors from the Electrical Simulation Laboratory of the Academy of Sciences of the USSR. The ferrites were irradiated with neutrons and γ rays in the vertical experimental column of an atomic power plant.

It was surmised that atoms would break away from the lattice junctions under the influence of irradiation of the ferrites by neutrons. This would lead to a modification in the occupation number of the sublattices [4, 5] that compose the spinel lattice of the ferrite. The effects of disordering would then change the magnitude of the magnetic saturation of the ferrites and should increase with the increase of the integral flux.

Certain parameters of the hysteresis loop were measured under pulse operation on a special apparatus. The rectangular pulses, $-I$, $+I$, $-I/2$ *formed by a current generator were delivered to the primary winding of the ferrite. The semiexcitation current I_s, which was equal to 60% of the total current, induced a small back-emf A_s in the secondary winding. The quantity A_s was less, the nearer the hysteresis loop approached an ideal rectangular shape. Thus, the degree of variation in the slope of the horizontal part of the hysteresis loop could be estimated from the variation in I_s.

In order to examine the question as to whether the ferrite would operate after the radiation was taken away, two batches of the ferrites (each consisting of ten identical samples, specially prepared for these experiments) were irradiated by a flux of $1.5 \cdot 10^{13}$ neutrons/cm^2 · sec. The total integral flux for the samples of the first batch was $2.15 \cdot 10^{17}$ neutrons/cm^2, that for the samples of the second batch was $6.5 \cdot 10^{17}$ neutrons/cm^2. A comparison of the data obtained for the irradiated ferrites with the data obtained prior to their irradiation showed that the amplitude of the semiexcitation current and the amplitude of the ferrite magnetization from the total current I, insofar as experimental error allowed, did not change after irradiation. (In connection with the high initial activity of the samples, the measurements were conducted every four days after withdrawal of the irradiation.)

Upon bombardment of the sample by neutrons, in addition to the structural changes in the lattice [7, 8], the ferrites also heated up, changing the form of the hysteresis loop. In order to segregate these effects, the dependence of the loop parameters on the temperature was recorded on a special assembly designed for operation in reactor experiments. The measurements inside and outside the reactor were made as follows. As the hysteresis loop breaks down (under the influence of temperature and irradiation), the semiexcitation current required to elicit a semiexcitation that does not exceed the permissible norm changes. In connection with this, in the operation of a matrix with the ferrites under these unfavorable conditions, it was determined by what amount ΔI the current must be changed in order that the cores could function normally (A_s = const). Moreover, it was determined how A_s and the useful amplitude A varied under these same conditions with a fixed value of the currents.

The results of the temperature measurements (from 20 to 58.8°C) showed that with an increase in the temperature, the width of the loop, i.e., the current for A_s = const, decreased, while the magnetization amplitude and, in particular, the semiexcitation amplitude for a constant value of the current increased. The rectangularity of the loop broke down considerably with increasing temperature, and at a temperature of 50 °C the useful amplitude A and the back-emf became almost identical in magnitude. (All the temperature variations in the loop were reversible.)

Upon irradiation in the reactor, the magnitude of the neutron and γ-ray flux could be varied within wide limits by changing the immersion depth of the samples in the channel. In order to avoid additional heating of the ferrites from the mounting that heated up during the irradiation, the samples were suspended in a container on thin copper wires, which simultaneously served as the windings for them. In order to observe the temperature, the junctions of two thin-wire (0.1 mm) copper–constantan thermocouples were attached to two of the samples.

In the figure a typical dependence of the variation in semiexcitation current and semiexcitation amplitude on the integral neutron flux is shown, along with a constant semiexcitation current (initial value A_s = 10). In the same

* An investigation of the cores in this regime is very essential in determining the suitability of the ferrite operation in the matrices of a two-current lock-on circuit [6].

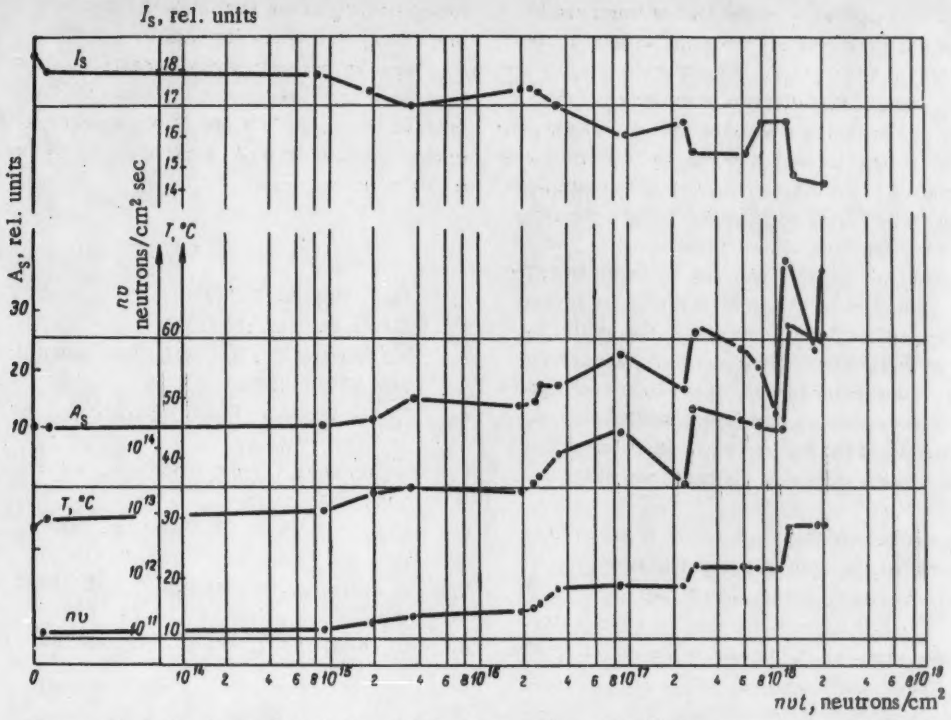

Figure. Variation in semiexcitation amplitude A_s and semiexcitation current I_s as a function of the integral neutron flux.

figure the temperatures of the samples and the neutron fluxes nv at the corresponding times of measurement are plotted. As evident from the figure, the variation in A_s and I_s pretty well follows the behavior of the variation in temperature of the ferrites and the neutron flux. The influence of the temperature on the properties of the ferrites could be seen from a comparison of the data obtained for a given value of the flux and integral fluxes, differing from one another by a factor of 2.7. For a larger value of the integral flux the temperature of the samples, which depends mostly, given the same value of the flux, on the heat-transfer conditions in the channel, was lower by 8 °C. The properties of the cores in this case were greatly improved, which lends support to the independence of the magnetic properties of ferrites from the integral flux. The mean value of the variation in the semiexcitation current (which is proportional to the coercive force) amounted to 12% for irradiation of the ferrites in a flux of $1.8 \cdot 10^{12}$ neutrons per cm² · sec (the temperature of the sample was equal to 46.3 °C). The mean variation in the quantity I_s was 13% for an increase in temperature to approximately the same value (47.2 °C), but without the irradiation. The maximum value of I_s in the largest flux applied for the investigation ($8.5 \cdot 10^{12}$ neutrons/cm² · sec) at a sample temperature of 60.5 °C amounted to 17%.

Variation of the magnetization amplitude and semiexcitation amplitude

	Nonirradiated		Irradiated
Temperature of the sample	52.7° C	58.8° C	60.5° C
Variation in magnetization amplitude*	39%	45%	15%
Variation in semiexcitation amplitude*	4 times	6.2 times	2.6 times
Ratio of the total magnetization amplitude	1.4	1.04	1.76

* In the table the mean values with respect to the initial value of these quantities at room temperature are given.
** The initial value of the ratio is 4.

During irradiation a much smaller increase was observed in the magnetization amplitude and the semiexcitation amplitude with an increase in the flux (temperature) in comparison with the temperature variation in these quantities without irradiation (table). These facts confirm the less sharply defined increase in the curvature of the horizontal part of the hysteresis loop upon irradia-

tion, i.e., the rectangularity of the loop is improved in comparison with its temperature variation without irradiation.

As already noted, the effects of disordering of the ferrite lattice should increase with the increase of the neutron flux. The absence of such a regularity is possibly connected with the fact that the temperature of the samples during the irradiation reached 320-333 °K. But the rate of disordering is a function of the temperature [7] and drops as the latter increases. Evidently, at the given temperatures, the vacancies and interstitial atoms are sufficiciently mobile and reorder a large part of the matter that is disordered by irradiation. More precisely, the observed improvement in the rectangularity of the loop at the poles of the n−γ radiation is also possibly connected with an additional ordering of the ferrite lattice in a flux of thermal neutrons [8], thus impeding the influence of the temperature.

As a consequence of this, with the application of ferrites as memory storage cells in equipment operating in neutron and γ-ray fluxes greater than $5 \cdot 10^{11} - 5 \cdot 10^{12}$ neutrons/$cm^2 \cdot$ sec, it is necessary that the equipment be designed for the variation of the matrix current or for the forced cooling of the ferrites to the necessary temperature during their operation with irradiation.

We take this opportunity to express our gratitude to L. A. Matalin for suggesting the topic and for his interest in it, to Yu. K. Gus'kov and N. V. Meshkov for assisting in the work, and to A. A. Kosarev for kindly furnishing the ferrite samples.

LITERATURE CITED

1. Elec. Mfg. 59, 312 (1957).
2. Electronics 30, 250 (1957).
3. M. Forestier et al., Compt. rend. acad. sci. France, 243, 1842 (1956).
4. Ya. G. Dorfman, Izvest Akad. Nauk SSSR, Ser. Fiz. 16, 412 (1952).
5. M. Bochiral, Compt. rend. acad. sci. France 233, 736 (1951).
6. L. A. Matalin, A. M. Shimanskii, and S. I. Chubarov, Pribory i Tekh. Éksp. No. 1, 64 (1957).
7. S. Zeitz, Dis. Faraday Soc. 5, 271 (1949); J. Glen, Uspekhi Friz. Nauk 60, 445 (1956).
8. C. Dixon and D. Bowen, Phys. Rev. 94, 1418A (1954).

THERMAL EXPANSION OF α PLUTONIUM

N. T. Chebotarev and A. V. Beznosikova

Original article submitted March 9, 1959

According to the data of [1], α plutonium has a monocrystalline structure with the following parameters: a = = 6.1835 ± 0.0005 A; b = 4.8244 ± 0.0005 A; c = 10.973 ± ± 0.001 A; β = 101.82 ± 0.02°.

As indicated in [2], the mean coefficient of thermal expansion for α plutonium in the temperature interval from -186 to + 100 °C is $[(46.85 \pm 0.05) + (0.0559 + +0.0004)t] \cdot 10^{-6}$. As the experimental part of this research was nearing its completion, there appeared some information [3] relative to the values of the coefficients of thermal expansion of α plutonium along the individual axes in the interval 21-104 °C (Table 1).

Table 1.

Directional thermal expansion coefficient	Temperature interval, °C		
	21–51	21–96	21–104
$\alpha_1 \perp c$	57	62	66
$\alpha_2 \parallel b$	58	71	73
$\alpha_3 \parallel c$	19	27	29
α_{av}	45	53	56

In the present paper a determination of the coefficient of thermal expansion of α plutonium along different directions in the temperature interval from -196 to +100 °C is described. With the investigated sample in the form of a wire (diameter 0.5 mm) x-ray exposures were obtained with copper radiation at room temperature, at the temperature of liquid nitrogen, and at 100 °C. X-ray photographs in the interval from -196 to + 20°C were obtained in an RKSO x-ray chamber by the method of photographic inversion. In order to obtain the x rays at -196 °C, the samples were continuously wetted with liquid nitrogen during the exposure. The x ray at +100 °C was obtained in an RKU x-ray chamber.

The lattice parameters of the sample investigated at room temperature were the following: a = 6.181 ± 0.002 A; b = 4.821 ± 0.001 A; c = 10.965 ± 0.005 A; β = 101.82°. The coefficients of thermal expansion in the indicated temperature interval were determined from the displacement of the following diffraction lines: $\bar{7}14$, 710, $\bar{5}45$, 248, 445, $\bar{7}24$, $\bar{4}52$, $\bar{3}56$, 060, $\bar{5}112$, $\bar{3}213$. These lines correspond to an interval of reflection angles from 63 to 81°.

Curves for the variation of the lattice parameters a, b, c of α plutonium in the temperature interval from -196 to +100 °C are shown in the figure.

Table 2.

Directional thermal expansion coefficient	Temperature interval, °C					
	−196 − +20		20−100		−196 − +100	
	$\alpha \cdot 10^6$	standard deviation, %	$\alpha \cdot 10^6$	standard deviation, %	$\alpha \cdot 10^6$	standard deviation, %
$\alpha_1 \perp c$	49±6	12	68±6	9	55±7	13
$\alpha_2 \parallel b$	53±3	6	77±4	5	60±5	8
$\alpha_3 \parallel c$	14±3	21	35±5	14	20±4	20
α_{av}	39±3	8	60±4	7	45±4	9

In Table 2 the coefficients of thermal expansion of α plutonium along three mutually perpendicular directions and the mean expansion coefficient α_{av} are given for the investigated temperature intervals; the standard deviation of the determinations is also shown.

It should be noted that there is a satisfactory correspondence between the results obtained and the data in the literature, both for the mean expansion coefficient in the interval from -196 to +100 °C and for the expansion coefficients along different directions in the interval 20-100 °C. Some of the discrepancy can be explained by the slight difference in the lattice parameters of the samples studied, as well as by the comparatively small temperature interval (particularly from 20 to 100 °C), which is limited by the α → β phase transition at 122 °C.

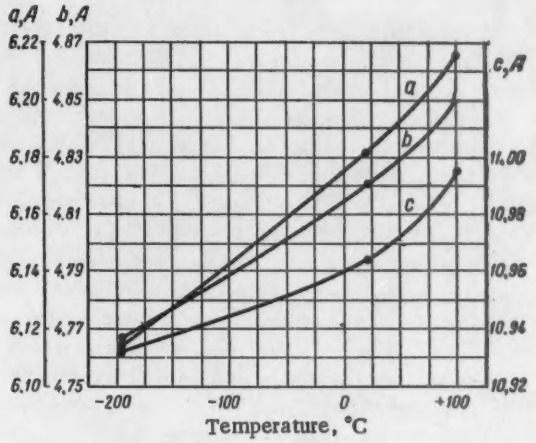

LITERATURE CITED

1. W. Zachariasen and F. Ellinger, J. Chem. Phys. 27, 811 (1957).
2. E. Cramer, L. Hawes and F. Schonfeld, Prog. Nucl. Energy 1 (V), 373 (1956).
3. A. Coffinberry, F. Schonfeld et al., "The physical metallurgy of plutonium and its alloys," Report No. 1046, presented by the USA at the Second International Conference on the Peaceful Uses of Atomic Energy (Geneva, 1958).

DISPROPORTIONATION OF Am (IV)

A. A. Zaitsev, V. N. Kosyakov, A. G. Rykov, Yu. P. Sobolev, and G. N. Yakovlev

Original article submitted November 17, 1958

Several anhydrous compounds of Am (IV) which are quite stable and may be obtained comparatively readily have now been synthesized [1, 2]. However, Am (IV) has not been detected in aqueous solutions up to now. Its instability is explained by the high value of the oxidation-reduction potential (2.4 v) of the Am (III)−Am (IV) couple [3] and, therefore, it is usually assumed [4-6] that Am (IV) must be reduced to Am (III) by water.

In an examination of the mechanism of Am (V) disproportionation, the observed ratio of Am (VI) and Am

(III) yields may be explained if it is assumed that one of the following reactions occurs in parallel with the disproportionation of Am (V) [7]:

$$2Am^{4+} + 2H_2O = Am^{3+} + AmO_2^+ + 4H^+; \quad (1)$$

$$Am^{4+} + AmO_2^+ = Am^{3+} + AmO_2^{2+}. \quad (2)$$

The rate of reaction (1) must depend on the hydrogen ion concentration and increase with a decrease in the acidity of the solution. Reaction (2) must proceed at a high rate that is independent of the hydrogen ion concentration.

In the present communication we present the result of preliminary investigations confirming the existence of (1) and (2).

EXPERIMENTAL

Americium dioxide was prepared by firing Am (III) oxylate at 600° C. Sulfuric acid solutions were prepared from distilled sulfuric acid. The acid concentration was determined by titration.

Americium dioxide was dissolved in 0.5, 1.0, and 2.0 M sulfuric acid at room temperature and in 4.0 and 6.0 M sulfuric acid with heating on a water bath. Solution lasted for 10-15 min. The solution was centrifuged and analyzed for americium in various valence states. The time between separation of the solution and the beginning of the measurements was 10-20 min. The Am (III), Am (V), and Am (VI) concentrations were determined spectrophotometrically on an SF-4 quartz spectrophotometer For this purpose, the absorption spectra of Am (III), Am (V), and Am (VI) were first studied in the sulfuric acid solutions investigated. Hermetically sealed cylindrical cells 2 cm long were used for the spectrophotometric measurements. The total americium concentration was determined radiometrically from the Am^{241} α radiation in a slit chamber with a counting coefficient of $4.85 \cdot 10^{-6}$.

DISCUSSION OF RESULTS

The compositions of the solutions obtained after solution of americium dioxide in sulfuric acid at various concentrations are given in the table.

As the table shows, when the americium dioxide had dissolved, the solution contained noticeable amounts of Am (VI) together with Am (III), but Am (V) was practically absent. The appearance of valence states above +4 indicates disproportionation of Am (IV) (reaction (1)). The absence from the solution of Am (V), which is one of the products of this reaction, and the formation of Am (VI) in 1.0 and 2.0 M sulfuric acid may only be explained by the presence of reaction (2), since the disproportionation of Am (V) in this solution may be neglected [8]. Consequently both reactions occur in this case with the second going practically to completion and apparently at a very high rate. The over-all disproportionation of Am (IV) may be written in the following way:

$$3Am^{4+} + 2H_2O = 2Am^{3+} + AmO_2^{2+} + 4H^+. \quad (3)$$

In 4.0 and 6.0 M sulfuric acid, Am (V) may also disappear as a result of disproportionation.

$$2AmO_2^+ + 4H^+ = AmO_2^{2+} + Am^{4+} + 2H_2O. \quad (4)$$

However, the over-all reaction also remains unchanged in this case.

It follows from this that in addition to the reduction of Am (IV), (3) also occurs in the solution of americium dioxide. By using the over-all reaction equation (3), we calculated the yields of Am (IV) disproportionation and reduction from the yields of Am (III) and Am (VI). The results obtained are given in the last two columns of the table. It can be seen that the yield of (3) increases with a decrease in acidity, and this reaction becomes the predominating one in weakly acid solutions. This indicates that the rate of the over-all reaction (3) is determined by the rate of (1), which is determined by the hydrogen ion concentration. However, the rate constant of (1) must be high as the disproportionation of Am (IV) is appreciable even in 6.0 M sulfuric acid.

For a conclusive demonstration of the existence of (2), experiments were carried out in which americium dioxide was dissolved in 0.5 M sulfuric acid containing a known amount of Am (V). When the original amount of Am (V) was approximately half that of the Am (IV) dissolved, Am (V) was practically absent after solution of the dioxide. Evidently, the original Am (V) reacted very rapidly with Am (IV) by (2) and the remaining Am (IV) partially disproportionated by (3) and was reduced. The yields of these reactions were as follows: reaction (2), 37%; reaction (3), 52%; and reduction of Am (IV), 11%.

In an experiment where the original amount of Am (V) was approximately twice that of Am (IV) dissolved, the probability of the reactions was calculated on the assumption that the decrease in the Am (V) concentration in solution was caused by (2) only. Here the probability of (2) was 77%, of (3), 10%, and of Am (IV) reduction, 13%. Since the experiments were with Am^{241}, there was

Disproportionation of Am (IV) in sulfuric acid

Acic concentration, M	Total concentration of americium in solution, mM	Solution composition, %			Reaction probability, %	
		Am (III)	Am (VI)	Am (V)	disproportionation of Am (IV)	reduction of Am (IV)
6.0*	29.4	87.7	11.7	0.6	36	64
4.0*	16.9	80.7	18.9	0.4	57	43
2.0	10.3	75.7	24.3	0.0	73	27
1.0	5.7	68.1	30.1	1.8	96	4

* Americium dioxide dissolved with heating on a water bath.

radiolytic reduction of Am (IV) and Am (VI) in parallel with the reactions described. The time from the moment of separation of the solution to the beginning of measurements was 10-20 min, during which Am (VI) could be partially reduced to Am (V) by radiolysis products. The small amount of Am (V) detected in the solution was apparently caused by precisely this reduction. Assuming this, it is possible to determine the amount of Am (VI) reduced up to the moment of the measurements. As can be seen from the table (third column from the right) this correction is insignificant. There is also radiolytic reduction of Am (IV) during solution of the dioxide and this cannot be neglected so that the percentage yield of the reduction reaction is the over-all result of reduction by water and radiolysis products. However, it was not possible to allow quantitatively for the contribution from radiolytic reduction as americium dioxide was present up to the moment of separation of the phases and the amount of americium in this was several times greater than the amount of americium in solution. The yield of Am (IV) reduction in 0.5 and 1.0 M sulfuric acid may be ascribed almost completely to radiolysis. It is only correct to consider Am (IV) reduction by water in the case of dioxide solution with heating.

A kinetic investigation of reactions (1) and (2) is very difficult due to their high rates. Nonetheless, the results obtained indicate that the absence of Am (IV) from moderately acid aqueous solutions is caused predominatly by reactions (1) and (2).

LITERATURE CITED

1. J. Perlman and K. Street, The Actinide Elements (McGraw-Hill Co., New York, 1954) Chapt. 14.
2. L. Asprey, J. Amer. Chem. Soc. 76, 2016 (1954).
3. L. Eyring, H. Lohr, and B. Cunningham, J. Am. Chem. Soc. 74, 1186 (1952).
4. S. Stephanon, L. Asprey, and R. Penneman, US, ASC-925 (1950).
5. G. Hall and P. Herniman, J. Chem. Soc. (1954) 2214.
6. G. Hall and T. Markin, J. Inorg. and Nuclear Chem. 4, 296 (1957).
7. G. N. Yakovlev and V. N. Kosyakov, "Investigations in geology, chemistry, and metallurgy," Reports of the Soviet Delegation to the International Conference on the Peaceful Uses of Atomic Energy (Geneva, 1955) [in Russian] (Izd. AN SSSR, 1955) p. 237.
8. G. N. Yakovlev, A. A. Zaitsev, V. N. Kosyakov, A. G. Rykov, and Yu. P. Sobolev, "Investigation of some oxidation–reduction reactions of americium," Trans. All-Union Sci. Tech. Conference on the use of radioactive and stable isotopes and radiation in the national economy and science. Coll.: Isotopes and Radiation in Chemistry [in Russian] (Izd. AN SSSR, 1958) p. 326.

NEUTRON SPECTRUM OF A Po–α–O SOURCE

A. G. Khabakhpashev

Original article submitted January 24, 1959

The oxygen isotope O^{18} has a large cross section for the (α, n) reaction. The neutron yield on a thick target made from the pure O^{18} isotope is 31 neutrons for 10^6 α particles with an energy of 5.3 Mev[1]. In the present paper the energy spectrum of a Po-α-O source has been measured.

The source was a nitric acid solution of polonium, prepared in water enriched to 24% with the isotope O^{18}. 2.3 cm^3 of a solution containing 1.38 C polonium was poured into a thin-walled stainless steel container with an inside diameter of 8 mm. The intensity of the neutron source was measured on a "long counter" [2] by comparison with a Pu-α-Be standard and was $2.3 \cdot 10^3$ sec^{-1}. The neutron yield on the thick O^{18} target, calculated from the data of this source, turned out to be equal to 30.7 neutrons for 10^6 α particles.

For the measurement of the energy of the Po-α-O source, a fast neutron scintillation spectrometer with a high efficiency was used.* A block diagram of the equipment is shown in Fig. 1.

The operating principle of the spectrometer is based on the measurement of the energy spectrum of recoil protons accompanied by scattered neutrons with a definite value of the energy. In this case the primary neutron energy can be defined as the sum of the energies of the recoil proton and the scattered neutron. In order to isolate the scattered neutrons having a given energy, amplitude-time selection was applied. Scattered neutrons with energies from 120 to 380 kev were segregated according to their transit time by a delayed coincidence circuit ($\tau = 5.5 \cdot 10^{-9}$ sec, delay time $1.9 \cdot 10^{-8}$ sec, transit distance 11.5 cm). A pulse selector in the second channel and a slow coincidence circuit made it possible to constrict the

* The spectrum will be described in detail in a separate publication.

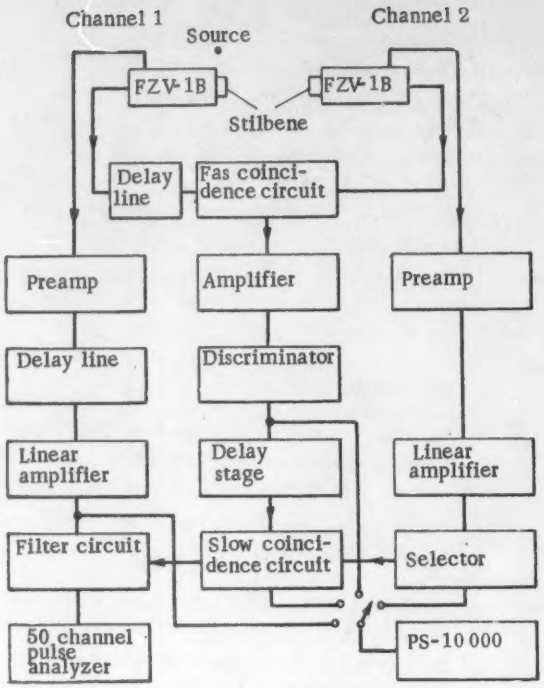

Fig. 1. Block diagram of the fast-neutron scintillation spectrometer.

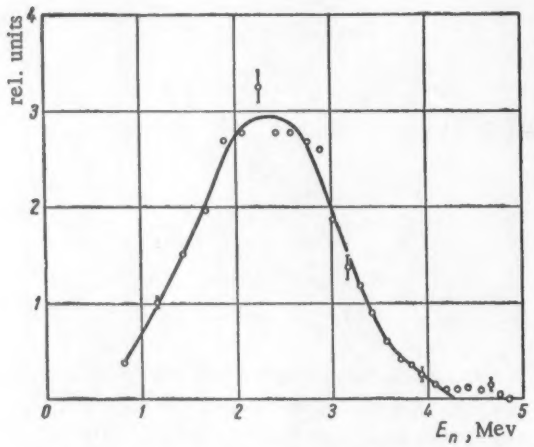

Fig. 2. Experimental neutron spectrum of the Po-α-O source.

energy interval of the scattered neutrons detected by the selector, to reduce the number of chance coincidences approximately ten times, and to exclude the detection of identical pulses. Identical pulses with a very large amplitude, elicited by γ quanta and cosmic particles, could pass through the fast coincidence circuit, since it has a sensitivity of ~100 kev (for protons). The energy of the scattered neutrons recorded by the spectrometer with pulse selector and slow coincidence circuit was equal to 260 ± ± 80 kev.

The amplitude distribution of the recoil-proton pulses was recorded on an AI-50 analyzer. For the transition to the energy spectrum of the recoil protons the data cited in [3] were used. The calibration of the spectrometer was performed according to the maximum with an energy of 4.85 Mev in the spectrum of the Po-α-Be source. The resolving power of the spectrometer was 100% for neutrons with an energy of 3 Mev.

The dependence of the spectrometer efficiency on the neutron energy can be expressed analytically if a crystal with a large diameter is used in the second channel and the distance between the source and the first crystal is not too small. For the case when both scintillators have approximately the same dimensions and the source is set up nearby the first crystal, the dependence of the efficiency on the energy should be determined experimentally. The spectrometer operation was checked out on the Po-α-Be source in two geometries.

For recording the neutron spectrum of the Po-α-O source the second geometry was used, for which the efficiency of the spectrometer was greatest. The dependence of the efficiency on the energy was determined from the Po-α-Be source, the spectrum of which has been quite satisfactorily measured in [4].

The neutron spectrum of the Po-α-O source is given in Fig. 2. The spectrum has a clearly pronounced maximum with an energy of 2.4 Mev. The maximum energy is equal to 4.3 Mev. The spectrum was recorded over a period of 20 hr. The total efficiency of the spectrometer, i.e., the ratio of the number of pulses detected to the number of neutrons emitted by the source, turned out to be equal to 10^{-6}.

The neutron spectrum of the Po-α-O source, as calculated on the assumption that the emission of neutrons excited by Ne^{22} nuclei proceeds isotropically in the center-of-mass system, is shown in Fig. 3. The method for calculating the spectrum was described in [4]. In the calculation data pertaining to the dependence of the cross section for the reaction $O^{18}(\alpha, n)Ne^{21}$ on the energy of the α particles [5] were used, as well as the results of a measurement of the γ radiation that accompanied the emission of neutrons.**

The results of the calculations and measurements are found to be in satisfactory agreement. The somewhat general displacement of the measured neutron spectrum in the direction of lower energies (by approximately 200 kev) could be connected with the scattering of neutrons at the source. Moreover, it is possible that the assumption of an isotropic emission of neutrons is not correct. In that case,

** According to these measurements, the decay of the Ne^{22} nucleus proceeds to the fundamental level of Ne^{21} (55%), the first excited level with energy 0.350 Mev (35%), and the second level with energy 1.73 Mev (10%) (a paper is to be published).

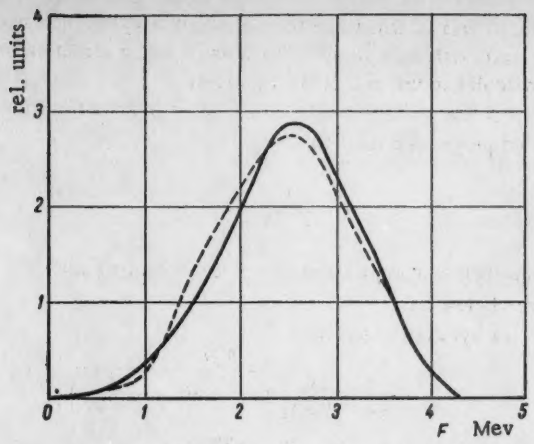

Fig. 3. Calculated neutron spectrum of the Po-α-O source.

the difference between the measured and calculated spectra must indicate the fact that the emission of neutrons in the direction of motion of an α particle is less probable.

Since the excitation functions for transitions to the fundamental and first two excitation levels of the Ne^{21} nucleus are clearly unknown, in the calculation it was assumed that they have the same form as the general excitation function given in [5]. However, the form of the excitation function is not too strongly manifested in the neutron spectrum. For the sake of comparison, the neutron spectrum, calculated on the assumption that the excitation function for a transition to the 0.350 Mev level has a rectangular form for an energy from 3.5 to 5.3 Mev, is illustrated by a dashed line in Fig. 3.

It is my privelege to thank É. M. Tsenter for his undivided attention to the work, and to V. V. Ivanova and L. P. Gaidukova for assistance in preparing the source.

LITERATURE CITED

1. I. A. Serdyukova, A. G. Khavakhpashev, and É. M. Tsenter, Izvest Akad. Nauk SSSR, Ser. Fiz. 21, 1017 (1957).
2. A. Hanson and J. McKibben, Phys. Rev. 72, 673 (1947).
3. C. Taylor, W. Jentschke, M. Remley, F. Eby, and P. Kruger, Phys. Rev. 84, 1034 (1951).
4. B. Whitmore and W. Baker, Phys. Rev. 78, 799 (1950).
5. T. Bonner, A. Kraus, J. Marion, and J. Schiffer, Phys. Rev. 102, 1348 (1956).

SPACE DISTRIBUTION OF IONS IN A LIQUID

V. I. Ivanov

Original article submitted January 12, 1959

The distribution of ions in a medium being exposed to radiation is determined to a large part by the structure of the tracks of the ionizing particles. The structure of the tracks depends in turn on the type of particles as well as the properties of the medium being irradiated. Several investigators [1-3] have concerned themselves with the study of these problems for different conditions of radiations. The special feature of liquids consists in the large density of ionization along the tracks of the ionizing particles which gives rise to a nonuniform distribution of the ion concentration.

For heavy particles, the specific volume appears to be a cylinder, while in the case of β or γ radiation, the ions are clustered into specific volumes of an approximately spherical form. As a result of recombination, the total number of ions decreases in time (within the limits of the specific volume), while the volume itself increases because of diffusion until the ions are not uniformly distributed over the whole volume being exposed to radiation.

Thus after a prolonged irradiation, part of the ions are uniformly distributed over the whole volume irradiated, and the other part is concentrated into nuclei of spherical or cylindrical form or some intermediate form.

The purpose of the present work is to determine the concentrations of ions of the uniformly distributed background and the concentrations of the ions concentrated in nuclei as a function of the conditions of the irradiation.

The method of investigation is based on the assumption that at the instant of their formation, all of the ions are concentrated into nuclei of volume V_0 (of identical form). As a result of recombination and diffusion, the ion concentration in the volume of the nucleus will decrease, and within a time τ (the time of the existence of the nucleus as an independent discrete portion in the irradiated volume) becomes equal to the concentration of ions of the background y_0. The variation in the concentration of ions of the background from the instant of the start of the exposure is determined by the equation

$$\frac{dy}{dt} = -\alpha y^2 + q, \qquad (1)$$

where α is the recombination coefficient of the ions, and q is the number of ion pairs being added to the background in unit time and unit volume because of the disappearance of nuclei.

In an equilibrium state, the concentration of ions of the background

$$y_0 = \sqrt{\frac{q}{\alpha}}. \qquad (2)$$

If the number of ions in a nucleus at the instant of its disappearance as an independent specific volume is equal to N_τ, and ν is the number of nuclei formed in unit time in unit volume, then

$$q = N_\tau \nu. \qquad (3)$$

For the given conditions of exposure, ν is proportional to the intensity of light.

From (2) and (3) we obtain

$$y_0 = \sqrt{\frac{N_\tau \nu}{\alpha}}. \qquad (4)$$

The problem of determining the equilibrium concentration of ions of the background y_0 thus leads to the determination of the number of ions N_τ in the nucleus at the instant of its disappearance.

The dependence of the number of ions in the nucleus on time can be represented in the form

$$N = N_0 f(t), \qquad (5)$$

where N_0 is the number of ions in the nucleus at the instant of its formation.

The function f(t) can be found from the condition of diffusion and recombination.

In the case of uniform formation of nuclei over the whole volume being irradiated, it is reasonable to assume that (for an equilibrium state) no new ions are formed in the volume occupied by the nucleus during the period of the independent existence of the nucleus; i.e., that

$$\tau = \frac{1}{\nu V_\tau}, \qquad (6)$$

where V_τ is the volume of the nucleus at the instant of its disappearance. The variation of the volume of the nucleus with time can be represented in the form

$$V = V_0 \varphi(t), \qquad (7)$$

where the function $\varphi(t)$ is found from the same conditions as was f(t). Relations (3) and (4) determine the equilibrium concentration of ions of the background.

The equilibrium concentration of ions concentrated in nuclei

$$x_0 = \overline{N} n_0, \qquad (8)$$

where $\overline{N} = \frac{N_0}{\tau}\int_0^\tau f(t)\,dt$ is the average number of ions in the nucleus for the period of its existence; $n_0 = \nu\tau$ is the equilibrium number of nuclei in unit volume.

Analytic expressions for x_0 and y_0 were obtained by this means for the case of cylindrical and spherical forms of nuclei. It was assumed that the volume of a cylindrical nucleus increases only as a result of diffusion along a direction perpendicular to the axis of the cylinder.

For the average displacement of an ion due to diffusion, we employed the relationship

$$\overline{r} = \sqrt{\frac{4}{\pi} Dt},$$

where D is the usual diffusion coefficient. Formulas are given below for:

1) cylindrical nuclei

$$y_0 = \left\{\frac{N_0 \nu}{\frac{1}{\alpha} + \frac{2N_0}{V_0 a^2}\left[\ln(1+ak) - \frac{ak}{1+ak}\right]}\right\}^{1/2},$$

where $k = \frac{1}{2a}\left[\left(1 + \frac{4a}{\sqrt[3]{\nu V_0}}\right)^{1/2} - 1\right]$,

$a = \sqrt{\frac{6\pi D l}{V_0}}$ (l is the length of the cylinder)

$$x_0 = \frac{N_0 \nu\tau}{1 + \frac{2\alpha N^0}{V_0 a^2}\left[\ln\left(1 + \frac{4}{3}a + \frac{1}{2}a^2\tau\right)^{1/2} + \frac{1}{1 + \frac{4}{3}a + \frac{1}{2}a^2\tau} - 1\right]};$$

2) spherical nuclei

$$y_0 = \left[\frac{N_0 \nu}{\frac{1}{\alpha} + \frac{1}{V_0}\left(\frac{k}{1+bk}\right)^2}\right]^{1/2},$$

where k is determined from the equation

$$\frac{1}{\sqrt[3]{k^2}} = \sqrt[3]{\nu V_0} + 1{,}82\sqrt[3]{\nu}\sqrt{D_1}k,$$

$$b = \frac{1{,}82\sqrt{D_1}}{\sqrt[3]{V_0}}, \quad D_1 = \frac{3}{2}\pi D;$$

$$x_0 = \frac{N_0 \nu\tau}{1 + \frac{a}{V_0}\left(\frac{k_1}{1+bk_1}\right)^3},$$

where $k_1 = \frac{\sqrt[3]{1+A} - 1}{b}$,

$$A = 2bk + \frac{3}{2}b^2k^2 + \frac{2}{5}b^3k^3.$$

x_0 is determined approximately according to the average volume of the nucleus during the period of its existence. The accuracy of the determination of the concentrations x_0 and y_0 depends on the accuracy of the original data. The relationships obtained for other similar conditions enable one to characterize the distribution of ions in the irradiated medium more accurately than by calculations made on the basis of the Magee [3] model. The Magee model is applicable only to cylindrical nuclei, and its underlying assumption as to the type of nuclear volume variation does not altogether strictly agree with diffusion theory.

It follows immediately from the relations obtained that the relative concentration of background ions increases with an increase of the initial volume of the nucleus and the intensity of the radiation. This explains some of the laws of behavior of liquid ionization chambers. The relationships for determining the concentrations x_0 and y_0 can be used in

the studies of reactions in radiation chemistry and of the effect of radiation on organisms.

LITERATURE CITED

1. G. Jaffe, Ann. Phys. 42, 303 (1912).
2. D. Lea, Proc. Cambridge Phil. Soc. 30, 80 (1934).
3. J. L. Magee, "The theory of radiation chemistry. (I) Effects of variation in ionization density," J. Am. Chem. Soc. 73, 3270 (1951).

RADIOACTIVITY OF AEROSOLS IN THE BUILDING HOUSING THE SYNCHRO-CYCLOTRON OF THE JOINT INSTITUTE FOR NUCLEAR STUDIES

V. P. Afanas'ev

Original article submitted January 10, 1959

It has been shown previously [1] that the air near the operating OIYaN syncrocyclotron becomes active, and that the activity is observed for several minutes after the accelerator is shut down. It is natural to assume that the aerosols suspended in the air are activated by the beam of high energy particles. The present investigation was conducted in order to determine the amount of radiation hazard due to the active aerosols and, insofar as possible, to determine their isotopic composition.

In order to select the aerosol samples, an arrangement was used which consisted of a dust-collecting fan, filter, and a counter which measured the volume of air which passed through the filter. The analytic filter, placed at the counter entrance, was a circle 28 mm in diameter, to which rubber washers were cemented from two sides to create a vacuum seal. We began to pump the air either immediately upon shutting off the accelerator or else a few hours afterward. The aerosol samples were collected from the most unsafe places. The activity of the filter was measured from 2 to 5 minutes after completing the pumping of the air. The beta radiation was measured with an end-window Geiger counter with a mica window whose thickness was ~ 5 mg/cm^2. The thickness of the filter (without considering its gauze backing) was 3 mg/ cm^2, while the distance from the filter to the sensitive volume of the counter was 15 mm. The value of the relative solid angle ω in this connection was equal to 0.06 [2].

In order to determine the portion of the aerosols r which was not captured by the filter, special measurements with two filters placed one above the other at the counter entrance were made. It was found that the portion of the aerosols not retained by the filter amounted to only 10%.

The maximum coefficient S of self-absorption of β particles in the filter was also determined. The coefficient of self-absorption S was equal to 0.98 for β particles emitted by the aerosols which were selected from the accelerator chamber; for β particles of aerosols obtained in the open air it was 0.85. The coefficients of absorption in the air layer K_1 and in the counter window K_2 were equal to 0.91 and 0.75, respectively.

Fourteen aerosol samples were taken in the accelerator chamber. Samples were simultaneously taken outside of the chamber. The value of the activity in the accelerator chamber was on the average equal to 84 pulses/ min/m^3, while in the open air it was 25 pulses/ min/ m^3. The average value of the activity caused by the operation of the accelerator thus amounted to 59 pulses/ min/ m^3. Half lives were also measured and the energy of the betas was estimated by measuring the absorption in aluminum. The half life and energy of the natural aerosols (samples taken outside the accelerator chamber) were all equal: T= 30 min $\pm$ 50% and E_β = 0.65 Mev $\pm$ 40%, respectively. Measurements of the constants of the radioactive decay of the aerosols selected in the synchrocyclotron chamber gave the following results: T = 14 hr $\pm$ 20% and E_β = 1.25 Mev $\pm$ 40%. The natural radioactivity of the aerosol is caused by one of the decay products of radon, that is Pb^{214} (RaB) [3].

On the basis of the measurements of the constants of the emission from the long-lived aerosols detected in the synchrocyclotron building, and also starting from the composition of the substances which were distributed in the vicinity of the accelerator (a massive concrete shield) and which were exposed to radiation consisting of the high energy particles, it is possible to assume that the activity of the aerosols in the accelerator chamber is caused in the main by the isotope Na^{24}.

The Na^{24} concentration in the air was calculated with the aid of the relation.

$$C_{Na^{24}} = \frac{N}{3{,}7 \cdot 10^{10} 60 \omega \cdot SKr \cdot 10^3} \text{ curie/liter,}$$

where N is the number of counts in 1 minute in 1 m^3 of the sampled air; 3.6×10^{10} is the conversion factor to units of curies; 10^3 is the conversion factor from cubic

meters to liters. The values of all of the other correction factors are listed above.

A correction factor will have to enter into the calculated formula for the general case in order to allow for the decay of the aerosols in the filter during the pumping period. However, in the present investigation such a factor was not introduced for two reasons: the pumping period was short compared with the half life of Na^{24}, and the pumping in the accelerator chamber and in the open air was carried out over equal intervals of time.

On substituting numerical values in the formula, we obtain $C_{Na^{24}} = (5 \cdot 10^{-13} \pm 50\%)$ curie/liter, which is 0.001 of the maximum allowable concentration of Na^{24} in air.

Let us estimate the Pb^{214} concentration in the air outside the synchrocyclotron building. Substituting the value for this case into the formula given, we obtain $C_{Pb^{214}} = 10^{-13}$ curie/liter. Such a value of the concentration of Pb^{214} (RaB) agrees with the data obtained in [4].

SUMMARY

1. It has been found that radioactive aerosols are formed in the chamber of the synchrocyclotron during its operation.

It is proposed that the activity of the aerosols in the acceleration chamber are due to the isotope Na^{24}. The Na^{24} concentration is equal to $(5 \cdot 10^{-13} \pm 50\%)$ curie per liter, which is 0.001 of the maximum allowable concentration. The concentration of the natural active aerosol Pb^{214} (RaB) in atmospheric air is equal to 10^{-13} curie/liter.

In conclusion, the author wishes to thank M. M. Komochkov and V. N. Mekhedov for critical comments and help in carrying out the present investigation.

LITERATURE CITED

1. M. M. Komochkov and V. N. Mekhedov, Atomnaya Énergiya 4, 71 (1958).*
2. N. G. Gusev, Handbook of Radioactive Radiations [in Russian] (MEDGIZ, 1955).
3. V. I. Baranov, Radiometry [in Russian] (Izd AN SSSR, 1955).
4. S. Zech, Czechoslovak Fiz. J. 7, 83 (1957).

* Original Russian pagination. See C.B. Translation.

THE PART TO BE PLAYED BY SCIENTISTS IN FULFILLING THE DECISIONS OF THE TWENTY-FIRST CONGRESS OF THE COMMUNIST PARTY OF THE SOVIET UNION

V. Korovikov

(From the Annual Conference of the Academy of Sciences of the USSR)

The annual general conference of the Academy of Sciences of the USSR took place on March 26-28, 1959, at the Moscow Home of Scientists. The conference was devoted to the ways and means for scientists to participate in fulfilling the decisions of the Twenty-First Congress of the Communist Party of the Soviet Union.

A. V. Topchiev, Vice President of the Academy of Sciences of the USSR, addressed the gathering in a report on the activities of the Academy over the past year and on tasks for the immediate future. A review report devoted to Soviet space research and upper atmosphere studies with the aid of rockets and artificial satellites was delivered by the President of the Academy, A. N. Nesmeyanov.

Over 20 persons took the floor in the discussion. A prominent place in the reports and statements of the participants at the conference was taken up by problems in the development of physics, particularly nuclear physics, and the development of engineering. The foremost in importance among some twenty odd prime problems in modern science were agreed upon as the control of thermonuclear fusion reactions and the study of elementary particles.

The physics and mathematics division was, and remains, the largest division in the Academy. Eleven new institutes have been established under the auspices of this division during the past three years, including five such institutes belonging to the Siberian section alone. Academician M. A. Lavrent'ev remarked that the building housing the Institute of Nuclear Physics is one of the first constructions going up at the site of the scientific city near Novosibirsk.

Control of thermonuclear reactions, the study of intranuclear forces, problems of neutron physics, radiochemistry and radiobiology, these are the most important tasks facing Soviet science in the next seven years. A broad scope has been attained in the construction of nuclear electric power stations. Further research on coolants, fuel elements and the choice of the most economically competitive reactor types are required in this area. New accelerators and reactors of novel design will be built.

Corresponding Member of the Academy of Sciences B. P. Konstantinov discussed in detail the work of the Physics and Engineering Institute, the oldest center of nuclear physics in the USSR, which has trained scores of first-rank research. Research work on the study of thermonuclear fusion will be expanded at the Institute, research on atomic nuclei will be extended, instrumentation is being devised and improved, e.g. a high-precision beta spectrometer, instruments for automating the monitoring of nuclear emulsion tracks.

A new Constitution for the Academy of Sciences was adopted at the conference. Its postulates are aimed at the further development of the methods of collective supervision of scientific activity, toward the all-around development of the creative initiative of the scientists, toward the development of democratic forms of organization. The conference devoted particular attention to the problems of organizing and coordinating scientific research, bridging the gap between completed research and production, assimilation of new discoveries, the material and technical needs of research institutes and laboratories. A resolution was passed on the establishment of scientific council bodies supervising the basic problems in research work. They will have the task of coordinating and directing the entire effort of academical and extra-academical research teams in the different areas of science and engineering.

NINTH ALL-UNION CONGRESS ON NUCLEAR SPECTROSCOPY

The Ninth All-Union (Annual) Congress on Nuclear Spectroscopy met in Kharkov on January 26 to February 2, 1959. The Congress was attended by over 300 scientific workers from research institutes and institutions of higher learning throughout the country. Over 100 reports were heard on the results of theoretical and experimental research work on differerent problems in the structure of nuclei, α and β decay. A short review of some of the papers read is given below.*

* Part of the proceedings of the Congress were published in Izvest. Akad. Nauk SSSR, Ser. Fiz. 23, No. 2 (1959); the remaining papers will appear in No. 7 of the same journal and in 24, No. 1 (1960).

Theory of the Nucleus; General Problems in Beta Decay. Problems in the theory of the nucleus were discussed at the first session of the Congress. In his report, A. S. Davydov (Moscow State University) gave a review of experimental results obtained in research on low excited states of nuclei, and presented a classification of excited states based on current theoretical concepts. As a possible explanation of the discrepancies between theory and experimental findings, and in particular of the anomalous rule of intervals in rotational bands, a deviation of the shape of the nucleus from the axisymmetric model was proposed. The nonaxiality parameter is determined from experimental data on the position of two energy levels of spin 2. The position of rotational levels and the intensity of transitions between those levels are computed on the basis of that parameter, and are found to agree well with the experimental data. In L. K. Peker's papers on new research on deformed nuclei, and the research of B. L. Birbrair, L. K. Peker, and L. A. Sliv (Leningrad Physics and Engineering Institute) on quadrupole oscillations of deformed nuclei, the older concepts retaining the axially symmetric shape of the nuclei were used in the interpretation of the experimental data. Two modes of oscillation of the nuclei are discussed in the latter report, oscillation along the axis of deformation (β mode) and oscillation transverse to that axis (γ mode), and expressions are derived for the energy of the first β and γ levels of vibration. Coupling between rotation and vibrations is taken into account, and the general corrective factor for the energy of the rotational band levels is derived.

A report presented by E. V. Inopin, V. Yu. Gonchar, and S. P. Tsytko (Kharkov Physics and Engineering Institute) was devoted to the use of the generalized model for an analysis of the experimental data available on β transitions in light nuclei. The ft values computed on the basis of that model and the values of the β-transition matrix elements showed better agreement with experimental data than the result of calculations using the shell model.

Results of theoretical research embodying new concepts on interactions between nucleons in nuclei were presented in several papers. S. T. Belyaev (Institute of Atomic Energy) told of the calculation of pair correlations in nuclei. The position of low excited states of the nucleus derived from that model is consistent with experimental data. The theory explains the familiar character of the dependence of the shape of the nucleus on the filling factor of the shell. A paper presented by A. B. Migdal (Institute of Atomic Energy) reported on the results obtained in applying the superconductivity model to nuclei, and on deriving general expressions for the moments of inertia of the nuclei, on the basis of that model. P. É. Nemirovskii (Institute of Atomic Energy) discussed the problem of the neutron stability of nuclei.

The general problems of β-decay theory were dealt with in the review paper presented by Ya. A. Smorodinskii (Institute of Atomic Energy).† Theoretical and experimental investigations conducted during recent years have made it possible to formulate a universal theory of weak interactions. The theory describes a number of events known at the present time, and predicts new processes which have yet to be detected experimentally. The report outlines the most interesting trends in the field of experimental β-decay research.

Among the interesting experimental research papers devoted to the general problems of β decay were the contributions of V. V. Vladimirskii, V. K. Grigor'ev, V. A. Ergakov, and Yu. V. Trebukhovskii (Institute of Theoretical and Experimental Physics) and of V. M. Lobashev, V. A. Nazarenko, and L. I. Rusinov (Leningrad Physics and Engineering Institute). The first paper reported measurements of the angular correlation between the directions in which electrons and neutrinos are deflected in the β decay of a free neutron. The correlation was studyed by investigating the spectrum of decay electrons at a fixed pulse of recoil protons. The authors estimated, with an appreciable statistical error to be sure, the value of the ratio of the Fermi and Gamow-Teller interaction constants. In the second paper, the correlation between transverse polarization of the decay electrons and circular polarization of the accompanying γ quanta is investigated. Preliminary measurements were carried out for Sc^{46} and Co^{60}. Further research on this correlation may succeed in resolving the question of the existence of an imaginary part in the Hamiltonian of β interaction.

Decay Schemes; γ Emission by Nuclei. The most popular subject for original papers at the Congress was research work on β spectra, internal conversion spectra of electrons and gamma radioactivity of nuclei. Here it is necessary to take note of the large quantity of papers presented by the staff of the Kharkov Physics and Engineering Institute including: Yu. P. Anufriev, A. K. Val'ter, Yu. V. Gonchar, E. G. Kopaneits, A. N. L'vov, P. M. Tutakin, S. P. Tsytko, P. V. Sorokin, A. S. Deineko, I. Ya. Malakhov, and A. Ya. Taranov, on research into the levels of several nuclei appearing in (p, γ) reactions. A proton beam of 4 Mev energy from an electrostatic generator was used. The reactions studied were $Si^{28,29,30}(p, \gamma)$, $Ne^{20}(p, \gamma)$, $S^{32,34}(p, \gamma)$, $A^{40}(p, \gamma)$, and $N^{14}(p, \gamma)$. As a result of the measurements performed, information was obtained on the position, width, and relative intensity of various resonances. For some hard γ lines, the polarization of the gammas was determined on the basis of observation of the photodisintegration of a deuteron.

An appreciable proportion of the reports was presented by colleagues of the Leningrad Physics and Engineering Institute. The papers contributed by D. G. Alkhazov, A. P. Grinberg, G. M. Gusinskii, M. Kh. Lemberg, V. V. Rozhdestvenskii, and K. N. Erokhina reported investigations of the Coulomb excitation of low levels in several nuclei, by bombarding them with a beam of multiply charged ions (C, N, O, and Ne) accelerated in a cyclotron. Results were

† Transl. note: Smorodinskii, Uspekhi Fiz. Nauk 68, 653 (1959).

presented of measurements of the excitation probabilities and lifetimes of low levels of several nuclei studied.

Several of the reports presented data on new measurements of beta spectra and spectra of internal conversion electrons. The results of that research serve to refine and supplement the decay schemes of the nuclei investigated. Several other papers presented by colleagues of the Leningrad institutes and the Joint Institute for Nuclear Studies were devoted to continued research on neutron-deficient nuclides of the rare-earth elements. The nuclides investigated were produced from fragmentation reactions effected by bombarding tantalum with fast protons (680 Mev). Following chromatographic analysis of the preparations, the β and γ spectra and the spectra of internal conversion electrons were studied. Some previously unknown γ transitions were detected in several nuclei. A paper submitted by A. V. Kalyamin, A. N. Murin, V. N. Pokrovskii, and V. A. Yakovlev (RIAN) presented proofs of the existence of radioactive isotopes Tm^{161}, Ho^{159}, Ho^{155}, and Ho^{157}. A study of the decay schemes of some neutron-deficient isotopes using the method of coincidences of internal conversion electrons was reported in papers submitted by B. S. Dzhelepov and V. A. Sergienko (Leningrad State University). A double-lens β spectrometer was used in the measurements.

Several of the reports dealt with theoretical and experimental research into the internal conversion of γ rays.

Spectroscopic Techniques. At the session devoted to problems arising in the techniques of α, β, and γ spectroscopy, new large magnetic spectrometers having excellent optical characteristics were discussed in some of the papers.

A paper by B. S. Dzhelepov, R. B. Ivanov, V. G. Nedovesov, and V. G. Chumin (RIAN) reported on a double focusing (angle $\pi\sqrt{2}$) α spectrometer. The instrument has a resolving power of 0.10% and aperture ratio of $3 \cdot 10^{-3}$ of the total solid angle. The radius of the central orbit is 33.5 cm. Work on designing an α spectrometer of the same type, but having higher characteristics, was discussed in a paper by S. A. Baranov, V. V. Beruchko, A. G. Zelenkov, A. F. Malov, and G. Ya. Shchepkin (Institute of Atomic Energy). The resolution of the spectrometer was 0.1%, and the aperture ratio $\sim 8 \cdot 10^{-4}$ of the total solid angle. The radius of the central orbit was 155 cm. The instrument exhibits high emissivity (product of the source area and the solid angle), and makes possible investigations of α lines at very low intensities. The spectrometer may also be operated as a spectrograph. In that case, the energy range of the α particles simultaneously recorded by the photographic plates reaches ~10%. An interesting report of the fabrication of a magnetic spectrograph for heavy charged particles was presented by I. F. Barchuk, G. V. Belykh, V. I. Golyshkin, and V. A. Kovtun (Physics Institute of the Academy of Sciences of the Ukrainian SSR). The instrument, small in size, simultaneously records the spectrum of protons over the 3-25 Mev range on photographic plates. The spectrograph is equipped to measure the angular distributions of charged particles in the range of angles from 5° to 170°.

Representatives of the Ministry of the Electronics Industry reported the development of new types of photomultiplier tubes possessing high spectral and time characteristics. It noted that the creation of highquality luminescent spectrometers is hampered at the present time not by the spectral response of the photomultipliers, but rather by the inadequacies of scintillators now being produced. The Conference discussed a report on the status of work in the field of scintillator manufacture, and took note of the need to effect considerable improvement in the spectral response of scintillator devices.

Bringing the Conference to a close, S. B. Dzhelepov briefly summed up the work accomplished, and noted the fundamental successes achieved in nuclear spectroscopy during the preceding year. The concluding remarks also directed attention to the desirability of achieving more rapid and more complete publication of the necessary reference materials and tables.

V. P. Rudakov

THE PHYSICS AND ENGINEERING DEPARTMENT AT THE URAL POLYTECHNIC INSTITUTE

Scientific research in various branches of physics is in progress at the Physics and Engineering Department of the S. M. Kirov Ural Polytechnic Institute (Dean, S. P. Raspopin).

The department, headed by D. A. Borodaev, boasts of a 15 Mev betatron commissioned in December, 1958. The department is planning to conduct research on the effects of irradiation of living organisms (mice, rats, rabbits) and testing new medicinal preparations. Studies of the properties of semiconductors subjected to radiation are scheduled Assembly has been completed on a cyclotron designed to accelerate α particles to 27 Mev. The machine is now being checked out. A manipulator designed at the Institute is used to periodically pulse the cyclotron. The cyclotron will contribute to the development of research in radiobiology, radiation chemistry, solid state physics, nuclear reactions at intermediate energies, and neutron dosimetry. Assembly of an ÉG-2.5 electrostatic generator has been started.

The Department of Theoretical Physics (under the supervision of Prof. G. V. Skrotskii), in collaboration with the Department of Organic Chemistry (supervised by Prof. I. Ya. Postovskii), is carrying on research on the structure of organic radicals, based on the electron paramagnetic resonance method. Attempts are being made to correlate

the reactivities of the free radicals with their physical properties. Two facilities are being assembled: one for the study of the hyperfine structure of the resonance line of organic radicals in the millimeter wavelength range and the other for isotopic analysis of substances using the nuclear magnetic resonance principle. An ÉM-3 electron microscope is being used to elaborate a procedure for research on the structure of ferrites, the processes of the formation and growth of crystals are being investigated, the structure of copper sulfide and nickel sulfide films is being studied, etc. One of the variants of the scanning method has been developed. Theoretical studies are being conducted on the widths of paramagnetic resonance lines and on the properties of systems of many interacting particles.

A group of undergraduate students, under the supervision of Khudenskii, carried out work during 1958 on constructing high-precision spectrometers for nuclear radiations. The possibility of designing fully automated spectrometers with high speed of response, on the basis of scintillation techniques and high-speed electronic computer techniques, was proved. This group designed and studied a 64 channel pulse-height analyzer. A conversion device was used to measure the amplitudes of the signal studied, by converting the amplitude into pulse duration and converting the latter into a pulse train with the number of pulses proportional to the signal amplitude. This intelligence is then stored in a magnetic memory. The height distribution of the pulses is read out on an oscillograph tube screen, with the aid of a decoder and special frequency generator.

The students' atomic physics lab (supervised by G. V. Solov'ev) is equipped with a facility for determining the magnetic moments of atomic nuclei by means of nuclear magnetic resonance, as well as a facility for measuring the magnetic moment of an electron using the electron resonance method.

Sverdlovsk P. K.

THE LATVIAN RESEARCH REACTOR

A 2000 kw(th) IRT research reactor is being built in Latvia (near Salaspils) for the Institute of Physics of the Academy of Sciences of the Latvian SSR (see Fig. 1). The decision to have the reactor built was taken because of the developing research underway in Latvia on the use of radioactive isotopes and nuclear research, requiring the powerful neutron source to be had in a nuclear chain reactor. Construction work on the reactor is scheduled for completion in 1960.

Construction. The IRT is a swimming-pool type (see Fig. 2). Ordinary distilled water will serve as both moderator and coolant. The reactor pool will be oval in shape. (2 m across, 4.5 m long). The core, containing 664 fuel rods (combined in assemblies) with enriched uranium, will be surrounded by beryllium oxide reflector and graphite. The fuel elements will be 50 cm long and ~1 cm in diameter. Forced cooling is used for the core. Rate of water flow is 400 m^3/hr, with about 300 m^3/hr passed through the core by ejection and 100 m^3/hr pumped by circulation pumps. The water of the primary loop is cooled in heat exchangers, and its temperature does not exceed 40°C while in the pool.

An inclined discharge chute built in the concrete biological shielding provides for the removal of spent fuel assemblies and irradiated samples or of stringers containing isotopes, the chute discharging into the pool. Removal of spent fuel is carried out by remote control.

Shielding and Health Physics. Biological shielding for the reactor is provided by a two-meter-thick layer of high-density concrete, laterally, and a layer of water 6 m deep

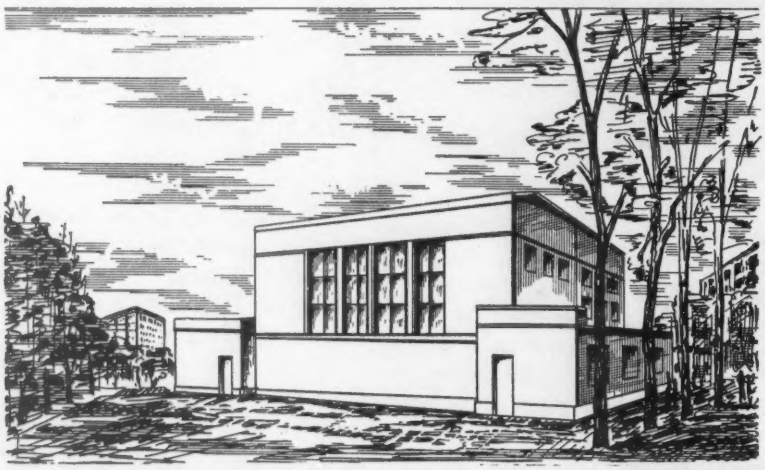

Fig. 1. General view of building housing reactor (projected).

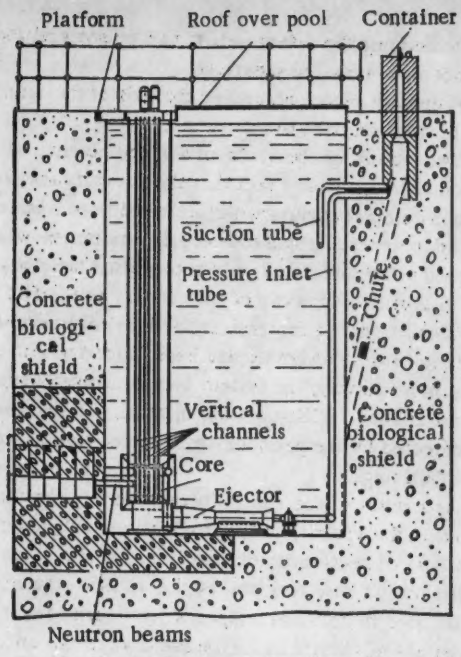

Fig. 2. Vertical cross section through reactor.

(on top of the reactor). The heat transfer loop of the reactor, including the swimming pool, is hermetically sealed, thus removing any hazard of radioactive contamination of the installation or reactor building. A ventilation system is being installed in the reactor building. The air is carefully filtered before being vented. The health service provides for strict monitoring of the radioactivity levels of the equipment, ground, clothing worn by personnel, etc. Special health monitoring booths are provided in the locker rooms. A zone of alienation stretching 1 km in radius has been established around the reactor. A special storage tank is being built to house hot wastes, and a burial ground for hot refuse is being set up.

Control System and Protection. Reactor control is effected by means of cadmium rods. 7 control rods, including 2 scram rods, are provided. The scram rods will be actuated whenever a 20% excursion beyond rated reactor power occurs, or when the rate of power buildup is excessive, or in case of faults in the electric control system circuits, etc. There is one rod in the automatic control system.

Experimental Equipment. The reactor incorporates a device for producing 9 horizontal neutron beams. The beam cross section is ~80 cm^2. Neutron flux in the beam will be $5 \cdot 10^8$ neutrons/$cm^2 \cdot$ sec. 7 vertical channels are provided for the production of radioactive isotopes and for obtaining samples with induced radioactivity. Six of these are passed through the reflector, and one through the center of the core. The flux through the central experimental channel is $1.2 \cdot 10^{13}$ neutrons/$cm^2 \cdot$ sec.

Research Programs Scheduled The scope of the problems being tackled by Latvian scientists is very broad. The projected research programs will cover the areas of nuclear spectroscopy, neutron physics, and solid state physics (including extensive research on radiation effects in materials). Chemical studies will be carried out on nuclear transmutation products, chemical reactions using radioactive isotope tracers will be studied, and the effects of neutron and gamma radiations on chemical reactions will also be investigated.

An appreciable portion of the research involves work in the areas of biology and medicine. The radioactive isotopes to be produced, particularly the short-lived isotopes, will be used for the treatment of malignant tumors, Basedow's goiter, and in diagnostics. The selective responses of different types of tumors to neutron bombardment when neutron-absorbing substances are introduced in the tumors will also be studied. A series of biological and physiological investigations involving the use of tagged atoms and radioactive sources, including research on metabolic processes in the organism, circulation of the blood, distributions of the various elements in different parts of the organism, is projected.

The radioactive isotopes produced in the pile will find use in the solution of many technical problems, particularly in wear studies on rubbing parts of machines.

In addition to the Institutes attached to the Academy of Sciences of the Latvian Republic, the Latvian State University, the Riga Polytechnic Institute, The Agricultural Academy, and the Research institutes under the auspices of the Ministry of Agriculture will also take part in the research and tests using the reactor facility.

To achieve coordination of the entire research effort, a Leningrad Council on the Peaceful Uses of Atomic Energy is being set up under the aegis of the Presidium of the Academy of Sciences of the Latvian SSR, with seats on the Council occupied by representatives of all of the organizations engaged in work with radioactive isotopes in the Republic. Scientists from Estonia and Lithuania will also use the reactor facilities.

Specialists for research work involving the use of the reactor and of radioisotopes will be trained primarily by the Physics and Mathematics Department of the Latvia State University and by the Chemistry Department of Riga Polytechnic Institute. Nuclear physics is being introduced as a new major at the university. Some of the students will complete their practical lab work at the atomic reactor being built in Tbilisi (Georgian SSR).

The Chemistry Department of Riga Polytechnic Institute has been engaged for some time in training specialists in radiochemistry. Students in this discipline will complete their practical lab training in laboratories in Moscow and Leningrad. Plans for the training of more highly skilled cadres envisage sending several teaching fellows to complete their graduate work in leading scientific institutions in Moscow, Leningrad, and other cities.

The start-up of the nuclear reactor will mark an important stage in the development of science in Latvia.

Yu. K.

In nuclear practice, as in any other branch of industry or technique, failure to observe safe work rules may result in severe, and sometimes tragic, consequences. As an example we note two fatal accidents which occurred during 1958: one in Yugoslavia (at the Boris Kidrič Institute of Nuclear Physics), the other in the United States (at Los Alamos Scientific Laboratory).

The accident at the Boris Kidrič Institute of Nuclear Physics took place on October 15, 1958 [1,2]. Experiments using the critical facility (see Fig. 1) of the Institute were in progress at the time, for the purpose of obtaining data on uranium–heavy-water lattices.

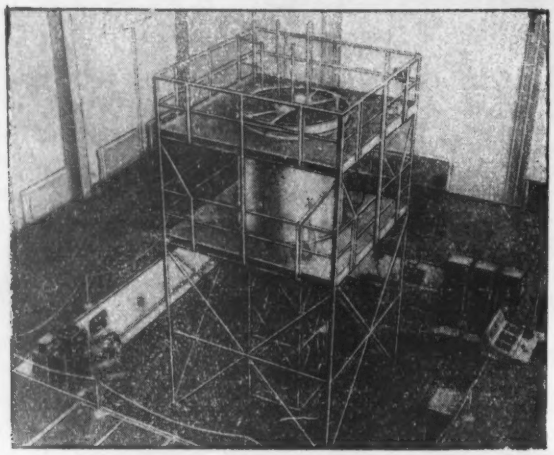

Fig. 1. General view of the critical facility in the Boris Kidrič Institute of Nuclear Physics.

The basic characteristics of the critical assembly in use are:

Inner diameter, cm	199.9
Height, cm	230
Natural uranium charge, kg	3995
Diameter of aluminum-clad uranium rods, cm	2.5
Critical level of moderator (at 22° C), cm	177.6 ± 1
Volume of moderator, m^3	6.36

Control of the critical facility was effected by varying the moderator level and by means of two cadmium control rods (50 cm long and 3 cm in diameter). The moderator level was varied with precision tolerances of 0.2 mm by means of electrical contact between the surface of the water and a level gage. Neutron flux was measured by three counters positioned around the periphery of the critical facility tank. The emergency control equipment consisted of two scram rods, a switch for emergency dropping of control rods, neutron detectors connected to a sonic annunciator panel, and an electric automatic shutdown circuit. The rods were held in place by electromagnets, which had to be operated from the emergency tripout switch dropping the safety rods to full poison position, and the rods were actuated separately.

A neutron source placed on the axis of the facility was used for the approach to criticality.

The reason for the accident was the absence of an interlock system, and the fact that the counters and the electric automatic shutdown circuit had been disconnected. (Radiation-recording and rod-release equipment were not designed as an integrated system providing interlocking control against a runaway of the critical assembly.) Under those conditions, an increase in the level of heavy water when the critical assembly had been loaded to critical resulted in a runaway; the system became strongly supercritical and the facility got out of hand. The runaway was detected by the personnel only by the smell of ozone in the building.

As a result of the abrupt increase in neutron flux, 8 persons in the vicinity of the reactor were subjected to a large dose of neutron irradiation (Fig. 2). To determine the irradiation dose received by the victims, the activities induced in gold and copper objects carried on the persons of the victims at the moment when the critical facility began to run away were measured.

Fig. 2. Diagram showing positions of victims (black dots) at the moment the critical facility started its runaway. Two workers, positions not shown in diagram, were some distance away from the facility at that moment, but also suffered exposures exceeding the maximum permissible dose.

Measurements showed that the integral flux of thermal neutrons alone reached an average of $2.2 \cdot 10^{11}$ neutrons per cm^2 at the points where the personnel were standing. From this, it was deduced that the energy developed by the reactor in the subcritical period was $8 \cdot 10^7$ watt-seconds. This figure fits well with the results of measurements of radioactive decay of fission products formed as a result of the facility runaway.

Further calculations showed that the victims received a mean whole-body irradiation of 116 RBE from neutrons at energies higher than 1 Mev, 223 RBE from neutrons of energies ranging from 1 Mev to thermal, and 49 RBE from thermal neutrons. The over-all mean neutron irradiation dose thus came to 388 RBE. It is important to note that some tissues and organs on the side of the body exposed to the critical facility received local doses of neutron irradiation going as high as 850 RBE, to a tissue depth of 10 cm.

Judging from data reported from experiments previously carried out to determine the intensity of γ radiation in the hall accomodating the critical assembly, it was established that the dose of γ radiation to which the Institute workers were exposed in the criticality accident reached 400r. Assuming the mean energy of the gammas to be 3 Mev, the dose of γ irradiation received by the whole organism, expressed in RBE units, would add another 295 RBE. The mean total dose of neutron and gamma irradiation accordingly comes to 683 RBE. Since the accident victims were standing at different distances from the critical facility, the differences in the exposures suffered ranged to $\pm 15\%$.

First aid was applied to the victims at the Institute. One of them died within the month. The two patients who had received the mildest exposures were treated in Belgrade, and the remainder were flown to Paris [1].

The fatality at Los Alamos Scientific Laboratory occurred on December 30, 1958, in the section where hot wastes left over from a plutonium extraction step are stripped and concentrated [3, 4]. The resulting slurries usually contain under 0.1 g/liter plutonium, with traces of americium. The plutonium and americium are removed by stepwise extraction using tri-n-butyl phosphate, with subsequent reextraction to an aqueous phase, which is concentrated by driving off the water. The final suspension, containing plutonium in quantities of several grams per liter, is recycled to an earlier extraction step.

In these processes, hydrolysis of the TBP occurs with resultant formation of mono- and dibutylphosphates in response to heat, nitric acid, and α radiation. The products of the hydrolysis tend to form stable complexes with plutonium, and must therefore be removed periodically from the extractant mixture. The suspended plutonium-containing solids then isolated are filtered off and directed in small batches to other sections for further processing.

An examination of the causes of the accident showed that the precipitate, containing a large quantity of plutonium which, had the process followed its normal course, would have been removed in small batches, this time issued from two vessels into the single large vat containing dilute aqueous and organic suspensions. After most of the aqueous slurry had been removed from the vessel, the remainder, amounting to ~150 liters, was transferred to a stainless-steel vat in which the critical mass formed (Fig. 3). Into this receptacle, already carrying ~300 liters of an aqueous-organic emulsion stabilized by caustic soda,

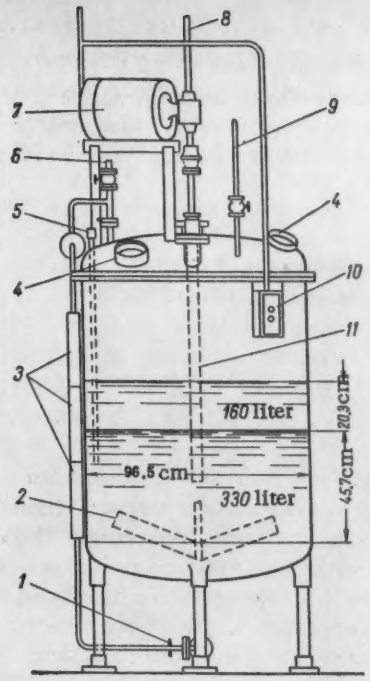

Fig. 3. Vat in which the critical mass formed.

were poured 49 more liters of concentrated nitric acid used for scrubbing residues of solid inerts from the bottom of the vessel in which the solvent was processed.

Accordingly, immediately prior to the accident, there were 330 liters of aqueous slurry, containing 40 g plutonium in the receptacle, with a layer of solvent about 160 liters in volume, and containing 3.27 kg plutonium, in the top of the vessel. Particulate solids containing 60 g plutonium were suspended in the aqueous and organic phases. Later calculations indicated that the layer was 20.32 cm thick, contained plutonium in amounts of 20 g per liter and was slightly subcritical. (The critical thickness of the layer would have been 20.95 cm.)

When he turned on the motor driving the mixer, the operator, observing the process through a viewing port on the top of the tank, saw a blue flash (Cerenkov radiation). The shock of the reaction accompanying the flash displaced the tank about 1 cm from its position. The motor was immediately turned off, and then restarted, by the operator. Two other operators rushing to the scene shut the motor off again. The supercritical mass formed because the layer of organic solvent in the receptacle rose 10 mm along the edges when the mixer was started up, corresponding to an increase of 12.7 mm in the effective radius of the system.

It was found that the amount of fissioned plutonium nuclei numbered $1.5 \cdot 10^{17}$. It was also revealed that induced activity showed up in objects situated 55 m distant from the receptacle in which the critical mass formed.

As a result of the accident, one operator received an exposure of 12,000 RBE and died in 36 hours. Two other

operators, suffering exposures of 134 and 53 RBE, displayed typical symptoms of radiation sickness.

A commission called to investigate the causes of the accident stated that it was due to an error on the part of the deceased operator, who set the entire mass of the slurry into agitation at once, instead of following the batch processing procedure.

It should be noted, in conclusion, that this is the third fatality resulting from overexposure to radiation at Los Alamos laboratory.

G. F.

LITERATURE CITED

1. Nucleonics 17, 28 (1959).
1. Nucleonics 17, 106 (1959).
3. Nucleonics 17, 21 (1959)
4. Nucleonics 17, 107 (1959).

HIGH-ENERGY ELECTRON SYNCHROTRONS

Until a very short time ago, the building of high-energy electron synchrotrons lagged far behind the rates of development of proton accelerators. This was associated first with the fact that the employment of nucleons proved preferable in nuclear reactions owing to the large interaction constant involved (approximately 100 times larger than the electromagnetic), and secondly because the construction of high-energy electron accelerators faced sizable engineering difficulties, principally with respect to compensating for rapidly mounting radiation losses.

However, it has been found in recent years that the low value of the interaction constant is fully offset by the possibility of obtaining comparatively high beam current in electron synchrotrons, and by the simplicity attained in interpretation of the experimental results.

Electron synchrotrons make possible a number of experiments of high interest for nuclear physics. These include experiments associated with:

a) photoproduction of π and μ mesons over a wide range of energies;

b) the Compton effect in hydrogen for high-energy γ quanta, probing into several fundamental questions in quantum electrodynamics;

c) photodisintegration of nuclei;

d) nuclear scattering of gamma photons and electrons, allowing further probing of the structure of nucleons.

When the peak energy of electrons or γ quanta is raised to several billion electron volts, pair production of heavy particles and multiple production of mesons become possible. It is important that the pair production threshold for γ quanta lie below that for protons. For purposes of illustration, a graph of the relative yield of pairs of heavy particles, as a function of energy is shown (see Figure)[1].

It has been shown in recent years that even with radiation losses accounted for, electron synchrotrons capable of accelerating electrons to ~10 Bev, may be designed with technically acceptable parameters.

In the design of large-scale electron synchrotrons, one of the basic problems to be faced is the choice between weak focusing and strong focusing. The weak focusing system, which is well developed at the present state of the art, presents the opportunity to obtain relatively high extracted-beam current for comparatively broad tolerance requirements in the various specifications of the magnetic system. However, this approach to focusing suffers from the important drawback expressed in the sharp increase in power supplies to the electromagnet, heavy weight penalty, large size, and, in consequence, high costs, as the exit particle energy is increased. Nonetheless, at low and intermediate energy ranges (up to 1-1.5 Bev), where the absolute value of the power supplied to the magnet is not so high, weak focusing may be preferable, in virtue of the simplicity of fabrication of the magnet. A further advantage in weak focusing is the presence of positive radiation damping of betatron oscillations. This may result in appreciably less stringent specifications for the magnetic system and operating vacuum.

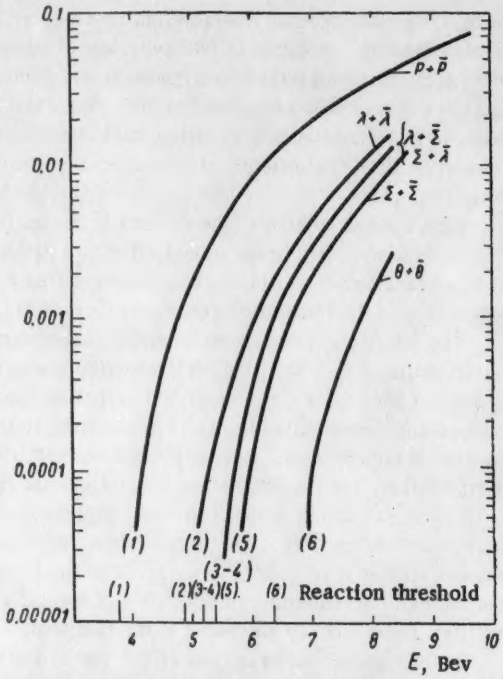

Relative yield of heavy-particle pairs as a function of peak electron energy.

The above considerations explain the fact that synchrotrons ranging 1 to 1.5 Bev in energy are being built at the present time on the weak-focusing principle (along with strong-focusing accelerators being currently designed or built).

Not long ago, a communication appeared to the effect that a 1 Bev weak-focusing synchrotron had been put into service at the Institute Nazionale di Fisica Nucleare (Frascati, Italy) [2]. The synchrotron was designed for experiments on the physics of π mesons and the production of strange particles (photoproductions of K mesons and hyperons at near threshold, multiple production of π mesons, etc.)

The first attempts to start up this facility were undertaken in December, 1958, when the electron injector (a 2.5 Mev Van de Graaff accelerator) was put into operation. At this stage, an energy of 300 Mev was attained by making use of only one of the two accelerating gaps. A maximun energy of 1 Bev was reached in February, 1959, when the second accelerating gap was connected. A maximum electron energy reaching 1.2 Bev is expected with the use of the same magnet, as work progresses.

A current of 3 ma was injected into the vacuum chamber of the synchrotron for 1 μsec. The peak beam intensity, according to preliminary measurements, was $8 \cdot 10^{10}$ equivalent quanta per minute with respect to γ radiation, at a pulse repetition rate of 20 cps.

Another large weak-focusing synchrotron in operation at present is the 1.4 Bev synchrotron at California Institute of Technology (Pasadena, USA). This synchrotron is based on a magnet designed after the magnet (scale 1 : 4) used in the Bevatron, the large 6.3 Bev proton synchrotron at Berkeley (USA). The frequency of the acceleration cycles (1/sec) is limited by the thickness of the steel plates (about 1 cm) in the magnet assembly. A pulse transformer yielding electrons at a kinetic energy of 1 Mev is used as injector. The number of accelerated particles per pulse is $10^{10} - 10^{11}$. This accelerator has been used to perform a number of interesting experiments on photoproduction of mesons, using hydrogen.

In line with the perspectives for further increasing the energy of accelerated electrons, the design and installation of strong-focusing synchrotrons is attracting particular attention. This is due to the characteristic features of the motion of relativistic electrons in the presence of radiation. It has been found in recent years that the random stochastic quantum character of the radiation results in the excitation of synchrotron oscillations, which render acceleration practically impossible in a weak-focusing system at energies considerably in excess of 1-1.5 Bev [3]. This difficulty is not encountered in strong-focusing synchrotrons which, incidentally, also have their negative aspects. In particular, the reaction of radiation in strong-focusing systems leads to instability of the radial betatron oscillations, requiring special damping techniques to correct this instability.

The first operating accelerator using strong focusing was installed at Cornell University (USA). A four-quadrant "racetrack" type magnet with removable pole shoes was used for the accelerator. These flux bars provide values of the field index $n^+ = 14.75$ and $n^- = -16.25$ with deviations $\Delta n = \pm 0.25$ over a track width of about 5 cm. At peak field strength of 13.2 kilogauss, the energy of the accelerated electrons should reach 1.5 Bev. The magnet is energized by a sinusoidal current at a frequency of 30 cps. The short acceleration time makes a damping system unnecessary. The limited weight of the magnet (20 tons) and the negligible pole gap allowed the use of a ready-made system for supplying the synchrotron with 300 Mev. The injector used is a Van de Graaff generator with a current of about 100 ma per pulse (plans call for raising the injection current to 1 amp). The peak intensity reached is 10^9 electrons per pulse; it has been proposed to increase the intensity by an order of 1-2.

The largest electron synchrotron currently in use is the strong-focusing accelerator at the Massachusetts Institute of Technology (Cambridge, USA), ~6 Bev [1]. The installation of this facility entails serious requirements imposed on the radio frequency, which must compensate for radiation losses which amount to about 5.7 Mev per revolution, at the termination of an acceleration cycle. The compensation is effected by 16 resonators producing an effective accelerating field with amplitude $\sim 8 \cdot 10^6$ v.

A characteristic feature of this accelerator is the very high value of the harmonic number (q = 352), enabling the short wavelength of the accelerating voltage ($\lambda \sim 0.5$ m) to be used to advantage, and allowing the use of small resonators as well. The total power radiated by the beam and scattered in the resonators reaches 455 kw at the end of a cycle. The repetition rate of the cycles is 15 cps, with the total power scattered in the windings and magnet amounting to about 750 kw. The total weight of the magnet is 230 tons, radius of the orbit 20 m. The element of periodicity in the magnetic system consists of two focusing and two defocusing magnets with the absolute value of the fall-off index of the magnetic field (n) = 89.5. Each structure of the element (known as a fofdod) yields rather high stability to disturbances and makes for ease of injection of particles. The comparatively high value of (n) allows the choice of a small aperture for the vacuum chamber (12.6 x 3.8 cm).

The injector used is a 40 Mev linear accelerator operated at a frequency of 2955 Mc. It has been suggested to produce a single-revolution injection of $8 \cdot 10^{11}$ electrons (injector current of 0.25 amp per pulse ~1 μsec).

The basic constants of the magnet will be assigned with a view to shedding light on the need for damping radial oscillations. Damping will evidently be effected by means of a magnet with its field direction reversed, included in the system.

The growing interest in the installation of large synchrotrons is also evinced in reports of new projects, e.g., a Japanese 1.4 Bev synchrotron and a German 7.5 Bev synchrotron (in Hamburg, West Germany) [4].

I.D., A. L.

LITERATURE CITED

1. M. Livingston, CERN Symposium 1, 439 (1956).
2. A. Alberigi et al., Nuovo Cimento 11, 311 (1959).
3. A. A. Kolomenskii and A. N. Lebedev, Elementary-Particle Accelerators [Suppl. No. 4 to Atomnaya Énergiya) [in Russian] (1957) p. 31.‡
4. Nucl. Engng. 4, 157 (1959).

‡Original Russian pagination. See C. B. Translation.

TOKYO SCHOOL FOR TRAINING LABORORATORY TECHNICIANS FOR WORK WITH RADIOACTIVE ISOTOPES

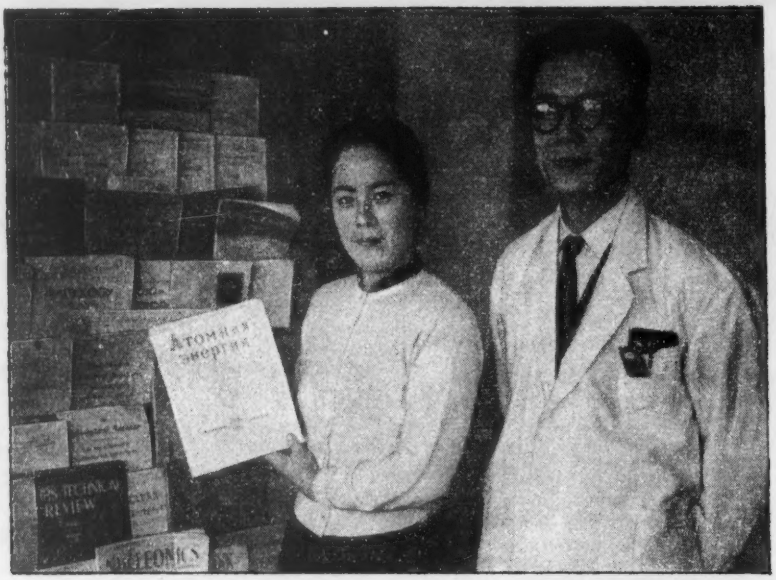

At the school library: Doctor Yatsui Hamada (on right) and librarian (holding recent copy of Atomnaya Energiya)

A school where laboratory technicians are being trained for work with radioactive isotopes in industry, medicine, agriculture, and scientific research, has been functioning in Tokyo during the past two years. Many of the students graduated from the school are directed to work in the Tokyo Institute of Physical and Chemical Research, and in the Center of Nuclear Research situated in the town of Tokai (over 100 km from Tokyo).

The period of tuition lasts 6 months. The school, organized to accomodate a class of 30, has at its disposal up-to-date laboratories for research in physics and chemistry involving the use of radioactive isotopes. Almost all of the instruments in use were manufactured in Japanese factories.

The school library receives periodical publications on nuclear physics and atomic energy from all over the world, including the Soviet Union (see photo). The library boasts of several thousand volumes.

The faculty consists in the main of scientific research workers on the staff of the Tokyo Institute of Physical and Chemical Research.

Tokyo

V. Parkhit'ko
(special correspondent)

BRIEF COMMUNICATIONS

USSR. A 12 channel magnetic pair spectrometer has been developed at the Joint Institute for Nuclear Studies. The instrument is capable of measuring spectra of gamma rays over the energy interval from 20 to 600 Mev. An SP-56 type electromagnet is used to establish a magnetic field in the 6 cm gap between the pole faces, with a peak field intensity of 18,000 oe. Proportional counters with high gas amplification, loaded only with methylal $CH_2(OCH_3)_2$

vapors at pressures of 160-200 mm Hg, usually employed as a quenching agent, are used in the spectrometer. The operating counter voltage is 1600-2000v, the effective dead time is less than 10^{-7} sec. The counter efficiency for particles with relativistic ionization reached 98% when the counter is operated with a coincidence circuit having a resolving time of $5 \cdot 10^{-7}$ sec. Delay of pulses due to electron drift in the counter gas is less than 10^{-7} sec. The pulse amplitude at the counter output is 1 v. Provisions are made for checking out separate components in the spectrometer. The instrument is to be used for research in gamma radiation due to the disintegration of neutral π mesons produced in a synchrocyclotron.

USSR. A technique for measuring the thermal ionization coefficient of a gas in the flow aft of a shock wave propagating through a shock tube to a speed of ~3 km/sec has been developed in the Physics Department of Moscow State University. The measurements were carried out with the aid of a cavity resonator operated at 10 cm wavelength. The stream of ionized gas, to be investigated without disturbing its fluid dynamic characteristics, was passed down the axis of a cylindrical high-frequency resonator. The variation in the Q of the resonator and the displacement of the resonant frequency as the gas advanced made it possible to monitor the ionization process directly, and to perform quantitative measurements. The duration recorded for the ionization process was dependent on the speed of the shock wave, and found to be ~200 μsec. The procedure enabled the ionization constant to be measured to an accuracy of ~10 % at several (10-15) points of the process under study, which in turn rendered it possible to measure the ionization pulse duration and the curvature of the forward and trailing wave fronts.

USSR. A 112 channel time analyzer with a minimum channel width of 1 μsec has been developed. The analyzer is capable of recording several pulses per cycle. The analyzer embodies the principle of arranging coincidence circuits in the form of a matrix with not only the triggering pulse, but also the pulse to be recorded passed through a time delay. The instrument passes signals only when two recorded pulses become superposed in a single change during the time the mechanical counter is in operation. Recording the pulses is carried out completely independently in the discrete channels.

USSR. A high-efficiency boron counter has been devised. The counter is BF_3-loaded to a pressure of 700 mm Hg. The counter cathode is a stainless-steel tube 25 mm in diameter and 400 mm long, the inner surface being ground. The anode is made of tungsten wire of 50 μ diameter. The forward face is fabricated in the form of a plane window of boron-free glass up to 1 mm thick. The rear face is a wrought flange with an opening for a glass insulator, having a protecting shim, and a device for keeping the filament in tension. For a parallel beam of thermal neutrons, the counter efficiency is close to 100%.

USSR. In the Central Scientific Research Institute for Wood Machining, the effects of radioactive emissions on wood, lumber materials, glues, and binders is being investigated.

USSR. Research is being conducted at the Uzbek State University into the effects of Co^{60} on physiological processes in the cotton plant, particularly on seed germination. The investigations demonstrated the effectiveness of treating seeds with gamma rays. Some of the experiments aimed at raising cotton productivity through radioactive treatment are being conducted in the fields, in kolkhozes of the Samarkand oblast.

USSR. A large section of the Soviet exposition opening in New York in late June is devoted to the successes achieved by Soviet science in the area of the peaceful utilization of atomic energy. The exhibits and models in the atomic section acquaint visitors with instruments and research methods in the field of nuclear physics, with scale models of existing or partially completed nuclear electric power stations, with a scale model of the atomic icebreaker "Lenin," and with the use of radioactive isotopes in medicine and industry.

IAE (International Atomic Energy Agency). The Agency published, in December, 1958, the first comprehensive handbook on the handling of radioactive isotopes, and postponed the effectuation of a resolution on the compilation of data pertinent to the technology and economics of low and medium power reactors, as well as data on the nuclear power requirements of poorly developed countries. A contract was signed with the University of Trieste for the development of a new technique of fast-neutron detection, and the conclusion of the first session of Agency experts on the disposal of hot wastes by burial in ocean waters was discussed.

IAEA. By March, 1959, the Agency had received propositions from various countries on the presentation of about 200 scholarships and admittances in special training institutions. In addition, the Agency proposes to set aside some of its own funds for that purpose. At the same time, requests for over 400 student placements were forwarded to the Agency.

German Democratic Republic. A method has been devised at the "Karl Zeiss" factory for the cutting and drilling of quartz, germanium, and other materials, based on electron beam bombardment. This principle is the basis for the design of an instrument which resembles an electron microscope in its external appearance, and is operated at a voltage of 100 kv and current of 10 ma. The electron beam is controlled by means of a programmed controller. The beam may be focused on a surface 1 μ in diameter. The instrument may be employed to cut through material without disturbing the crystal-lattice structure, and leaving practically no mechanical flaws.

NEW LITERATURE

Proceedings of the Second Conference on the Peaceful Uses of Atomic Energy. Papers of Soviet Scientists. Vol. 1. Nuclear Physics. (Edited by Academician A. I. Alikhanov, Academician V. I. Veksler, Candidate in Physical and Mathematical Sciences N. A. Vlasov). Atomizdat, 1959. 552 pages, 26 rubles.

The Proceedings of the Second International Conference on the Peaceful Uses of Atomic Energy (Geneva, September 1-13, 1958), are being published in Russian in 16 volumes, 6 volumes comprising all of the papers submitted by Soviet scientists to the Conference, and 10 remaining volumes containing selected papers by foreign scientists.

The first volume of papers by Soviet scientists, the volume on Nuclear Physics, consists of two parts. Part I, the Physics of Plasma and the Problem of Controlling Thermonuclear Reactions, consists of 17 papers. A survey article by L. A. Artsimovich gives a detailed analysis of the problem of the controlled thermonuclear reaction and the pathways taken toward resolving that problem in the Soviet Union. Appraising the present state of the art, L. A. Artsimovich (P. 2298) feels that no particular one of the approaches known up to now in controlled reaction problems exhibits any decisive advantage over the competing approaches. Research must therefore be pushed along the broadest possible front in the coming period. One of the possible avenues of approach is the use of electric discharges at high current strengths. Experimental research involving such discharges is dealt with in papers by A. M. Andrianov (P. 2301). V. S. Komel'kov, et al.; in papers submitted by S. M. Osovets (P. 2225), G. G. Dolgov-Savel'ev, K. D. Sinel'nikov, I. N. Golovin, V. S. Komel'kov et al., (P. 2527), experimental research on the behavior of plasma in magnetic fields of different types is described. Spectroscopic investigations of high-temperature plasma is discussed in a paper by S. Yu. Luk'yanov and V. I. Sinitsyn (P. 2228). Several papers contain theoretical studies of plasma stability (A. A. Vedenov, R. Z. Sagdeev, B. B. Kadomtsev, (P. 2214), high-frequency plasma oscillations (A. I. Akhiezer et al., P. 2300), plasma radiation (B. A. Trubnikov and V. S. Kudryavtsev, P. 2213) and plasma absorption of the energy in an electromagnetic field (R. Z. Sagdeev and V. D. Shafranov, P. 2215).

Part II, Nuclear Physics, contains 26 reports on different problems of neutron physics, nuclear reactor physics, particle acceleration, and the physics of cosmic rays. The report by Academician V. I. Veksler tells of the commissioning of the world's largest particle accelerator, the giant proton synchrotron of the Joint Institute for Nuclear Studies, and of scientific work being conducted with that accelerator. A report by S. N. Vernov and A. E. Chudak deals with the results of cosmic ray studies using Soviet rockets and earth satellites. The launching of the space satellites made it possible for the first time to bring physical equipment designed to record cosmic rays to an altitude of over 1000 km above the surface of the earth. As a result of processing of the data received from the satellites, the existence of a peculiar aureole of electrons of moderate energy around the earth may be considered proven. The accumulation of electrons is explained by the effects of the geomagnetic field, acting as a magnetic trap for low-energy electrons. A paper submitted by L. V. Groshev et al. adduces data on γ rays arising in the capture of low-energy neutrons by different nuclei. This question is intriguing from two points of view. First, such data are necessary to calculate the shielding required for nuclear reactors to hold in gamma radiation. Secondly, studies in that area may provide much information on the structure of nuclei.

Several papers (A. I. Leipunskii, M. V. Pasechnik, V. M. Pankratov) were devoted to interactions between fast neutrons and various nuclei. These data must be available when designing fast breeder reactors.

New theoretical and experimental findings in the field of fission physics were related in papers by B. T. Geilikman, I. I. Bondarenko et al.

The study of the properties of a number of previously unknown fission fragments was taken up in papers submitted by B. S. Dzhelepov, T. A. Mostova, B. V. Ershler, I. V. Gordeev, et al.

A paper by V. V. Vladimirskii et al., compiled new data on the interaction of neutrons of various energies with fissioning isotopes and with a number of heavy elements recently produced in the USSR. A description of pulsed neutron sources, recently modernized, and up-to-date radioelectronic circuitry of analyzers used in neutron detection is to be found in papers by V. V. Vladimirskii, V. V. Sokolovskii, and A. P. Tsitovich.

The papers by Soviet scientists published in the first volume of "Proceedings of the Second International Conference on the Peaceful Uses of Atomic Energy" attest to the broad sweep of research on controlled thermonuclear reactions now in progress in the Soviet Union, and to the great steps forward taken by Soviet nuclear physics as a whole.

Proceedings of the Second International Conference on the Peaceful Uses of Atomic Energy. Papers of Soviet Scientists. Vol. 2, Nuclear Reactors and Nuclear Power. Edited by Corresponding Member of the Academy of Sciences of the USSR N. A. Dollezhal', Doctor in Physical and Mathematical Sciences A. K. Krasin, Acting Member of the Academy of Sciences of the Ukranian SSR A. I.

Leipunskii, Corresponding Member of the Academy of Sciences of the USSR I. I. Novikov, and Doctor of Physical and Mathematical Sciences V. S. Fursov. Atomizdat, 1959, 708 pp, 32 rubles, 60 kopeks. [in three parts, papers not listed here]

Handbook on Dosimetric, Radiometric, and Electronic and Physical Instruments, Counters, Scintillators, and Photomultipliers. Atomizdat, 1959, 254 pp, 6 rubles, 30 kopeks.

The handbook contains concise technical data on instrumentation for individual dosimetric monitoring, measurements of the dose rate of α , β , and γ radiations, measurements of neutron flux, determinations of contamination of air by radioactive substances, data on amplifiers and pulse discriminators, rectifier-stabilized scalers, counters for recording ionizing radiations, scintillators, phototube multipliers. The handbook is written for engineers and scientific research workers working with radioactive substances.

Korotkov, V. I., Chernysh, A. M., Ships of the Future, Voenizdat, 1959, 112 pages, 2 rubles, 10 kopeks.

The book presents a general picture of atomic energy as the principle underlying the operation of atomic reactors; a brief description is given of atomic power plants for ship propulsion and of atomic-powered ships; the perspectives of development os fuch ships is discussed. The book is illustrated with photographs and diagrams, with a brief list of the literature consulted as an appendix.

Naumenko, I. A., Atomic Power Plants, Voenizdat, 1959, 190 pages, 3 rubles, 15 kopeks.

The book outlines the physical fundamentals of nuclear power and provides a concept of the structure of matter, of the atom and the nucleus, nuclear forces, and nuclear reactions. Methods and instruments for obtaining nuclear energy, airborne and sea-going atomic engines, stationary atomic power plants, the problems facing the use of atomic engines for overland transportation, direct conversion of nuclear energy to electric energy, etc. The book is well illustrated and written for a broad readership.

Articles from the Periodical Literature

D. M. Abdurasulov "On the effect of small doses of ionizing radiation on the organism," Med. zhur. Uzbekistana No. 12, 3 (1958).

K. K. Alintsev et al., "Determination of work of ionization in air for gamma emissions of Co^{60}," Izmerit. Tekh. No. 2, 52 (1959).

D. L. Belyaev and Z. L. Zaturenskii, "Determination of rate of flow of pieces of coke in dry slaking chambers, with the aid of radioactive cobalt isotopes," Koks i khimiya No. 3, 34 (1959).

N. A. Borzunov et al., "Studies of a high-power pulsed discharge in conical chambers," Zhur Éksp. i Teor. Fiz. 36, 717 (1959).

S. Vartazarov "Radioactive isotopes aid in construction work," Stroitel' No. 2, 22 (1959).

I. A. Vasil'ev and K. A. Petrzhak, "Effectiveness of an end-window counter as a function of the hardness of beta spectra," Priboryi Tekh. Éksp. No. 1, 57 (1959).

P. A. Vlasyuk, "Natural radioactivity of plants and potassium fertilizers," Doklady VASKhNIL No. 2, 3 (1959).

V. V. Volkov et al., "Formation cross sections of californium isotopes on bombarding U^{238} with accelerated carbon ions," Zhur Éksp. i Teor. Fiz. 36, 762 (1959).

L. A. Vulis and A. A. Kostritsa "Hydrodynamic analogy to neutron diffusion and the critical state of a nuclear reactor. Reports 1, 2," Izvest. Akad. Nauk Kaz. SSR, Ser. Énerget. No. 2, 111 (1959).

G. S. Gol'din et al., "Industrial testing of a radioactive pulp densitometer," Gornyi Zhur. No. 3, 55 (1959).

Yu. I. Gribanov, "A portable neutron dosimeter," Pribory i Tekh. Éksp. No. 1, 133 (1959).

K. M. Efremova et al., "Investigation of the composition of alkali uranates obtained by the dry process," Doklady Akad. Nauk SSSR 124, 1097 (1959).

A. E. Zerschikov "Use of radioactive isotopes for monitoring acidification of an oil field," Geologiia nefti i gaza No. 2, 17 (1959).

A. M. Ivanitskii "Summary of the second scientific conference on problems of the effect of ionizing radiation on higher branches of the central nervous system (Moscow, May, 1958)," Patol. Fiziol. i Éksp. Terapiya 3, 93 (1959).

G. G. Iordan et al., "Safety measures in the widespread use of radioactive instruments," Priborostroenie No. 3, 21 (1959).

A. G. Karabash et al., "Chemical-spectral method of analysis of metallic beryllium and beryllium oxide of high purity," Zhur. Anal. Khim. 14, 94 (1959).

L. M. Kovrizhnykh, "On the oscillations of a cylindrical cavity in a fully ionized plasma," Zhur. Éksp. i Teor. Fiz. 36, 839 (1959).

A. D. Kostyuchenko and L. I. Petrova, "Effect of Ca^{45} and P^{32} on the development of perennial flax and red clover," Trudy Vsesoyuz. Nauchnoissled. Inst. l'na No. 5, 171 (1958).

A. M. Kuzin and V. I. Tokarskaya, "Continuous tagging of organic plant constituents with radiocarbon as a method of studying disturbances in metabolism" Biokhimiya 24, 80 (1959).

I. A. Kuzin and A. M. Semushin, "Use of ion exchange techniques for isotope separations," Trudy Lenigr. Tekh. Inst. im Lensoveta No. 48, 209 (1958).

V. I. Kuznetsov, "Colored reactions of uranium and thorium with o-arsono-o-oxyazocompounds," Zhur. Anal. Khim. 14, 7 (1959).

V. A. Leonova, "Contribution to the mineralogy and crystal chemistry of uraninites of Northern Karelia," Zapiski Vsesoyuz. Min. Obshchestva 88, 89 (1959).

Yu. V. Morachevskii and I. A. Tserkovinitskaya, "Gravimetric and photometric assay of thorium content in (natural) uraninites, with the aid of anthranilic acid," Zhur. Anal. Khim. 14, 55 (1959).

A. I. Moskvin and P. I. Artyukhin, "Determination of composition and instability constants of ethylenediaminetetraacetate complexes of Pu(III) by the ion exchange method," Zhur. Neorg. Khim. 4, 591 (1959).

E. P. Nadeinskaya, "Use of radioactive isotopes for studies of wear on cutting tools," Izvest. Vyssh. Ucheb. Zaved. Mashinostroenie No. 3-4, 134 (1958).

E. I. Nikitina, "Complexometric assay of zirconium in borides and nitrides," Zavodskaya Lab. 25, 142 (1959).

A. Ozol, "Plant research using a radiation field with gamma rays," Izvest. Akad. Nauk. Latv. SSR No. 12, 75 (1958).

V. I. Panasyuk and N. A. Miroevskaya, "Simplification of the complexometric assay of zirconium in zirconium glasses and concentrates," Zavodskaya Lab. 25, 147 (1959).

G. A. Pik-Pichak, "Anisotropy of angular distribution of fission fragments of a rotating nucleus," Zhur. Éksp. i Teor. Fiz 36, 961 (1959).

I. A. Piontovskii, "Effect of ionizing radiation on heredity," Patol. Fiziol. i Éksp. Terapiya 3, 12 (1959).

S. M. Polikanov and V. A. Druin, "Fission of heavy-element nuclei in interactions with carbon, nitrogen, and oxygen nuclei," Zhur. Éksp. i Teor. Fiz. 36, 744 (1959).

A. N. Protopopov et al., "On the angular anisotropy of the separation of fragements in the fission of Am^{241} induced by neutrons of 14.7 Mev energy," Zhur. Éksp. i Teor. Fiz. 36, 920 (1959).

A. M. Protopopov and B. M. Shiryaev, "Gammas accompanying the fission of U^{238} by 2.8 Mev and 14.7 Mev neutrons," Zhur. Éksp. i Teor. Fiz. 36, 954 (1959).

V. Ya. Savel'ev and V. A. Kononenko, "Investigation of slow neutron counters," Priboryi i Tekh. Éksp. No. 1, 61 (1959).

E. M. Savitskii and V. F. Terekhova, "Mechanical properties and recrystallization diagram of zirconium iodide," Trudy Baikova Inst. Metallurg. No. 3, 181 (1958).

G. A. Semenov and Yu. A. Zonov, "Contribution to the mass-spectrometric assay of the isotopic composition of boron," Zhur. Anal. Khim. 14, 137 (1959).

A. G. Sitenko, "On the fission of aspherical nuclei," Zhur. Éksp. i Teor. Fiz. 36, 793 (1959).

S. A. Sysomyatin, "Production of rutile and zircon concentrates by the method of reduction by roasting and magnetic separation," Trudy Nauchnoissled. i Proekt. Inst. "Uralmekhanobr" No. 4, 136 (1958).

L. I. Torozova, "Contribution to the problem of the origin of radioactivity in the Tskhaltubo mineral wells," Trudy Inst. Geofiz. (Akad. Nauk Gruz. SSR) 17, 383 (1958).

N. Ya. Turova et al., "On beryllium phenolates," Zhur. Neorg. Khim. 4, 549 (1959).

N. V. Fedorenko et al., "Dissociation of the molecular ion H_2^+ in collisions with gas," Zhur. Éksp. i Teor. Fiz. 36, 385 (1959).

D. G. Fleishman and L. G. Shakhidzhanya, "Lowering of the background in measuring low activity levels in liquid scintillation counters," Priboryi i Tekh. Éksp. No. 1, 135 (1959).

A. I. Shashenshtein and Yu. I. Antonchik, "Semimicrotechniques in the isotope analysis of substance with close to 100% deuterium content," Zhur. Anal. Khim. 14, 100 (1959).

I. S. Shpigel', "Plasma acceleration," Zhur. Éksp. i Teor. Fiz. 36, 411 (1959).

V. V. Yankov, "On the behavior of a conducting gas sphere in a quasi-istationary electromagnetic field," Zhur. Éksp. i Teor. Fiz. 36, 560 (1959).

T. Asaoka, Nuclear Sci. and Eng. 5, 57 (1959).

G. Bäckstrom, Nuclear Instr. and Methods 4, 5 (1959).

R. Balzer et al., Nuovo Cimento 11, 609 (1959).

L. Barney et al., Nuclear Sci. and Eng. 5, 28 (1959).

D. Beard, Phys. Rev. Letters 2, 81 (1959).

R. Brackmann and W. Fite, Rhys. Rev. 112, 1157 (1958).

R. Bradley, J. Appl. Phys. 30, 1 (1959).

B. Brockhouse, Rev. Sci. Instr. 30, 136 (1959).

A. Cameron, Canad. J. Phys. 37, 323 (1959).

P. Campion et al., Canad. J. Phys. 37, 377 (1959).

W. Clendenin, Nuclear Sci. and Eng. 5, 1 (1959).

G. DeSaussure and F. Silver, Nuclear Sci. and Eng. 5, 49 (1959).

J. Drummond, Phys. Rev. 112, 1460 (1958).

J. Elliot and F. Young, Nuclear Sci. and Eng. 5, 55 (1959).

W. Fite and R. Brackmann, Phys. Rev. 112, 1141 (1958).

W. Fite and R. Brackmann, Phys. Rev. 112, 1151 (1958).

W. Fite et al., Phys. Rev. 112, 1161 (1959).

A. Futch, Nuclear Sci. and Eng. 5, 61 (1959).

H. Gebauer, Atomkernenergie 4, 62 (1959).

K. Geiger and G. Whyte, Canad. J. Phys. 37, 256 (1959).

E. Gelbard et al., Nuclear Sci. and Eng. 5, 36 (1959).

J. Groover, Ind. Chemist. 35, 59 (1959).

"Halden BHWR," Nuclear Eng. 4, 106 (1959).

G. Hall, Ind. Chemist 35, 3 (1959).

E. Harris, Phys. Rev. Letters 2, 34 (1959).

L. Holland, J. Sci. Instr. 36, 105 (1959).

P. Huebotter and W. Seitz, Nuclear Sci. and Eng. 5, 11 (1959).

G. Keiholtz et al., Nuclear Sci. and Eng. 5, 15 (1959).

P. Kisliuk, J. Appl. Phys. 30, 51 (1959).

T. Krieger and P. Zweifel, Nuclear Sci. and Eng. 5, 21 (1959).

I. Kügler, Atomkernenergie 4, 67 (1959).

H. Landon et al., Phys. Rev. 112, 1192 (1958).

B. Leonard et al., Nuclear Sci. and Engr. 5, 32 (1959).

D. Montgomery, Phys. Rev. Letters 2, 36 (1959).

A. Morton and W. Smith, Nuclear Instr. and Methods 4, 36 (1959).

H. Mott-Smith, Nuclear Sci. and Engr. 5, 68 (1959).

R. Murray et al., Nuclear Sci. and Eng. 5, 69 (1959).

S. Neddermeyer, J. Appl. Phys. 30, 16 (1959).

Nuclear Eng. 4, 113 (1959).

R. Perkins and J. Nielsen, J. Science 129, 94 (1959).
D. Reagan, Phys. Rev. Letters 2, 82 (1959).
A. Sauer, Nuclear Sci. and Eng. 5, 71 (1959).
J. Slepian, Phys. Rev. 112, 1441 (1959).
A. Strasser, Nuclear Eng. 4, 131 (1959).
M. Sumi, Phys. Rev. Letters 2, 37 (a959).
J. Uhler and T. Alvāger, Arkiv Fysik 14, 473 (1959).
E. Weibel, Phys. Rev. Letters 2, 83 (1959).
R. Wille and R. Fink, Phys. Rev. 112, 1950 (1958).
B. Wolfe and D. Fisher, Nuclear Sci. and Eng. 5, 5 (1959).
D. Wood, Nuclear Sci. and Eng. 5, 45 (1959).

ATOMIZDAT

1. Nuclear Physics. First volume of reports by Soviet scientists at the Second Geneva Conference. 26 rubles.
2. Nuclear Reactors and Nuclear Power Engineering. Second volume of reports by Soviet scientists at the Second Geneva Conference. 32 rubles, 60 kopeks.
3. Handbook on Dosimetric, Radiometric, Electronic, and Physical Instruments, Counters, Scintillators, and Photomultipliers. 6 rubles, 30 kopeks.
4. N. A. Doronin, Calcium Metallurgy. 2 rubles, 60 kopeks.
5. N. G. Gusev and E. E. Kovalev, Nomograms for Design of Shielding Against Gammas Emitted by Radium, Cobalt-60, Scandium-137, Iridium-137. 2 rubles.
6. A. N. Komarovskii, Accelerator Design Details. 6 rubles.
7. A. N. Komarovskii, Structural Materials for Shielding Against Radiation from Nuclear Reactors and Accelerators. 5 rubles, 50 kopeks.
8. A. D. Galanin, Theory of Thermal Reactors, 2nd edition, revised and augmented.
9. Charlotte Auerbach, Genetics in the Atomic Age.
10. O. I. Leipunskii, Gamma Radiations from an Atomic Explosion.
11. Electrostatic Generators. Symposium of articles edited by A. K. Val'ter.

Nonresidents of Moscow may order C.O.D., no down payment. Remit orders to: Moscow, K-31, Stoleshnikov per., 14., magazine No. 77, Otdel "Kniga-Pochta."

JUST OFF THE PRESS: AN ATLAS OF NEUTRON CROSS SECTIONS. Atomizdat. 1959, 376 pages, 103 rubles.

The Atlas may be ordered from Atomizdat (Moscow, V-180, Staromonetny per. 26) or may be acquired by personally addressing the editorial office of ATOMNAYA ÉNERGIYA (Moscow, Tsentr, ul. Kirova, 18).